Aus der II. Medizinischen Klinik
der Medizinischen Fakultät Mannheim
(Direktor: Prof. Dr. med. Matthias P Ebert)

Hierarchical regulation of albumin transcription in liver cells under physiologic and pathophysiologic conditions

Inauguraldissertation
zur Erlangung des medizinischen Doktorgrades (Dr. med.)
der
Medizinischen Fakultät Mannheim
der Ruprecht-Karls-Universität
zu
Heidelberg

vorgelegt von
Rilu Feng

aus
Zhejiang, China
2021

Dekan: Prof. Dr. med. Sergij Goerdt
Referent: Prof. Dr. rer. nat. Steven Dooley

CONTENTS

Page

LIST OF ABRREVIATIONS

°C	Grad Celsius
µ	Micro (10^{-6})
2-DG	2-deoxyglucose
2DG6P	2-deoxyglucose-6-phophate
Abcc6	ATP Binding Cassette Subfamily C Member
ALF	Acute liver failure
BP	Base pair
BDL	Bile duct ligation
bZIP	basic region leucine zipper
C/EBPα	CCAAT/enhancer-binding protein alpha
CCl_4	Carbon tetrachloride
Cdk8	Cyclin dependent kinase 8
ChIP	Chromatin immunoprecipitation
CLF	Chronic liver failure
CPM	Counts per million
CREB	cAMP regulatory element-binding protein
CTD	Heptapeptide repeats in the C-terminal domain
Cyp	Cytochromes P450
DAB	3,3-diaminobenzidine
DC	Decompensated cirrhosis
DPE	Downstream promoter element
EDTA	Ethylene Diamine Tetraacetic Acid
EGF	Epidermal growth factor
ELISA	Enzyme-linked immunosorbent assay
EMT	Epithelial-to-mesenchymal transition
F5	Coagulation Factor V
F7	Coagulation Factor VII
F9	Coagulation Factor IX
F11	Coagulation Factor XI
Fbp2	Fructose-bisphosphatase 2
FBS	Fatal bovine serum
FC	Fold change

FDR	False discovery rate
FOXA2	Forkhead box protein A2
GLUT2	Glucose transporter Type 2
GLI2	Glioblastoma family zinc finger 2
Gpt2	Glutamic-pyruvic transaminase 2
GSEA	Gene Set Enrichment Analysis
GSK3	Glycogen synthase kinase-3
HCC	Hepatocellular carcinoma
HH	Hedgehog
HNF4α	Hepatocyte nuclear factor 4 alpha
HPH	Human primary hepatocyte
HRP	Horse radish peroxidase
IGF	Insulin-like growth factor 1
IHC	Immunohistochemistry
INR	International normalized ratio
IRS-1	Insulin receptor substrate 1
ITS	Insulin-Transferrin-Selenium
KDM5C	Lysine-specific demethylase 5C
LETF	Liver-enriched transcription factors
LPC	Liver progenitor cell
LPS	Lipopolysaccharides
LTx	Liver transplantation
Med14	Mediator 14
MELD	Model of end stage liver disease
MPH	Mouse primary hepatocyte
NES	Normalized enrichment score
NR2A1	Nuclear receptor subfamily 2, group A, member1
PBS	Phosphate-buffered saline
PDGF	Platelet-derived growth factor
PEPCK	Phosphoenolpyruvate carboxykinase
PI3K	Phosphatidylinositol-3-kinase
Pol II S2	RNA polymerase II phosphorylation of Ser2
Pol II S5	RNA polymerase II phosphorylation of Ser5
Pparα	Peroxisome proliferator activated receptor alpha

P/S	Penicillin-streptomycin
qPCR	Quantitative polymerase chain reaction
RNAi	RNA interference
RNA-SEQ	RNA Sequencing
RIN	RNA integrity number
RT	Room temperature
SAG	Smoothened agonist
SBE	SMAD-binding element
SD	Standard deviation
SDS-PAGE	Sodium dodecyl sulfate polyacrylamide gel electrophoresis
SHH	Sonic hedgehog
siRNA	small interfering RNA
Slc10a1	Solute Carrier Family 10 Member 1
Slc27a5	Solute Carrier Family 27 Member 5
TAF	TBP-associated factor
TBIL	Total bilirubin
TBP	TATA-box binding protein
TBST	Tris buffered saline with 0.05% Tween 20
TFIID	Transcription factor II D
TGF-β	Transforming growth factor beta
TNF-α	Tumor necrosis factor alpha
TSS	Transcription start site
WB	Western blotting

1 INTRODUCTION

1.1 Albumin synthesis is an essential liver function

The liver performs more than 500 vital functions, which can be divided into six categories: (1) filtration and storage of blood; (2) metabolism of carbohydrates, proteins, fats, hormones, and foreign chemicals; (3) formation of bile; (4) storage of vitamins and iron; (5) formation of coagulation factors and (6) synthesis of albumin [1]. Physiologically, most liver functions are carried out by hepatocytes. In the condition of liver failure (e.g. massive hepatocytes loss), liver progenitor cells (LPC) residing in intrahepatic bile ductules, called the "Canals of Hering", are activated to take over key hepatocyte functions [2].

1.2 Albumin function

Albumin is the most abundant serum protein synthesized by hepatocytes. The concentrations of albumin are 3.5-5.0 g/dL, accounting for more than 50% of total serum proteins in a healthy adult [3]. Albumin possesses many functions in maintaining homeostasis. The key role of albumin is acting as a plasma expander, which contributes to 75~80% of the plasmatic oncotic pressure [4]. Therefore, albumin was initially introduced in clinical practice as plasma volume expander for circulatory support [5]. Albumin performs many additional important functions, such as binding multiple drugs and other molecules, antioxidant, immunomodulation, endothelial stabilization, and antithrombotic function [6]. Through binding to a variety of substances, including fatty acids, bilirubin, bile acids, endotoxin, hormones, pharmaceuticals, and metabolites, albumin contributes to bilirubin elimination, maintaining a normal level of bile acids, drug delivery and detoxification, and antioxidant protection [7]. Albumin exerts antioxidant functions through binding and neutralizing free copper and iron to reduce highly toxic reactive metal species. Thiol groups from the cysteine-34 residue of albumin act as potent scavengers of reactive oxygen species [8]. Through nitric oxide (NO)-albumin complexes, albumin prolongs the activity of NO to promote vasodilation and inhibit platelet aggregation [9]. Recently, the anti-inflammatory effect of albumin has been investigated. Fernández J et al. reported that increasing serum albumin levels to more than 30 g per liter reduced systemic inflammation in patients with decompensated cirrhosis [10]. They also found that albumin infusion reduced the incidence of nosocomial infection in cirrhotic

patients with nonspontaneous bacterial peritonitis infections [11]. However, a recent clinical trial demonstrated that albumin infusions to increase the albumin level to 30 g per liter or more was not more beneficial than the current standard care in patients hospitalized with decompensated cirrhosis [12]. In contrast to additional key parameters such as bilirubin and international normalized ratio (INR), which are rapidly increased in response to the development of liver failure, albumin levels remain stable even in patients with terminal liver failure (ALF). These observations imply an efficient regulatory mechanism in the liver that maintains albumin synthesis even in the condition of liver failure.

1.3 Transcriptional regulation of albumin

The liver possesses a transcriptional network that regulates the expression of the hepatic functional genes, including albumin. Functional analysis reveals that numerous hepatocyte-specific DNA regulatory regions are composed of multiple cis-acting DNA sequences that are bound by different liver-enriched transcription factors (LETFs) [13–15]. LETFs are also named hepatocyte nuclear factors (HNFs), including at least five types based on structurally related DNA-binding domains. They are variant homeodomain-containing proteins (HNF-1α, HNF-1β); the winged-helix family proteins HNF-3α, β, and γ (also called FoxA1, 2, and 3); members of the nuclear hormone receptor family (HNF4, COUP-TFII, LRH-1, FXR, and PXR); the basic leucine zipper-containing factor CCAAT/enhancer-binding protein alpha (C/EBPα); and the onecut homeodomain protein HNF-6 [16,17]. During embryonic development, the specification of hepatoblasts in the endoderm requires HNF-3α and HNF-3β [18–21]. HNF-4α and GATA6 are essential for liver bud expansion and hepatocyte differentiation [22,23]. Hepatoblast differentiation into hepatocytes or cholangiocytes requires C/EBPα, HNF-6, and HNF-1 [24–26]. Little is known about when and how this network is established during hepatic development. It is also largely unknown when and how the network is disrupted in severe diseased conditions, such as terminal liver failure, resulting in dysregulated expression of hepatic function genes. In this study, we mainly focus on the role of HNF4α, C/EBPα, and FoxA2 in the regulation of albumin transcription during conditions of severe liver damage.

1.3.1 HNF4α

HNF4α, also known as NR2A1 (nuclear receptor subfamily 2, group A, member1), is a member of the nuclear receptor superfamily. Among the liver-enriched transcription

factors, HNF4α acts as a master transcription factor [27,28], given that up to 50% of functional genes in human adult hepatocytes are regulated by HNF4α, including albumin, metabolic enzymes, transporters, coagulation factors, even other nuclear receptors [29,30]. In contrast to many other nuclear receptors, HNF4α is constitutively expressed in hepatocytes throughout fetal growth and adult life [31]. Forced re-expression of HNF4α can restore hepatocyte functionality, thereby reversing terminal chronic hepatic failure in CCl_4-treated rats [32]. These observations highlight a key role of HNF4α in controlling liver function and maintaining organ homeostasis.

1.3.2 C/EBPα

C/EBPα is a member of the subfamily of basic region leucine zipper (bZIP) transcription factors [33]. It plays a pivotal role in the regulation of cell proliferation and differentiation, as well as in the expression of several lineage-specific genes [34]. During liver development, C/EBPα directs hepatoblasts towards the hepatocyte lineage. C/EBPα-deficient embryonic hepatoblasts give rise almost exclusively to biliary epithelial cells in a transplantation setting [35]. Physiologically, C/EBPα regulates genes encoding hepatic lipogenesis and glucose metabolism [36]. In addition, C/EBPα expression in the nucleus of hepatocytes [37] acts as a transcriptional activator regulating liver-specific genes, including transthyretin, α-1-antitrypsin, and albumin [38].

1.3.3 FoxA2

FoxA2 belongs to the subfamily of the forkhead box (FOX) proteins, which were initially discovered in liver nuclear extract specific for the promoters of the hepatic genes on the basis of DNA binding activity [39]. During development, the *FOXA2* gene is active throughout the period of definitive endoderm and the derived organs such as liver and pancreas [40], indicating an important role of the transcription factor in hepatogenesis. Another evolutionarily conserved function of FoxA2 is protecting the organism from hypoglycemia. Genes for the gluconeogenic enzymes can be activated by FoxA2 in response to fasting [41]. In addition, FoxA2 plays a role as pioneer transcription factor, possessing the capability to open chromatin by displacing linker histone, thereby enabling other transcription factors to bind to the functional regulatory sequences of target genes [42,43]. Unlike HNF4α, FoxA2 is a signal-driven transcription factor, which is driven by specific signals. Insulin and glucagon have been previously investigated to exert opposite effects on FoxA2 through regulating nuclear translocation in response to fasting or feeding state [44,45].

Therefore, FoxA2 is not stably localized in nuclei of hepatocytes to be the main regulator of albumin expression in the normal condition.

1.4 Insulin in albumin expression

Albumin synthesis in humans is an insulin-sensitive process [46]. Albumin expression was significantly decreased in livers from diabetic animals, but restored with insulin treatment [47]. A similar phenomenon was observed *in vitro* in primary rat hepatocytes: insulin stimulation maintained albumin gene transcription, protein synthesis and secretion [48,49]. These studies highlight the importance of insulin in albumin synthesis. Insulin is a pivotal hormone that regulates metabolism and growth. In the liver, insulin promotes glucose storage through mediating translocation of the glucose transporter (GLUT) from cytoplasm to the plasma membrane [50]. It exerts its functions through activating the phosphatidylinositol-3-kinase (PI3K)-AKT signaling pathway and phosphorylating a variety of substrates, including glycogen synthase kinase-3 (GSK3) [51], the forkhead (FOXO) transcription factors, and cAMP regulatory element-binding protein (CREB) [52]. CREB, FOXO1, and C/EBPα are transcription factors involved in gluconeogenesis [53–55]. The detailed mechanisms of how insulin maintains albumin expression require further investigation.

Insulin resistance occurs in patients with sepsis [56], obesity and diabetes [57], implying a role for severe or persistent inflammation. With insulin resistance, hepatocytes exhibit lower sensitivity to insulin signaling, thus leading to suppression of glucose transport [58]. Accordingly, the insensitivity of hepatocytes to insulin signaling might influence downstream factors, including albumin.

1.5 Inflammation in albumin expression

1.5.1 TGF-β

Inflammation is the main factor inhibiting hepatic nuclear factors and functional gene transcription. Among a plethora of inflammatory factors, Transforming growth factor-beta (TGF-β) is the best-known HNF4α inhibitory cytokine [59]. In cultured hepatocytes, TGF-β inhibits HNF4α expression by upregulating Snail, a transcription repressor that binds to the *Hnf4a* promoter, leading to epithelial-to-mesenchymal transition (EMT) of hepatocytes [60]. However, high levels of TGF-β do not always lead to loss of HNF4α in hepatocytes *in vivo*. As TGF-β mediates its biological function through activating downstream protein SMAD2 and SMAD3 [61], a previous study had

examined serum TGF-β concentrations and liver p-SMAD2 expression in patients with chronic liver disease of different severity [62]. TGF-β and p-SMAD2 levels positively correlated with inflammatory grades and fibrotic stages [62]. In these patients, loss of HNF4α was only observed in a portion of cirrhotic patients (unpublished data). These observations raise an interesting question: What is the underlying reason that some patients with chronic liver disease are capable of maintaining HNF4α expression in hepatocytes despite high levels of TGF-β, while hepatocytes in other patients lose HNF4α expression when their disease progresses into liver cirrhosis or terminal liver failure? Identification of the mediators of TGF-β effect on HNF4α is crucial for understanding the mechanisms involved in hepatic decompensation in cirrhosis or acute liver failure.

1.5.2 TNF-α

In the condition of inflammation, Tumor necrosis factor-alpha (TNF-α) is the key factor leading to insulin resistance[63]. TNF-α inhibits insulin signaling through blocking the phosphorylation of insulin receptor substrate 1 (IRS-1) [63]. It is worth noting that the mRNA level of C/EBPα is dramatically decreased in the liver, lung, and fat tissue of mice following intraperitoneal administration of lipopolysaccharides (LPS), which develop an acute phase response [64]. To date, it is not known how TNF-α regulates HNFs.

1.5.3 Hedgehog

In liver injury, hedgehog (HH) ligand synthesis is significantly induced, which correlates with the severity and duration of the injury, regardless of the etiology [65]. Multiple factors, including inflammatory factors such as TGF-β [66] and platelet-derived growth factor (PDGF) [67], epidermal growth factor (EGF) [68], and insulin-like growth factor (IGF) [69], can activate HH signaling. During development, Sonic hedgehog (SHH), one of the HH ligands, is strongly expressed in the ventral foregut endoderm, and later in hepatoblasts [70]. A previous study has shown that transcriptional activation of FoxA2 is directly regulated by the Glioblastoma (Gli) family of transcription factors, the canonical HH downstream signaling factors, during embryonic development [71]. Whether and how SHH regulates FoxA2 in severe liver disease requires investigation.

1.6 Aims of this study

Based on the state of art, albumin synthesis is an essential function of hepatocytes. In the condition of massive hepatocyte loss, why and how the severely damaged liver is still capable of producing albumin remains unknown to date. In this study, we propose that liver progenitor cells are activated to take over key hepatocyte functions, including albumin synthesis in massive hepatocyte loss-induced acute liver failure. There is an efficient transcriptional regulatory network existing in hepatocytes and liver progenitor cells in response to various pathophysiological conditions. We hypothesize that HNF4α, C/EBPα, and FoxA2 constitute this transcription factor network that regulates albumin expression in the liver. The aims of this study are (i) Analyzing the *ALB* core promoter DNA sequencing and nucleosome structure to identify potential binding sites of transcriptional activators, in particular HNF4α, C/EBPα, and FoxA2; (ii) Clarifying the effects and mechanisms of how HNF4α, C/EBPα, and FoxA2 regulate albumin transcription in hepatocytes and LPC; (iii) Examining the expression of HNF4α, C/EBPα, and FoxA2 in healthy and severely damaged livers; and (iv) Determining how microenvironmental factors such as hormones and inflammatory factors affect expression of HNF4α, C/EBPα, and FoxA2 in different pathophysiological conditions.

2 MATERIALS AND METHODS

2.1 Materials

2.1.1 Patients and liver tissues

In total, 98 patients, including 56 non-cirrhosis and 42 cirrhosis, were analyzed in the Department of Medicine II, University Medical Center Mannheim, Medical Faculty Mannheim, Heidelberg University and the Department of Gastroenterology and Hepatology, Beijing You'an Hospital, Affiliated with Capital Medical University. Among 42 cirrhotic patients, 30 had compensated cirrhosis, while 12 suffered from acute decompensation (AD) and received liver transplantation. Acute decompensation was defined by the development of one or more major complications of liver diseases: (i) development of grade 2 to 3 ascites within <2 weeks; (ii) hepatic encephalopathy; (iii) gastrointestinal hemorrhage; (iv) bacterial infections (spontaneous bacterial peritonitis, spontaneous bacteremia, urinary tract infection, pneumonia, cellulitis) [72].

The study protocol was approved by local Ethics Committees (Jing-2015-084, and 2017-584N-MA). Written informed consent was obtained from patients or their representatives. A portion of patients has been investigated in a previous study [62].

2.1.2 Primary hepatocyte and cell lines

Table 1. Cell and culture medium used in the study

Cell		Culture medium	Reference
Primary cell	HPH	Williams E, 10%FBS, 1% L-Glutamine, 1% P/S, 0.5% ITS, 0.1% Dexamethasone	Provided by Dr. Stefan Munker [73,74]
	MPH	Williams E, 10%FBS, 1% L-Glutamine, 1% P/S, 0.5% ITS, 0.1% Dexamethasone	
Cell line	AML12	DMEM/F-12, 10% FBS, 1% L-Glutamine, 1% P/S, 0.5% ITS, 0.1% Dexamethasone	Provided by Dr. Nelson Fausto
	HepaRG	Williams E, 10% FBS, 1% L-Glutamine, 1% P/S, 50uM Hydrocortisone, 5ug/ml Insulin	Saint Gregoire, France
	BMOL	Williams E, 10% FBS, 1% L-Glutamine, 1% P/S, 10ug/ml Insulin	Provided by Dr. George Yeoh
	HEK293T	DMEM, 10% FBS, 1% L-Glutamine, 1% P/S	[75]

2.1.3 Chemicals and reagents

Table 2. Chemicals and reagents

Chemical and reagents	Company	Cat.No.
Acetic acid	Sigma-Aldrich	338826
Acrylamide/Bis solution 37,5:1	Serva	10688.01
Agarose	Biozym	840.004
Ampicillin Natriumsalz	Carl Roth	K029.4
APS	Sigma-Aldrich	A3678
Bovine Serum Albumin	Serva	11930
Chloroform	Sigma-Aldrich	C2432
Citric acid	Sigma-Aldrich	C2404
Collagen, Rat Tail	Roche	11179179001
3,3'-Diaminobenzidine Tablets	Sigma-Aldrich	D5905
Deoxyribonucleic acid sodium salt from salmon testes	Sigma-Aldrich	D1626
DEPC treated water	Thermo Fisher	4387937
Dexamethasone	Sigma-Aldrich	D4902
DMEM	Biozym	BE12-709F/12-M
DMEM/F-12	Gibco	21331-020
DMSO	Sigma-Aldrich	41639
dNTP Mix	Thermo Fisher	R0191
DPBS	Thermo Fisher	14190144
Dual Endogenous Enzyme Blocking	DAKO	S200389-2
EDTA	Sigma-Aldrich	E9884
Ethanol 96%	Carl Roth	T171.4
Ethanol 99.8%	Carl Roth	K928.4
Ethanol absolut zur Analyse	Neolab	LC-4045.1
FBS	Lifetechnologies	10270-106
Formaldehyde	Sigma-Aldrich	f1635
GelRed	GeneOn	S420
GeneRuler 100 bp DNA Ladder	Thermo Fischer	SM0323
GeneRuler 1 kb DNA Ladder	Thermo Fischer	SM0314
Glycine	Carl Roth	3790.2

Hematoxylin Connterstain	VectorLaboratories	H-3401-500
Hydrocortisone hemisuccinate	Sigma-Aldrich	PHR1926
Hydrogen Peroxide 30%	Merck	1072102500
Insulin solution from bovine pancreas	Sigma-Aldrich	I0516
Insulin-Transferrin-Selenium (100x)	Lifetechnologies	41400-045
Isopropanol	VWR	1096342511
Kanamycin	Sigma-Aldrich	K1876
LB Broth miller	Carl Roth	X968.1
L-Glutamine 200mM	Sigma-Aldrich	G7513
Lithium chloride	Sigma-Aldrich	L-4408
2-β-Mercaptoethanol	Sigma-Aldrich	516732
Methanol	Carl Roth	4627.6
Milk	Carl Roth	T145.3
Mounting Medium	Sigma-Aldrich	C9368
$NaHCO_3$	Biochrom	L1713
Nonidet P40 Substitute	Sigma-Aldrich	11754599001
NuPAGE™ LDS Sample Buffer (4X)	Lifetechnologies	NP0007
Opti-MEM	Gibco	31985-070
Pageruler protein ladder	Thermo Fisher	26619
PBS	Biochrom	L182-50
Penicillin Streptomycin	Sigma-Aldrich	P0781
Phosphatase inhibitor cocktail 2	Sigma-Aldrich	P5726
Protease Inhibitor Cocktail	Sigma-Aldrich	S8820
PowerUp SYBR Green Master Mix	Thermo Fisher	A25918
Protein A/G Plus Agarose	Santa Cruz	SC-2003
Protein Assay Reagent A	Bio Rad	5000113
Protein Assay Reagent B	Bio Rad	5000114
Protein Assay Reagent S	Bio Rad	5000115
Random Hexamer	Thermo Fisher	SO142
Recombinant KDM5C	Active Motif	31433
Recombinant Shh	PeproTech	100-45
Recombinant TGFβ1	PeproTech	100-21
RevertAid H Minus Reverse Transcriptase	Thermo Fisher	EP0452

RiboLock RNase Inhibitor	Thermo Fisher	EO0382
Sample Reducing Agent	Lifetechnologies	NP0009
SDS	Carl Roth	2326.2
Smoothened Agonist	Millipore	566660
Sodium chloride (NaCl)	Carl Roth	3957.2
DH5α Competent Cells for Subcloning	ThermoFisher	18265017
TEMED	Sigma-Aldrich	T9281
Tris	Carl Roth	5429.5
Triton™ X-100	Sigma-Aldrich	X100
Trizol reagent	ThermoFisher	15596018
Trypsin-EDTA Solution (10X)	Sigma-Aldrich	T4174
Tween20	Neolab	1247ML500
Williams E medium ohne Phenolrot	Sigma-Aldrich	W1878
Xylol (Isomere) >98 %	Carl Roth	9713.2

2.1.4 Antibodies

Table 3.1. Antibodies used for immunohistochemistry

Antibody	Species	Dilution	Company	Cat.No.
HNF4α	Rabbit	1:200	Cell Signaling	CST#3113
C/EBPα	Rabbit	1:500	Sigma-Aldrich	HPA065037
FOXA2	Mouse	1:100	Santa Cruz	SC-101060
Albumin	Sheep	1:1000	Abcam	Ab8940
GLI2	Mouse	1:100	Santa Cruz	SC-271786
p-SMAD2	Rabbit	1:100	IBL	28027
GLUT2	Rabbit	1:300	Sigma-Aldrich	HPA028997
Anti-Rabbit/HRP	Swine	1:200	DAKO	P021702-2
Anti-Mouse/HRP	Goat	1:200	DAKO	P0447
Anti-Goat/HRP	Rabbit	1:200	DAKO	P0449

Table 3.2. Antibodies used for immunoblotting

Antibody	Species	Company	Cat.No.
HNF4α	Rabbit	Cell Signaling	CST#3113
C/EBPα	Rabbit	Cell Signaling	CST#8178
FOXA2	Rabbit	Abcam	Ab108422
p-SMAD2	Rabbit	Cell Signaling	CST#3108S
p-SMAD3	Rabbit	Abcam	Ab63403
SMAD2	Rabbit	Cell Signaling	CST#5339S
SMAD3	Rabbit	Cell Signaling	CST#9523S
p-AKT(Ser473)	Rabbit	Cell Signaling	CST#4060
AKT	Rabbit	Cell Signaling	CST#4691
MED14	Mouse	Santa Cruz	SC-81236
GAPDH	Mouse	Santa Cruz	SC-25778
β-ACTIN	Mouse	Santa Cruz	SC-47778
Anti-Rabbit IgG	Mouse	Santa Cruz	SC-2357
Anti-Mouse IgG	Goat	Santa Cruz	SC-2005

Table 3.3. Antibodies used for ChIP assay

Antibody	Species	Company	Cat.No.
H3K4me3	Rabbit	Abcam	Ab8580
RNA PolI Ser2	Rabbit	Abcam	Ab193468
RNA PolI Ser5	Rabbit	Abcam	Ab5131
Histone 3	Rabbit	Abcam	Ab1791
Histone 3.3	Rabbit	Abcam	Ab176840
HNF4α	Rabbit	Abcam	Ab181604
C/EBPα	Rabbit	Invitrogen	PA5-77911
FOXA2	Mouse	Sigma-Aldrich	17-10258
GLI2	Rabbit	Novus Biologicals	NB600-8744
TBP	Mouse	DIAGENODE	C15200002
SMAD2	Rabbit	Cell Signaling	CST#5339S
SMAD3	Rabbit	Cell Signaling	CST#9523S
IgG Control	Mouse	Cell Signaling	CST#5415S
IgG Control	Rabbit	Cell Signaling	CST#3900S

2.1.5 Buffer preparation

Table 4. Buffer

Chemicals	Ingredient
RIPA (Western blotting, WB)	Tris 50mM
pH 7.2	NaCl 250mM
	Nonident P40 2%
	EDTA-Na 2.5mM
	SDS 0.1%
	Deoxycholic acid Na-salt 1.6g
Running buffer (WB) (10x)	Glycin 144g
pH 8.3	Tris 30.34g
	SDS 10g
Transfer buffer (WB) (10x)	Glycin 144g
	Tris 30.2g
	Methanol (add before use, 200ml/l)
TBST (WB) (10x)	Tris 12.1g
pH 7.5	NaCl 87.66g
	Tween-20 10 ml
Stripping buffer (WB)	Tris 7.56g
pH 6.7	SDS 20g
	2-β-Mercaptoethanol (1:1250)
ECL buffer (WB)	Solution 1
	Tris buffer (pH 8.5) 0.1M
	Luminol 250mM
	p-coumaric acid 90mM
	Solution 2
	Tris buffer (pH 8.5) 0.1M
	hydrogen peroxide solution 30%
Lysis buffer (ChIP)	SDS 1%
	EDTA 10mM
	Tris-Cl (pH 8.0) 50mM
Dilution buffer (ChIP)	SDS 0.01%
	Triton X-100 1.1%

	EDTA 1.2mM
	Tris-Cl (pH 8.0) 16.7mM
	NaCl 167mM
TSE I (ChIP)	SDS 0.1%
	Triton X-100 1%
	EDTA 2mM
	Tris-Cl (pH 8.0) 20mM
	NaCl 150mM
TSE II (ChIP)	SDS 0.1%
	Triton X-100 1%
	EDTA 2mM
	Tris-Cl (pH 8.0) 20mM
	NaCl 500mM
Buffer III (ChIP)	LiCl 0.25M
	NP-40 1%
	Deoxycholic acid 1%
	EDTA 1 mM
	Tris-Cl (pH 8.0) 10mM
TE buffer (ChIP)	Tris-Cl (pH 8.0) 10mM
	EDTA 1mM
Elution buffer (ChIP)	SDS 1%
	NaHCO3 0.1M
TAE buffer (50x)	Tris 242g
	Na_2EDTA (pH 8.0) 0.5M 100ml
	Glacial acetic acid 57.1ml
Citrate buffer (IHC)	Citrate acid 1.92g
pH 6.0	Tween-20 500ul
EDTA buffer (IHC) pH 8.4	EDTA 0.3722g

2.1.6 Commercial assays

Table 5. Commercial assays

Product	Company	Cat.No.
Lipofectamine 3000 kit	Thermo Fischer	L3000008
Lipofectamine® RNAiMAX kit	Thermo Fischer	13778-075
PureLink Quick Plasmid Miniprep Kit	Invitrogen	K210010
PureLink® HiPure Plasmid Maxiprep Kit	Invitrogen	K210007
Phusion® High-Fidelity DNA Polymerase	New England Biolabs	M0530S
Bio-Rad protein assay kit	Bio Rad	5000113-115
SYBR Green Master Kit	Thermo Fisher	A25918
Glucose uptake assay	Promega	J1341
Human Albumin ELISA Kit	Abcam	Ab108788
Mouse Albumin ELISA Kit	Abcam	Ab108792

2.1.7 Small interfering RNA

Table 6. Small interfering RNA

Product	Species	Company	Cat.No.
siHNF4A	Human	Dharmacon	M-003406-02-0005
siHnf4a	Mouse	Dharmacon	M-065463-00-0005
siCEBPA	Human	Santa Cruz	SC-37047
siCebpa	Mouse	Santa Cruz	SC-37048
siFOXA2	Human	Santa Cruz	SC-35569
siFoxa2	Mouse	Santa Cruz	SC-35570
siGli2	Mouse	Santa Cruz	SC-145421
siSMAD2	Human	Thermo Fisher	107873
siSmad2	Mouse	Thermo Fisher	156216
siSMAD3	Human	Thermo Fisher	107876
siSmad3	Mouse	Thermo Fisher	156947
siTbp	Mouse	Thermo Fisher	188336
siTaf6	Mouse	Thermo Fisher	186593
siTaf9	Mouse	Thermo Fisher	81626
siCdk8	Mouse	Thermo Fisher	223930

siMed14	Mouse	Thermo Fisher	70692
Control siRNA		Santa Cruz	SC-37007

2.1.8 Plasmids

Table 7. Plasmids

Recombinant DNA	Company	Cat.No.
pFlag-CMV4-CEBPA	Biomed	BM1310
pFlag-CMV4	Biomed	
pScalps-mcebpa	Addgene	79551
pScalps	Addgene	

2.1.9 Materials

Table 8. Materials

Material	Company	Cat.No.
10 µl white Tip	StarLab	S1111-3000
200µl yellow Tip	StarLab	S1111-0006
1000µl blue Tip	StarLab	S1111-6001
Safe lock tubes 0.5ml	Eppendorf	30121023
Safe lock tubes 1,5ml	Eppendorf	30120086
Safe lock tubes 2.0ml	Eppendorf	30123344
PCR tubes 0.2 mL	Eppendorf	30124359
Cryotubes, 2 ml	Greiner	126280
50 ml Falcons	Greiner	227261
15 ml Falcons	Greiner	188271
Serol. Pipette 50ml, single packed	Greiner	768180
Serol. Pipette 25ml, single packed	Greiner	760180
Serol. Pipette 10ml, single packed	Greiner	607180
Serol. Pipette 5ml, single packed	Greiner	606180
Aspiration pipette 2mL	Greiner	710183
6-well Plate	Greiner	657160
12-well Plate	Greiner	665180

24-well Plate	Greiner	662160
48-well Plate	Greiner	677180
96-well Plate	Greiner	655180
Cell Culture Dishes, 100 x 20mm	Greiner	664160
Cell Culture Dishes, 145/20 mm	Greiner	639161
Greiner Petri Dish 100 x 20 mm, sterile	Greiner	P5737-360EA
Cell Culture Flask 25cm2, 50ml	Greiner	690175
Cell Culture Flask 75cm2, 250ml	Greiner	658175
Cell Culture Flask 175cm2, 550ml	Greiner	660175
Filtropur S 0.45	Sarstedt	831826
Filtropur S 0.2	Sarstedt	831826001
MicroAmp Fast Optical 96-Well Reaction Plate	Lifetechnologies	4346907
Adhesive seals 100 sheets	Thermo Fisher	AB-0558
96 MicroWell™ Platten, Nunc™	Thermo Fisher	732-2717
Amersham Protran® 0.2 µm NC	Carl Roth	4685.1
Sponge Pad	Invitrogen	EI9052
Blotting Paper, 100/PAK	Whatman	WH3030-917
Mini-protean Spacer Plates 1.5mm Integrated Spacers	Bio-Rad	1653312
Mini-PROTEAN® Short Plates	Bio-Rad	1653308
Mini-PROTEAN® comb, 15well, 1.5mm	Bio-Rad	1653366
Mini-PROTEAN® comb, 10-well, 1.5 mm	Bio-Rad	1653365
Mini-PROTEAN® Casting Frame	Bio-Rad	1653304
Microscope cover glasses, No 1, 18 mm	Paul Marienfeld	0111580
Microscope cover glasses, No 1, 12 mm	Paul Marienfeld	0111520
Microscope slides	Carl Roth	ET081
Microtom Klingen R35	Hartenstein	0207500005
DAKO PEN	DAKO	S2002
XCEED Nitrile Gloves, Powder Free, Blue	Star Lab	XC-INT-S
Parafilm 10cm x 38m	Häberle	743311

2.1.10 Instruments

Table 9. Instruments

Instruments	Company	Cat.No.
Ultra-clean workbench	Kendro	KS 9
CO2 Incubator	Thermo Scientific	HERACELL 240i
Benchtop Centrifuge	Heraeus	30023354
Microscope for cell culture	Leica	521665
Water Bath	VWR	10128
Counting Chambers	BRAND	NA
Cryo 1 °C Freezing Container	NALGENE	5100-0001
Liquid nitrogen tank	Cryotherm	78204183
4 °C refrigerator	LIEBHERR	22336
-20 °C refrigerator	Premium NoFrost	3366
-80 °C refrigerator	Thermo Scientific	HFU T SERIES
Shaker for bacteria	CERTOMAT HK	8863245
Incubator	BINDER	9010-0080
Centrifuge for 96-well plate	Heraeus Christ	00097349
Multimode microplate reader	TECAN	Spark 10M
PCR analyzer	VWR	732-2548
StepOnePlus Real-Time PCR System	Thermo Fisher	4376600
Thermomixer compact	Eppendorf	5382000015
Vortex Mixers	VWR	444-1372
Duomax 1030 Shakers & Mixers	Heidolph	543-32210-00
RM5	CAT	60207-0110
Sprout Mini-Centrifuge	Heathrow Scientific	120611
Electrophoresis Chambers	Bio-Rad	1658004
Trans-Blot Cell	Bio-Rad	1703939
Power Supplies	Bio-Rad	1645070
Imaging system	Vilber Lourmat	Fusion SL
Microtome	Leica	RM2245
Microwave oven	MDA	44577
Microscope for IHC	Leica	DMRBE
Microscope for IF	Leica	DFC450C

Autoclaves	Systec	VX-150
Ice Machine	Manitowoc	UD0310A
1 ml Pipette	Eppendorf	2897987
200 µl Pipette	Eppendorf	293339
100 µl Pipette	Eppendorf	1007324
20 µl Pipette	Eppendorf	1969964
10 µl Pipette	Eppendorf	1984124
2.5 µl Pipette	Eppendorf	1966584
DualRange Balance	Sartorius	BP211D
Digital Balance	Sartorius	LP6200
Gel Electrophoresis Device	CLP	75.1214
Gel iX 20 Imager	INTAS	NA
Rotator	Stuart	SB3
Hot plate magnetic stirrers	IKA-Werke	RCT basic
Pipette filler pipetus	Hirschmann	13014
pH/mV/°C meters	inoLab	pH7110

2.1.11 Software

Table 10. Software

Software	Company	Source
GraphPad Prism 7.0a	GraphPad	https://www.graphpad.com/scientific-software/prism/
SPSS statistics 23	IBM Corporation	http://www.spss.com.hk/software/statistics/
BioRender	Crunchbase	https://biorender.com/

2.2 Methods

2.2.1 Immunohistochemistry

Tissue type: formalin-fixed, paraffin-embedded specimens

Note: Do not allow slides to dry at any time during this procedure.

Day 1

Step 1: Deparaffinization and rehydration

1) Incubate sections in three times xylene for 5 mins each time;

2) Incubate sections in one time of 100% ethanol for 10 mins;
3) Incubate sections in one time of 100% ethanol for 5 mins;
4) Incubate sections in one time of 96% ethanol for 5 mins;
5) Wash sections two times in PBS for 5 mins each time.

Step 2: Antigen Unmasking

Heat-induced epitope retrieval using a microwave with 1mM EDTA solution, pH 8.4 or citrate acid buffer, pH 6.0.

Total 10 mins (EDTA) or 20 mins (Citrate acid buffer):

10 to 15 seconds boiling

45 to 50 seconds waiting

Cool slides on the bench to RT.

Step 3: Blocking to eliminate non-specific staining.

1) Wash sections in PBS three times for 10 mins each time;
2) Blocking: incubate sections in DAKO blocking peroxide for 30 mins.

Step 4: Staining primary antibody

1) Wash sections in PBS twice for 10 mins each;
2) Dilute the primary antibody to the indicated concentration (Table 3.1) and add the diluted antibody to the sections;
3) Incubate sections overnight at 4 °C.

Day 2

Step 5: Staining secondary antibody

1) Remove primary antibody and wash sections in PBS three times for 10 mins each;
2) Add corresponding secondary antibody diluted to the indicated concentration (Table 3.1) in PBS to each section and incubate for 45 mins at RT;
3) Remove secondary antibody and wash sections three times with PBS for 10 mins.

Step 6: Staining to detect horse radish peroxidase (HRP)

1) Prepare DAB solution: add 10 mg DAB in 15 mL 50 mM Tris (hydroxymethyl)-aminomethane solution (pH 7.6), and then filter the clumps.
2) Add 12 µL H_2O_2 to the DAB solution to activate DAB, and then add the activated DAB to each section and monitor staining under a microscope.

Note: Let the sections develop 10 mins but do not exceed 10 mins and immerse slides in ddH_2O.

3) Counterstain sections in hematoxylin for 10 to 30 seconds.

4) Wash sections using tap water for 10 mins.

Step 7: Dehydrate sections

1) Incubate sections in 95% ethanol two times for 1 min each time;
2) Repeat in 100% ethanol, incubating sections two times for 1 min each time;
3) Repeat in xylene, incubating sections two times for 1 min each time;
4) Mounted the sections with malinol mounting medium.

Step 8: Record the staining results using Leica upright research microscope.

2.2.2 Mouse primary hepatocyte isolation

FVB wild-type mice were purchased from Jackson Lab. All animal protocols were performed in full compliance with the guidelines for animal care and approved by the local Animal Care Committee. 6 to 12 weeks old mice were used.

1) Setup perfusion station: Warm water bath to 42 °C, place perfusion buffer in the water bath.
2) Prepare the peristaltic pump: Run 70% ethanol through the tubing; Run air through the tubing for 30–60 s; Wipe the end of the tubing with a paper towel; Connect 27-gauge needle to the outlet end of the tubing.
3) Prime the tubing with warm perfusion buffer (pump speed 3 mL/min).
4) Anesthetize mouse by intraperitoneal injection of 10% ketamine hydrochloride (5mg/100mg body weight) and 2% xylazine hydrochloride (1mg /100 mg body weight). Place mouse on the edge of the dissection tray and secure limbs using needles.
5) Wet the fur thoroughly with 70% ethanol. Make a ‘‘U’’-shaped incision through the skin, secure the skin near the head using a needle.
6) Move the intestine to the right to reveal the portal vein and vena cava, place a stable and heavy object adjacent to the mouse hind legs to support the tubing such that it is slightly higher than the mouse, lay the tubing and the needle on the object. The edge of the needle should rest on the vena cava at a flat angle.
7) Turn on the pump and let the warm perfusion buffer reach the needle, while the buffer is running through the needle, insert the needle into the vena cava above the kidney.
8) Immediately upon appearance of white spots and/or portal vein swelling (occurs 2–3 s after cannulation), cut the portal vein with scissors.
9) Clamp the portal vein with forceps for 7–10 s. Make sure no fluid is passing through. After 30 s perform a second clamp, make sure you observe liver

swelling and relaxation.

10) Clamp the liver one more time, prior to digestion buffer arriving to the liver. Make sure the liver swells and relaxes.
11) While digestion buffer is perfused into the liver, clamp the portal vein every minute but no more than 3–4 times.
12) Remove the needle before the air gets into the liver. Dissect out the liver gently (it is now very flimsy and frail): using forceps, grab the central connective tissue between the lobes and slightly lift upwards, using it as an anchor point.
13) Transfer liver and media to a 10 cm plate. Rupture liver sack with fine tip forceps in a few locations along the liver surface and gently release cells using a cell lifter.
14) Filter 5 mL of suspension through a 70mm cell strainer into a 50 mL tube. Add another 10 mL of cold plating media to rinse the plate, add 5 mL of it to each filter. Spin at 50g for 2 mins at 4°C.
15) While the samples are spinning, prepare fresh Percoll solution from pre-chilled ingredients, aspirate most supernatant, leave 1 mL and resuspend the cells by swirling the tube.
16) Add 10 mL plating media and resuspend by gentle swirling.
17) Add 10 mL Percoll solution and mix thoroughly by inverting the tube several times. Spin at 200g for 10 mins at 4°C.
18) Aspirate supernatant, add 20 mL plating media.

2.2.3 Cell culture and treatment

Cells and culture medium used in this study are presented in Table 1.

Mouse primary hepatocytes were isolated as described above. Primary human hepatocytes were isolated by the Cell Isolation Core Facility of the Biobank Großhadern, University Hospital, LMU Munich. All the cells were cultured at 37°C in a humidified atmosphere containing 5% CO2. For transient transfection of siRNA or plasmid, cells were treated with indicated culture medium without penicillin/streptomycin. Cells underwent starvation without FBS medium for 4 to 6 hours before treating with 5ng/ml transforming growth factor-beta (TGF-β). After seeding, cells were cultured in complete medium without insulin for 24 hours before insulin treatment.

2.2.4 Chromatin immunoprecipitation and quantitative real-time PCR

Chromatin immunoprecipitation and quantitative real-time PCR (ChIP-qPCR) analyses were performed as described previously with minor modifications [76]. For each ChIP, Cells were grown to 95% confluence (8~9x10^6 in a 10cm cell culture dish) in complete culture medium for at least 3 days. Cells were washed twice with PBS and were subsequently incubated with 1% formaldehyde at 37 °C for 10 min to crosslink proteins and DNA. Following twice washing with ice-cold PBS, the cells were collected in lysis buffer containing 1% protease inhibitor cocktail. The chromatin was sonicated at 4 °C with 40 pluses each 30 seconds followed with subsequent 30 seconds to produce DNA fragments with an average length of 200-500 bp as determined by resolving the purified DNA on a 1.5% agarose gel. The sample was then centrifuged at 4 °C in an Eppendorf centrifuge at 15000 rpm for 10 mins to remove the cell debris from the crude chromatin lysate. Twenty microliters of the lysate were diluted with 80 µl of the dilution buffer and set aside as the input chromatin. The sheared chromatin from the cells was diluted at 1:10 and mixed with 50% protein A/G Plus Agarose, which blocked with 2 µg of salmon serum DNA at a concentration of 2 µg/mL. After shaking gently for 2 hours, the samples were centrifuged at 1700 rpm for 5 mins at 4 °C. The supernatant was collected and added the indicated antibodies (Table 3.3) to 2 µg/ml and shaken overnight at 4 °C. The samples were then mixed again with 50% protein A/G Plus Agarose (about 50 µl in 1 ml sample) and 2 µg of salmon sperm DNA to a final concentration of 2 µg/ml. After shaking 1 hour, the samples were centrifuged at 1700 rpm for 10 mins to remove the supernatant. Pellets were consecutively washed with 1 ml of TSE I, TSE II, buffer III and TE buffer for 10 mins each on a shaker at 4 °C. Antibody-protein-DNA complexes were eluted from protein A/G Plus Agarose with 100 µl of elution buffer by shaking on a rotatory platform for 10 mins. Eluted complexes, as well as the input chromatin, were incubated in a water bath at 65 °C for 6 hours to remove protein. The pulled down DNA fragments were extracted and purified using phenol-chloroform extraction/ethanol precipitation. The samples were stored at -20 °C until use.

The PCR employed in the ChIP assay consisted of 12 µL of the PCR reaction mix containing 2 µL of the DNA template, 1.25 µL of each primer (0.625 µL forward and 0.625 µL reverse primer, Table 11), 2.5 µL of PCR buffer (5x), 0.25 µL of 10 mM of

dNTPs, 0.125 µL of Taq polymerase and 5.875 µL ddH_2O which was subjected to amplification in a thermocycler. The PCR parameters were initially at 95 °C for 2 mins, followed by 38 cycles at 94 °C for 30 s for denaturation, 52 °C for 30 s for annealing, and 72 °C for 30 s to extend the DNA. The final PCR amplified product was identified on a 1.5 % agarose gel together with the 100 bp DNA ladder.

The samples were also subjected to quantitative PCR using SYBR green assay. The primer sets used for these assays are listed in Table 11. The PCR result was normalized to input fragments and the recruitment of target proteins (listed in Table 3.3) was presented as a fold change of PCR amplification in these samples compared with controls.

Table 11. Primers used for ChIP assay in this study

Gene	Forward primers (5'-3')	Reverse primers (5'-3')
ALB(-144~+75bp)	TTGTAATCGGTTGGCAGCCA	ATCTCGACGAAACACACCCC
Alb(-219~+87bp)	GGGTTAGAGGGGAACAGCTC	ACTCTTACGTGCTTCTCGGC
ALB(-1568~-1104bp)	AGGCACACTTGTTTTATGTCTGT	TACCTCTGCCCTTTTGCTCA
Alb(-1763~-1337bp)	GCTCAAGCGCCTACTTCATT	AGGGTGGGTGGCAGAATTAA
Foxa2(-1108~-545bp)	ACTGAGGTGGGTAGCCAGAA	TAGGTGAGAGGAAGCCAGGG
HNF4A(-250~+67bp)	TTGGGGTTGGCTCTCTAGGA	CAGGCAGATGTGGAGTCAGG
Hnf4a(-172~+160bp)	CCTGGTTCCAAGAAGCCACT	ATCTGCCAGGTGATGCTCTG
Hnf4a(-1750~-1172bp)	TGGCTCTCTCTGTCCTCTCC	AAAATGGGGTGACGATGGCT
CEBPA(-1070~-677bp)	ACGCAGGCAGGTAAAGCTAA	TCAAGAACCCACCCAGCATC
Cebpa(-1997~-1509bp)	GTGTTCCCTTTCCCCTCAGG	TCTAGGGTCGCAGGTCAAGA

2.2.5 RNA extraction, cDNA synthesis, and quantitative real-time PCR.

All reagents and containers used for RNA processing were RNase-free grade or treated with 0.1% DEPC to eliminate RNase contaminants.

1) RNA extraction

Total RNA was extracted in TRIzol according to the manufacturer's instructions.

a) Add 200 µL per well TRIzol to the 6-well plate, scrape the cells, collect lysate and transfer to a 1.5 mL Eppendorf tube;
b) Incubate at RT for 5 mins, centrifugation at 12,000 rpm at 4°C for 10 mins;

c) Collect the supernatant into a new 1.5 mL Eppendorf tube, add 40 µL Chloroform, shake well, incubate at RT for 2 mins, centrifugation at 12,000 rpm at 4°C for 10 mins;

d) Collect the supernatant into a new 1.5 mL Eppendorf tube, add 120 µL Isopropanol, shake well, incubate at RT for 15 mins, centrifugation at 12,000 rpm at 4°C for 15 mins, discard the flow-through;

e) Add 200 µL 75% ethanol (750 µL Absolute ethanol plus 250 µL DEPC water), rinse precipitation, centrifugation at 12,000 rpm at 4°C for 5 mins, discard the flow-through;

f) Add 40 µL DEPC H_2O to dissolve RNA. The concentrations of RNA were quantified in Infinite M200 by measuring absorbance at 260 nm.

2) cDNA synthesis

a) Prepare the following RNA/primer mixture in each tube:

Total RNA 500 ng
Primer (random) 0.5 µL
Water (nuclease-free) to 6.25 µL

Incubate the samples at 65°C for 5 min and then on ice for at least 1 min.

b) Prepare reaction master mixture. For each reaction:

5x Reaction Buffer 2 µL
10 mM dNTP mix 1 µL
RevertAid H Minus Reverse Transcriptase 0.25 µL

c) Add the reaction mixture to the RNA/primer mixture, mix briefly, incubate at 25°C for 5 mins; incubate the tubes at 42°C for 60 mins, heat inactivates at 70°C for 5 mins, and then chill on ice; Store the cDNA at -20°C until used for real-time PCR.

3) Quantitative real-time PCR

Normalize the primer concentrations and mix gene-specific forward and reverse primer pairs. Each primer (forward or reverse) concentration in the mixture is 5 pmol/ml. Set up the experiment and the following PCR program on a StepOnePlus system using SYBR Green Master Kit. 20 µl mixtures contained 5 µl template cDNA, 4 µl SYBR Green, 1µl forward and reverse primer PCRs, and 10 µl ddH_2O were run in triplicate. Polymerase chain reaction conditions were 95°C for 15 mins, followed by 40 cycles of 95 °C for 15 s, 60 °C for 20 s, and 72 °C for 20 s. The final extension

period consisted of 15 s at 95 °C and 1 min at 60 °C. Three biological replicates per condition were measured. The relative abundance fold changes of each target gene compared with a set of internal controls were determined by the $-2^{\Delta\Delta CT}$ formula [77]. Primers for quantitative RT-PCR were chosen using the PRIMER 3 software (http://primer3.wi.mit.edu/, see Table x). All primers were aligned with BLAST to avoid nonspecific annealing and cross-amplifications (https://blast.ncbi.nlm.nih.gov/Blast.cgi). Primers were synthesized by Eurofins.

Table 12. Primers used for qRT-PCR in this study

Gene	Forward primers (5'-3')	Reverse primers (5'-3')
Ppia	AGGATTCATGTGCCAGGGTG	GCCATCCAGCCATTCAGTCT
Hnf4a	AGATGCTTCTCGGAGGGTCT	GCCACTCACACATCTGTCCA
Cebpa	GCAAAGCCAAGAAGTCGGTG	CACCTTCTGTTGCGTCTCCA
Foxa2	CCCTACGCCAACATGAACTCG	GTTCTGCCGGTAGAAAGGGA
Smad2	TCCGGCTGAACTGTCTCCTA	CTGTGACGCATGGAAGGTCT
Smad3	AGAGGTGTGCGGCTCTACTA	GGGCAGCAAATTCCTGGTTG
Alb	TGTCCGTCAGAGAATGAAGTGC	AAGACATCCTTGGCCTCAGCA
Gli2	AGAGCCCACGGTGTAAACTG	CCTCCAGACCAATTCCACCC
Taf6	CACTCACCATCACACAGCCT	AGGAGGAGAAGGCTGAGGAG
Taf9	ACCCCTTTGCCACTGATCAA	TGGAGTCGGTGTACCTAGGG
Tbp	AAGAGAGCCACGGACAACTG	TTCACATCACAGCTCCCCAC
Cdk8	CCTCCGACTATCAGCGTTCC	GCTGAGTATCCCATGCTGCT
Med14	AGGGGCCAGTTTTGCTAGTC	CAGTTTCCTGCTCGTCCACT
Slc2a2	GCATCGACTGAGCAGAAGGT	CTCCACAAGCAGCACAGAGA
Foxa3	GCTGACCCTGAGTGAAATCTAC	ACGAAGCAGTCATTGAAGGAC
Cyp21a1	GCAGATCCAAGAGAGTCGGG	CTTTCCATTGGCCTGCAACC
Cyp3a25	TATGAACTGGCCACTCACCC	CCATCAGGGCGTCATAGGTG
Cyp2d26	GCCATCTTCCTGCTTCTGGT	GTTCTCGAAGTCCACCTGCA
Abcc6	ACTGCTATGGAGGGGCTACA	CCATTGCAGCTTCTCCTCCA
Slc27a5	GTAACGTCCCTGAGCAACCA	TAAGCCCACATTGCCCTCTG
Slc10a1	CCTCAAGGCAGGCATGATCA	ATCAGGGAGGAGGTAGCCAG
F5	CGCAACTAAGGCAGTTCTATGT	GCTAGATCGTGGCTTTTCTTTCT
F7	TGTAGGGACCAAGCGTACCT	CCACACAGCAATAACCCATTGAT
F9	ATGCTGGTGCCAAGTTGGATT	CTCAGTGCAGGAACAAATTACCT
F11	GAAGGATACGTGCAAGGGAGATT	CAAGTGCCAGACCCCATTGT
Fbp2	TGAATGCAATCCTGTGGCCT	CTCTTGCACATCCTCAGGGG

Gpt2	GTACTCCGCGGTCATCTCTG	CACAGTGGTCTTTGGCTTGC
Ppara	AGAGCCCCATCTGTCCTCTC	ACTGGTAGTCTGCAAAACCAAA
GAPDH	GGAGCGAGATCCCTCCAAAAT	GGCTGTTGTCATACTTCTCATGG
HNF4A	CACGGGCAAACACTACGGT	TTGACCTTCGAGTGCTGATCC
CEBPA	TATAGGCTGGGCTTCCCCTT	AGCTTTCTGGTGTGACTCGG
FOXA2	CCAGGAATTTGCTGCTCTTC	TCCATAGGGACCACACACAA
ALB	CACGCCTTTGGCACAATGAA	ATCTCGACGAAACACACCCC
GLI2	GAAGCCTCCACCCTTTCCTC	TGCCACTTCTGTCTGCTGAG
SMAD2	CCAGGAATTTGCTGCTCTTC	TCCATAGGGACCACACACAA
SMAD3	GGCTCCCTCATGTCATCTACT	AGTAGGTAACTGGCTGCAGGT

2.2.6 Protein extraction, concentration determination, and Western blotting

1) Whole cell protein extraction

Wash the cells twice with ice-cold PBS and immediately add RIPA buffer (80 µL per well of 6-well plate) supplemented with protease inhibitors and phosphatase inhibitors on ice for 10 mins. Thereafter, scrape the cells to collect lysate and transfer to a 1.5 mL Eppendorf tube. Subsequently, centrifuge at 13,000 rpm at 4°C for 10 mins. Collect the supernatant in a fresh 1.5 mL Eppendorf tube.

2) Protein concentration determination

The total protein concentration in the supernatant was determined using a Bio-Rad protein assay kit. 20 µL Reagent A diluted with Reagent S (50:1) was added into a 96-well plate followed by 2 µL of each sample and mixed with 200 µL Reagent B. The plate was incubated for 10 mins at RT on the shaker. Then, the concentrations of samples were quantified by Infinite M200 at 595 nm. A standard curve was produced by quantifying BSA samples of standard concentration (0.125, 0.25, 0.5, 1, 1.5, 2 mg/mL). After the addition of LDS sample buffer, the samples were boiled at 90°C for 10 mins and kept at -20°C until use.

3) Western blotting

Twenty microgram proteins were separated by 10-15% sodium dodecyl sulfate polyacrylamide electrophoresis (SDS-PAGE) gel and transferred onto 0.2 µm nitrocellulose membranes. Following blocking with 5% non-fat milk or BSA in tris buffered saline with 0.05% Tween 20 (TBST) for 1 hour at RT, the membranes were

incubated with primary antibodies at 4°C overnight. The next day, the membranes were incubated with secondary antibodies for 1 hour. Beta-ACTIN and GAPDH were used as loading controls. After washing with TBST for three times, the membranes were incubated visualized by the Pierce™ ECL Plus Western Blotting Substrate.

2.2.7 Enzyme-linked immunosorbent assay

Before treatment, cells were replaced with fresh culture medium, and supernatants were collected 48 hours after knocking down. All the samples and standards were assayed in triplicates. The assay was performed at RT.

1) Add 50 μL of Albumin Standard or sample per well. Gently tap the plate to thoroughly coat the wells. Break any bubbles that may have formed. Cover wells with a sealing tape and incubate for 2 hours. Start the timer after the last addition.
2) Wash five times with 200 μL of Wash Buffer manually. Invert the plate each time and decant the contents; hit 4-5 times on absorbent material to completely remove the liquid.
3) Add 50 μL of Biotinylated Albumin Antibody to each well and incubate for 1 hour.
4) Wash the microplate as described in step 2).
5) Add 50 μL of Streptavidin-Peroxidase Conjugate per well and incubate for 30 mins. Gently tap plate to thoroughly coat the wells. Break any bubbles that may have formed. Turn on the microplate reader and set up the program in advance.
6) Wash the microplate as described in step 2).
7) Add 50 μL of Chromogen Substrate per well and incubate in ambient light for 20 mins or until the optimal color density develops. Gently tap the plate to ensure thorough mixing and break the bubbles in the well with pipette tip.
8) Add 50 μL of Stop Solution to each well. The color will change from blue to yellow. Gently tap the plate to ensure thorough mixing and break the bubbles in the well with pipette tip.
9) Read the absorbance on a microplate reader at a wavelength of 450 nm, subtract readings at 570 nm from those at 450 nm to correct optical imperfections.

Analyze the data from triplicate measures for each sample. The concentrations were calculated according to the standard curve.

2.2.8 siRNA transfection

siRNA targeting the indicated genes (listed in Table 6) were transfected into cells using Lipofectamine RNAiMAX reagent. A non-targeting negative stealth siRNA was used as a negative control.

Day 1: Seeding the cells at a density of $2x10^5$ cells per well in 12-well plate with 1 mL corresponding growth medium.

Day 2: siRNA transfection using Lipofectamine RNAiMAX Kit

Step 1: Change the culture medium with fresh medium.

Step 2: Prepare RNA-lipid complexes

1) Dilute RNAiMAX reagent in Opti-MEM medium by adding 1.5 µL RNAiMAX into 75 µL Opti-MEM medium in tube A;
2) Dilute siRNA in Opti-MEM medium by adding 20 pmol siRNA into 75 µL Opti-MEM medium in tube B;
3) Add diluted siRNA to diluted RNAiMAX with a ratio of 1:1, then incubated the mixture for 5 mins at RT.

Step 3: Add RNA-lipid complexes to cells. RNA and whole cell protein were extracted 48 hours after transfection.

2.2.9 Plasmid transfection

Recombinant DNAs for transfection were listed in Table 7, using Lipofectamine 3000 reagent. An empty vector was used as a negative control.

Day 1: Seeding the cells at a density of $2x10^5$ cells per well in 12-well plate with 1 mL corresponding growth medium.

Day 2: Plasmid transfection using Lipofectamine 3000 Kit

Step 1: Change the culture medium with fresh medium.

Step 2: Prepare DNA-lipid complexes

1) Dilute DNA master mix in Opti-MEM medium by adding 1.25 µg DNA and 2.5 µL P3000 reagent into 62.5 µL Opti-MEM medium in tube A;
2) Dilute Lipofectamine 3000 reagent in Opti-MEM medium by adding 2.8 µL Lipofectamine 3000 into 62.5 µL Opti-MEM medium in tube B;
3) Add diluted DNA master mix to diluted Lipofectamine 3000 with a ratio of 1:1, then incubated the mixture for 5 mins at RT.

Step 3: Add DNA-liposome complexes to cells. RNA and whole cell protein were extracted 72 hours after transfection.

2.2.10 Glucose uptake assay

Cells were seeded in a 24-well plate and were cultured with medium without insulin 24 hours before treatment. Subsequently, the cells were incubated with TNF-α (1 nM) for 1 day at 37°C and 5% CO_2. Added insulin (1 µM) into the medium for 1 hour.

1) Remove medium and wash with 100 µL PBS twice;
2) Add 50 µL of the prepared 1mM 2DG per well, shake briefly, and incubate 10 minutes at RT;
3) Add 25 µL of Stop Buffer and shake briefly;
4) Add 25 µL of Neutralization Buffer and shake briefly;
5) Add 100 µL of 2DG6P Detection Reagent and shake briefly;

Note: Be sure to prepare 2DG6P Detection Reagent 1 hour before use to minimize assay background.

6) Incubate for 4 hours at RT;

Record luminescence using a 0.3–1 second integration on a luminometer.

2.2.11 RNA sequencing

Total RNA was extracted as described above. RNA quality was checked with the Agilent 2100 Bioanalyzer and the RNA 6000 Nano Kit (Agilent, Waldbronn). Samples with RNA integrity number (RIN) above 9.5 were used for RNA sequencing. The sequencing work was performed by BGI Tech Solutions Co. (Hong Kong, China).

2.2.12 Bioinformatic analyses of RNA sequencing

Most of the procedure was done with R and bioconductor using the NGS analysis package systempipeR [78]. Quality control of raw sequencing reads was performed using FastQC (Babraham Bioinformatics). Low-quality reads were removed using trim-galore (version 0.6.4). The resulting reads were aligned to human genome version GRCh38.p12 and mouse genome version GRCm38.p6 from Gene code and counted using Kallisto (version 0.46.1) [79]. The count data were transformed to log2-counts per million (logCPM) using the voom-function from the limma package [80]. Differential expression analysis was performed using the limma package in R. A false positive rate of α= 0.05 with FDR correction was taken as the level of significance. Volcano plots and heatmaps were created using the ggplot2 package (version 2.2.1) and the complex heatmap (version 2.0.0) [81].

2.2.13 Statistical analyses

Statistical analyses were performed using SPSS Statistics 23.0. Variables were summarized as mean ± standard deviation (SD). The unpaired Student's t-test was used to determine statistical significances between two groups. The number of technical and experimental replicates can be found in the figure legends for each experiment. *P* values less than 0.05 were considered significant and represented graphically as *, $P<0.05$; **, $P<0.01$; and ***, $P<0.001$.

3 RESULTS

Part I A hierarchical regulatory network guarantees albumin synthesis under pathophysiological challenges

3.1 Serum albumin concentrations in the patients with end-stage liver disease are more than 30 g/L

First, we compared serum albumin concentrations in 84 patients with hepatocellular carcinoma (HCC), 38 decompensated cirrhosis (DC), and 35 acute liver failure (ALF). The mean values of serum albumin concentrations in the three cohorts were 40.37 g/L, 30.82g/L and 30.55 g/L, respectively (**Figure 1A**). Although albumin levels in the patients with liver failure significantly lower than HCC patients, the average albumin concentrations in them were more than 30 g/L.

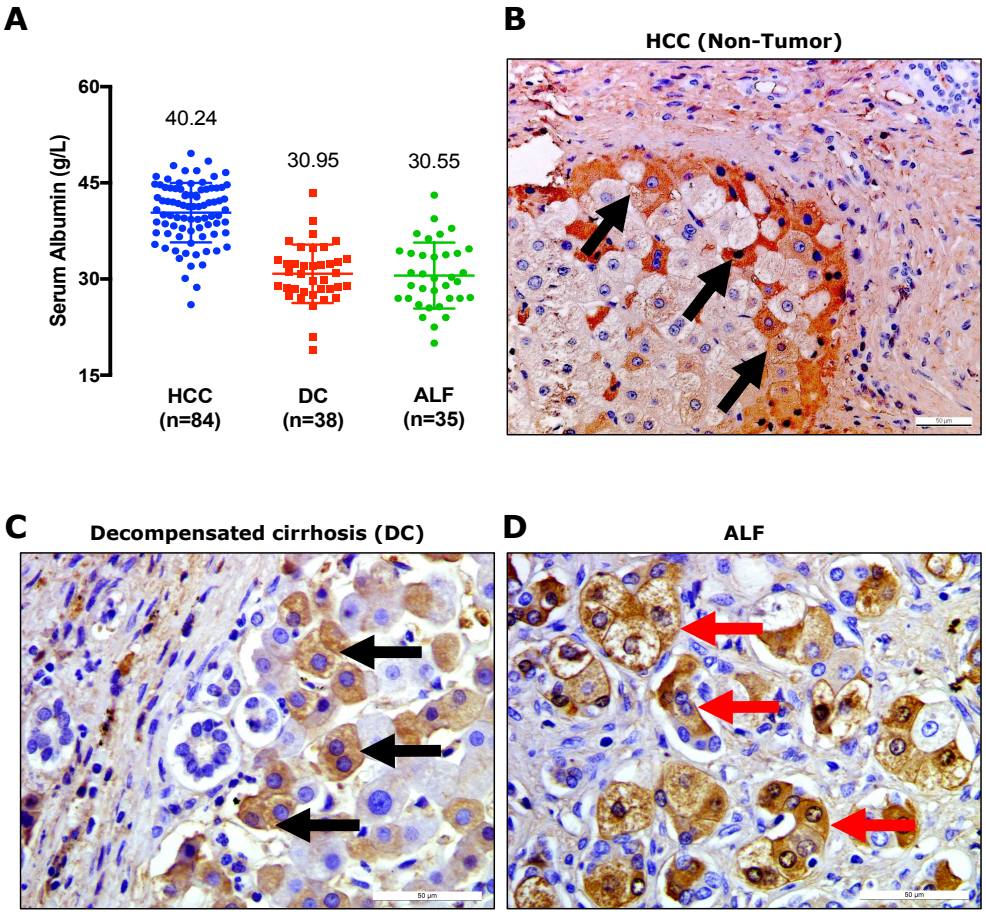

Figure 1. Serum albumin levels and hepatic albumin expression in patients with ESLD.

A. Serum albumin concentrations were measured in patients with ESLD. **B-D.** Immunohistochemistry shows albumin expression in 3 representative liver tissues with HCC, decompensated cirrhosis or ALF. Black and red arrows depict albumin expression in hepatocytes and liver progenitor cells, respectively. Original magnification: x40. Bars represent the mean ± SD.

Subsequently, we performed immunohistochemical staining (IHC) for albumin in the liver tissues from these patients. Albumin was expressed in all examined liver tissues (**Figure 1A**). In the liver tissues without massive hepatocyte loss, albumin was only expressed in hepatocytes (black arrows in **Figure 1B-C**), whereas in ALF patients with massive hepatocyte loss, liver progenitor cells (LPC) expressed albumin (red arrows in **Figure 1D**). These results imply that both hepatocytes and LPC synthesize albumin in different disease conditions.

3.2 The *ALB* core promoter possesses a TATA box and nucleosome-free area

Next, we analyzed the DNA sequence of the *ALB* gene core promoter. In both humans and mice, the *ALB* core promoter possesses a TATA box (**Figure 2A**). In a gene with TATA box, its core promoter is usually nucleosome free [82,83]. We confirmed the nucleosome-free area in the *ALB* core promoter by performing ChIP assays for histone H3 and H3.3 (**Figure 2B**). ChIP assays also showed that Pol II with phosphorylation on serine 5 (S5) and serine 2 (S2) of the heptapeptide repeats in the C-terminal domain (CTD) of the Rbp1 subunit bound to the *ALB* core promoter (**Figure 2B**), indicating transcription initiation and elongation of the *ALB* gene in normal hepatocytes.

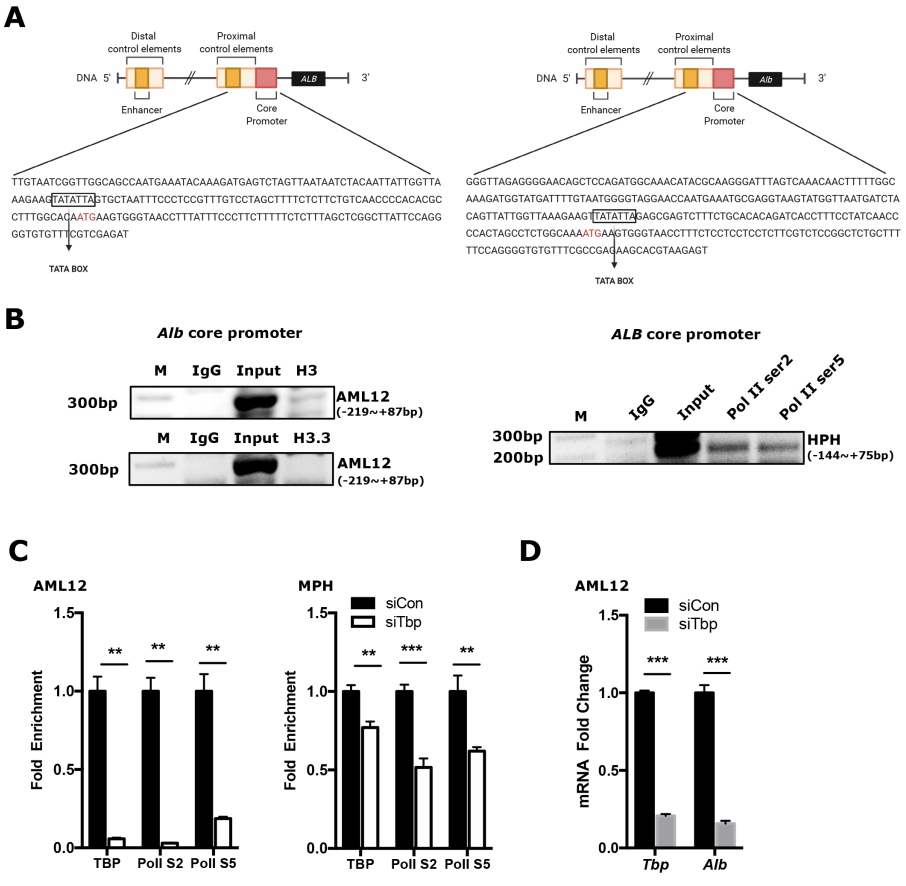

Figure 2. The *ALB* gene core promoter possesses a TATA box and nucleosome-free area.
A. A scheme depicts the *ALB* core promoter sequence and TATA box in human and mouse species. **B.** ChIP assays were performed to examine Histone 3 and Histone 3.3 binding to the *Alb* (-219~+87bp) core promoter in AML12 cells. ChIP assays measured Pol II S2 and Pol II S5 binding to the *ALB* (-144~+75bp) gene core promoter in HPH; **C.** ChIP-qPCR assays were performed to analyze TBP, Pol II S2 and Pol II S5 binding to the core promoter of *Alb* (-219~+87bp) gene in AML12 cells and MPH with or without Tbp siRNA treatment for 24 h. **D.** qPCR analyzed *Alb* mRNA expression in AML12 cells with or without Tbp siRNA treatment for 48 h. Data information: *P*-values were calculated by unpaired Student's t-test (C, D). Bars represent the mean ± SD, **, $P<0.01$; ***, $P<0.001$. Except the experiments performed in HPH, other experiments were repeated for three times.

To further clarify the role of the TATA box in the *ALB* transcription, we knocked down TATA box binding protein (TBP) by RNAi in both AML12 cells and mouse primary hepatocytes (MPH) (**Figure 2C-D**). ChIP assays and qPCR analyses showed that knockdown of TBP reduced S5-P and S2-P Pol II binding to the *Alb* core promoter (**Figure 2C**) and mRNA expression of albumin (**Figure 2D**) in hepatocytes.
These results suggest that presence of the TATA box and nucleosome-free promoter region in the *ALB* gene, provide an epigenetic structure in hepatocytes, which leads to constitutive albumin expression.

3.3 HNF4α and C/EBPα regulate albumin transcription in hepatocytes

Given that a sufficient transcription requires transcriptional activator(s) binding to the gene promoter, we assumed that constitutively albumin expression in hepatocytes requires constitutively expressed master transcription factor(s). Among the master hepatocyte transcription factors, HNF4α controls near half hepatocyte function genes, including albumin, given that HNF4α possesses binding sites on these genes' promoter [29]. In addition to HNF4α, DNA sequence analyses showed that C/EBPα also possesses binding sites on the *ALB* promoter. Own previous study shows that HNF4α and C/EBPα are required for each other in hepatocytes (unpublished data). In 10 controlled liver tissues collected from patients who received surgery due to bile duct stone, HNF4α and C/EBPα were constitutively expressed in hepatocytes (**Figure 3A**). Therefore, we hypothesized that HNF4α and C/EBPα are the major transcriptional activators for albumin transcription in normal hepatocytes.

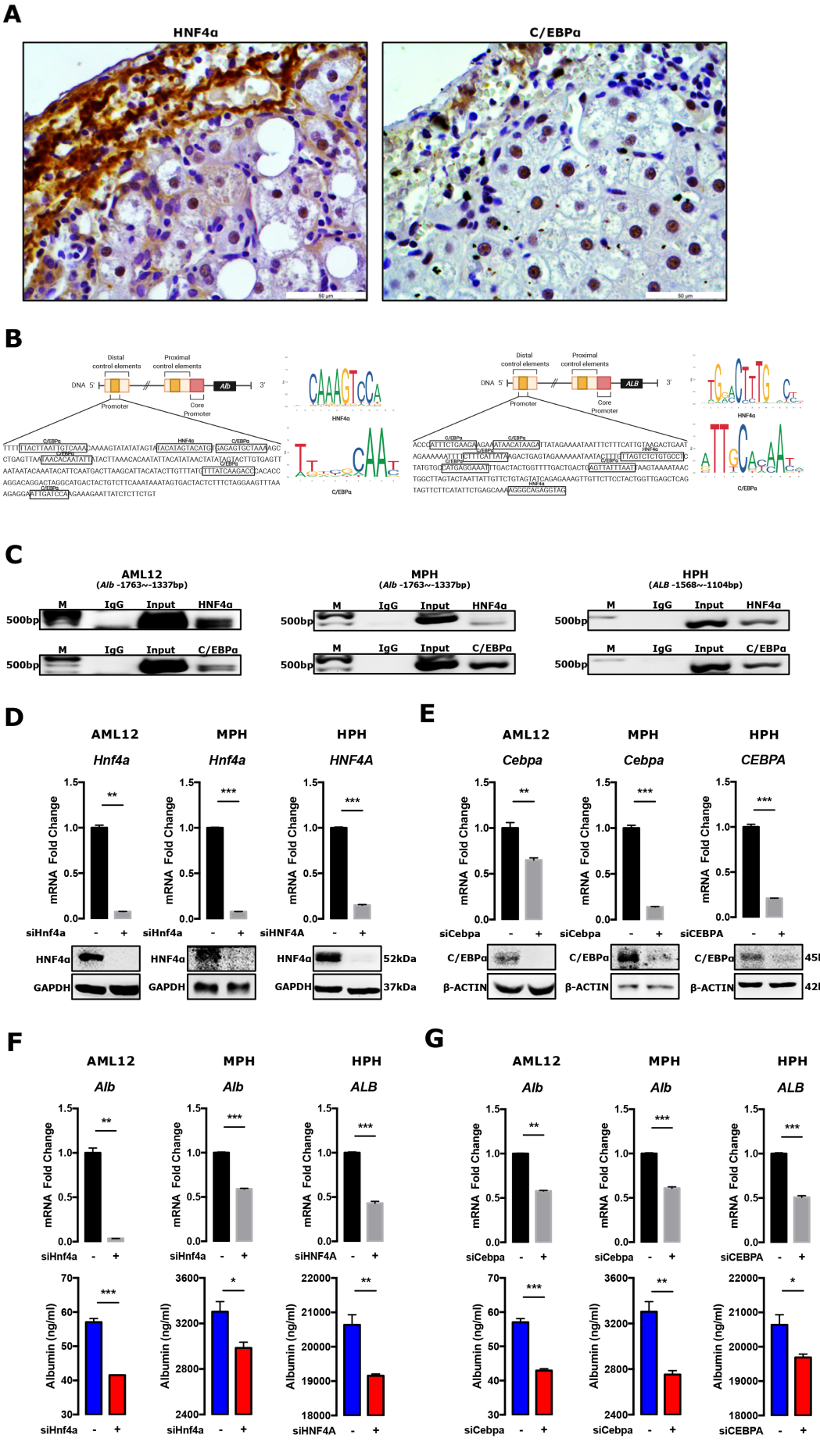
A
HNF4α
C/EBPα
B
Distal control elements
Proximal control elements
Promoter
Core Promoter
Alb
ALB
HNF4α
C/EBPα
C
AML12
(Alb -1763~-1337bp)
MPH
(Alb -1763~-1337bp)
HPH
(ALB -1568~-1104bp)
M
IgG
Input
HNF4α
C/EBPα
500bp
D
AML12
MPH
HPH
Hnf4a
Hnf4a
HNF4A
mRNA Fold Change
siHnf4a
siHNF4A
GAPDH
52kDa
37kDa
E
Cebpa
Cebpa
CEBPA
siCebpa
siCEBPA
β-ACTIN
45kDa
42kDa
F
Alb
Alb
ALB
Albumin (ng/ml)
G

Figure 3. HNF4α and C/EBPα regulate albumin transcription in hepatocytes.
A. Immunohistochemistry shows HNF4α and C/EBPα expression in a representative patient with chronic HBV infection. Original magnification: x40. **B.** In silico analysis shows the predictive binding sites of HNF4α and C/EBPα on the *ALB* promoter (human: -1568~-1104bp, mouse: -1763~-1337bp) [84]. **C.** ChIP assays were performed to examine HNF4α and C/EBPα binding to the *ALB* gene promoter (human: -1568~-1104bp, mouse: -1763~-1337bp) in AML12 cells, MPH and HPH. **D-E.** qPCR and western blotting show the knockdown efficiency of HNF4α (D) and C/EBPα (E) siRNA following 48 h transfection in AML12 cells, MPH and HPH for 48 h. **F-G.** qPCR and ELISA measured albumin expression in hepatocytes with or without HNF4A (F) or CEBPA (G) siRNA treatment for 48 h. Data information: *P*-values were calculated by unpaired Student's t-test (D-G). Bars represent the mean ± SD. *: $P<0.05$; **: $P<0.01$; ***: $P<0.001$. Except the experiments performed in HPH, other experiments were repeated for three times.

DNA sequencing analyses showed that there were binding sites of HNF4α and C/EBPα on the *ALB* promoter (**Figure 3B**). ChIP assays confirmed that both HNF4α and C/EBPα bound to the *ALB* distal promoter in AML12 cells, MPH and human primary hepatocytes (HPH) (**Figure 3C**). Subsequently, we efficiently knocked down HNF4α or C/EBPα expression by RNAi in the three hepatocytes (**Figure 3D-E**). qPCR and ELISA assays revealed that mRNA expression of albumin and the albumin concentrations in culture medium were significantly reduced when the cells were transfected by either HNF4α or C/EBPα siRNA for 48 h (**Figure 3F-G**). These results suggest that both HNF4α and C/EBPα are required for albumin expression in normal hepatocytes.

3.4 FOXA2 maintains albumin transcription in the hepatocytes lacking both HNF4α and C/EBPα expression

Hepatic HNF4α and C/EBPα expression is often inhibited by inflammation in severely damaged livers. However, albumin expression in hepatocytes is still robust (**Figure 1C**). To clarify the potential transcription factor(s) maintaining albumin transcription in the hepatocytes lacking HNF4α and C/EBPα, we performed RNA sequencing in MPH, in which both Hnf4a and Cebpa were knocked down by RNAi (**Figure 4A-B**).

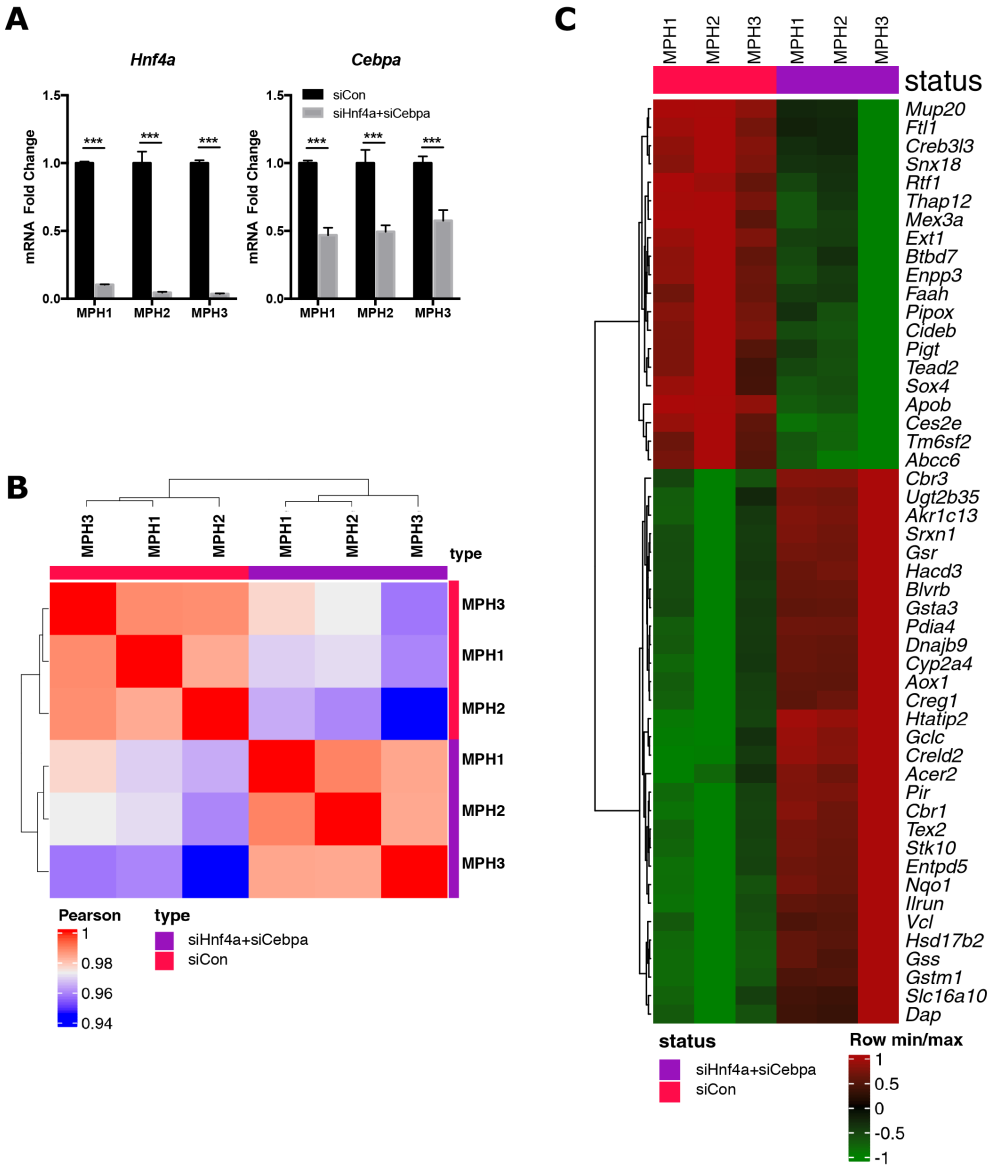

Figure 4. RNA-Sequencing in mouse primary hepatocytes with or without knock-down of Hnf4a and Cebpa.
Primary hepatocytes were freshly isolated from three mice: Mouse1 (MPH1), Mouse2 (MPH2), Mouse3 (MPH3). MPH was transfected by Hnf4a and Cebpa siRNA for 48 hours. The knockdown efficiency of siRNA is measured by qPCR (**A**). RNA extraction and sequencing were performed as described in Materials and Methods. The heatmap shows the clustering situation of the examined samples (**B**), and top altered 50 significant genes (**C**).

Knockdown of both Hnf4a and Cebpa reduced transcription factors such as Foxa3, Hnf6b, Hnf1a and Hnf6a, but did not affect Foxa2 (**Figure 4C, Figure 5A**). Pearson correlation analysis showed that Foxa2 transcription was not related to either Hnf4a or Cebpa expression (**Figure 5B**). qPCR confirmed that knockdown of Hnf4a or Cebpa in MPH and HPH, Foxa2 mRNA expression was not altered (**Figure 5C**).

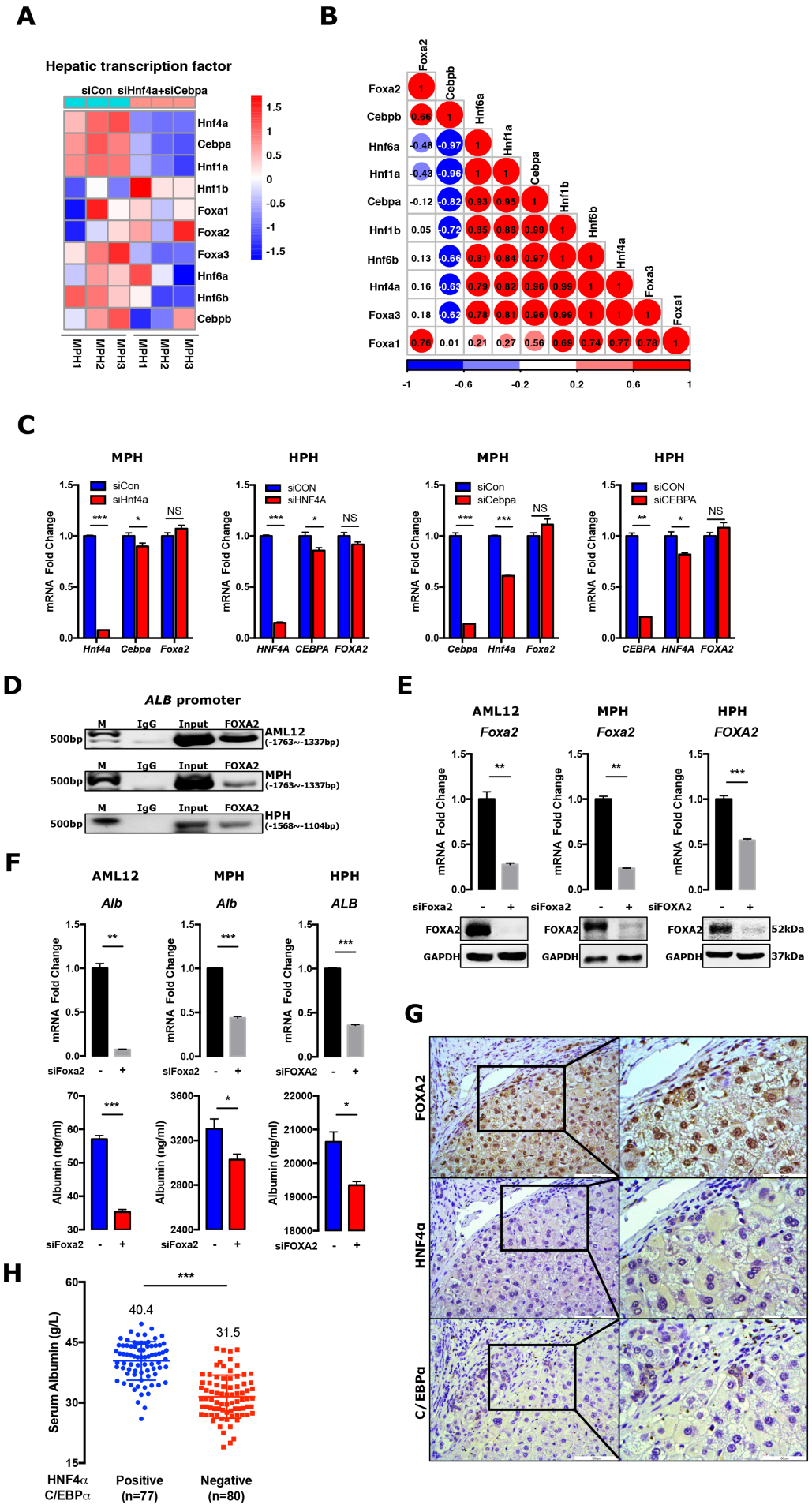
A
Hepatic transcription factor
siCon siHnf4a+siCebpa
Hnf4a
Cebpa
Hnf1a
Hnf1b
Foxa1
Foxa2
Foxa3
Hnf6a
Hnf6b
Cebpb
MPH1 MPH2 MPH3 MPH1 MPH2 MPH3
1.5 1 0.5 0 -0.5 -1 -1.5
B
Foxa2 Cebpb Hnf6a Hnf1a Cebpa Hnf1b Hnf6b Hnf4a Foxa3 Foxa1
-1 -0.6 -0.2 0.2 0.6 1
C
MPH
HPH
MPH
HPH
siCon
siHnf4a
siCON
siHNF4A
siCon
siCebpa
siCON
siCEBPA
mRNA Fold Change
Hnf4a Cebpa Foxa2
HNF4A CEBPA FOXA2
Cebpa Hnf4a Foxa2
CEBPA HNF4A FOXA2
NS
D
ALB promoter
M IgG Input FOXA2
500bp
AML12 (-1763~-1337bp)
MPH (-1763~-1337bp)
HPH (-1568~-1104bp)
E
AML12 Foxa2
MPH Foxa2
HPH FOXA2
mRNA Fold Change
siFoxa2 - +
siFOXA2 - +
FOXA2
GAPDH
52kDa
37kDa
F
AML12 Alb
MPH Alb
HPH ALB
mRNA Fold Change
Albumin (ng/ml)
siFoxa2 - +
siFOXA2 - +
G
FOXA2
HNF4α
C/EBPα
H
Serum Albumin (g/L)
40.4
31.5
HNF4α C/EBPα
Positive (n=77)
Negative (n=80)

Figure 5. FOXA2 maintains albumin transcription in the hepatocytes lacking HNF4α and C/EBPα.

A. A heatmap depicts hepatic transcription factors expression in MPH with Hnf4a and Cebpa knockdown by RNAi. **B.** Pearson's correlation analyzed the relationship between indicated hepatic transcription factors in MPH with Hnf4a and Cebpa siRNA treatment. Positive correlations are displayed in red and negative in blue. The color intensity and the size of the circle are proportional to the correlation coefficients. Pearson's correlation coefficient values were shown in the circles. **C.** qPCR analyzed the effects of HNF4α and C/EBPα disruption on FOXA2 expression in MPH and HPH. HNF4α and C/EBPα were knocked down by siRNA. **D.** ChIP assays examined FOXA2 binding to the promoter of *Alb*/*ALB* gene in AML12 cells, MPH (-1763~-1337bp), and HPH (-1568~-1104bp). **E-F.** qPCR and western blotting showed the knockdown efficiency of FOXA2 siRNA following 48 h transfection in AML12 cells, MPH and HPH. qPCR and ELISA (F) analyzed the effects of FOXA2 siRNA on albumin expression in three cells. **G.** IHC staining shows HNF4α, C/EBPα, and FOXA2 expression in a representative patient with decompensated cirrhosis using series sections. Original magnification: x20 and x40. **H.** Comparison of serum albumin concentrations in patients with or without HNF4α and C/EBPα expression. Data information: *P*-values were calculated by unpaired Student's t-test (C, E, F, H). Bars represent the mean ± SD. *: $P<0.05$; **: $P<0.01$; ***: $P<0.001$; and NS, no significance. Except the experiments performed in HPH, other experiments were repeated for three times.

ChIP assays further revealed that FOXA2 bound to the ALB promoter in AML12 cells, MPH and HPH (**Figure 5D**). Knockdown of FOXA2 significantly decreased mRNA and protein expression of FOXA2 in the three cells (**Figure 5E**). qPCR and ELISA assays showed that knockdown of FOXA2 by RNAi reduced albumin transcription in AML12 cells, MPH and HPH and protein secretion in culture medium (**Figure 5F**). Further, we performed serial sections to examine HNF4α, C/EBPα and FOXA2 expression by IHC in 11 patients with decompensated cirrhosis or ALF. All examined patients lacked both HNF4α and C/EBPα expression in hepatocytes, however, these cells were expressed FOXA2 (**Table 13, Figure 5G**).

Subsequently, we divided enrolled patients into two cohorts based on whether their hepatocytes expressed HNF4α and C/EBPα and compared their serum albumin concentrations. The mean serum albumin concentrations were 40.4 g/L and 31.5 g/L in the patients with or without both HNF4α and C/EBPα expression in hepatocytes, respectively ($P<0.001$, **Figure 5H**).

These results suggest a crucial role of FOXA2 in the maintenance of albumin transcription in hepatocytes losing both HNF4α and C/EBPα expression. However,

the capability of hepatocytes to synthesize albumin might be compromised in the absence of HNF4α and C/EBPα expression.

Table 13. IHC staining for HNF4α, C/EBPα, FOXA2 and GLI2 in 6 CLF and 5 ALF patients.

	Patient	HNF4α	C/EBPα	FOXA2	GLI2
CLF	1	-	-	+	+
	2	-	-	+	+
	3	-	-	+	+
	4	-	-	+	+
	5	-	-	+	+
	6	-	-	+	+
ALF	7	-	-	+	-
	8	-	-	+	+
	9	-	-	+	+
	10	-	-	+	+
	11	-	-	+	-

3.5 HNF4α and FOXA2 upregulate albumin transcription in liver progenitor cells in patients with massive hepatocyte loss

Acute liver failure is a severe consequence of massive hepatocyte necrosis [85]. In such a risky condition, remaining hepatocytes are not capable of maintaining hepatocyte functions, including producing albumin. We assume that patients exploit LPC to take over the function to produce albumin (see **Figure 1D**). To clarify the transcription factors regulating albumin transcription in LPC, we performed RNA sequencing to compare transcriptome between hepatocytes (HPH and AML12 cells) and LPC (HepaRG and BMOL cells). Hepatocytes and LPC demonstrated different gene transcriptome (**Figure 6**). Distinct from hepatocytes, C/EBPα expression is very low in LPC (**Figure 7A**). mRNA expression of HNF4α in LPC was at the similar level as in hepatocytes, while FOXA2 expression in LPC was higher than that in hepatocytes (**Figure 7A**). The results suggested that HNF4α and FOXA2 might play a crucial role in the regulation of albumin transcription in LPC.

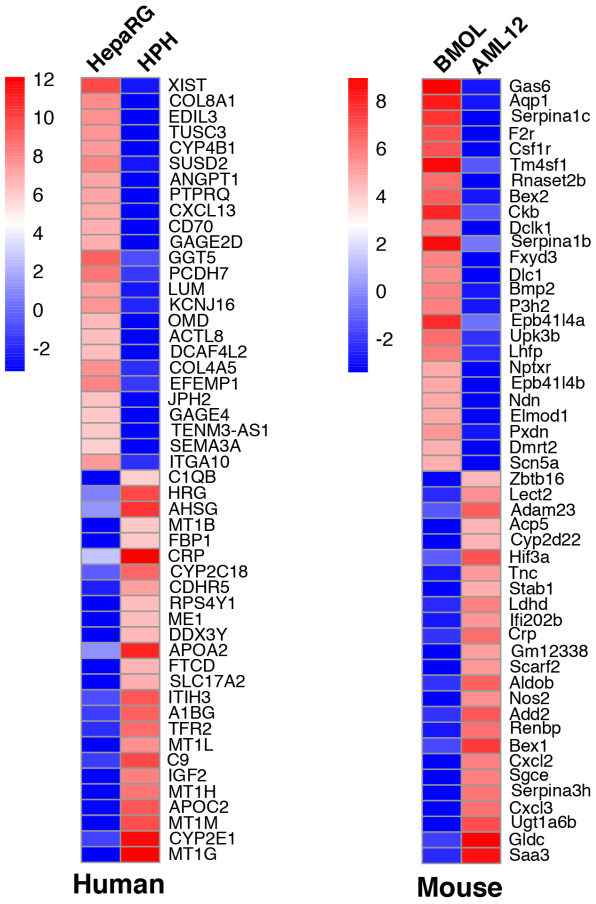

Figure 6. RNA-Sequencing in human and mouse hepatocytes and liver progenitor cells.
RNA extraction and sequencing were performed as described in Materials and Methods. The heatmap shows the top altered 50 differential genes between Hepatocytes (HPH and AML12) and LPC (HepaRG and BMOL).

ChIP assays confirmed that both HNF4α and FOXA2 bound to the *ALB* promoter in HepaRG and BMOL cells (**Figure 7B**). Subsequently, we efficiently knocked down HNF4α and FOXA2 by RNAi in BMOL and HepaRG cells, respectively (**Figure 7C-D**). qPCR and ELISA assays revealed that knockdown of either HNF4α or FOXA2 reduced albumin transcription in both cells and protein secretion in the culture medium (**Figure 7C, E**). We further performed serial section in liver tissues collected from 5 ALF patients who receiving liver transplantation. IHC analyzed confirmed that LPC in these patients expressed albumin. Impressively, the LPC in these patients expressed FOXA2, but not HNF4α.

These results suggest that HNF4α and FOXA2 are the two transcription factors that regulate the albumin gene transcription in LPC. In the ALF patients with poor clinical outcome, FOXA2 is the master transcription factor controlling albumin expression in LPC.

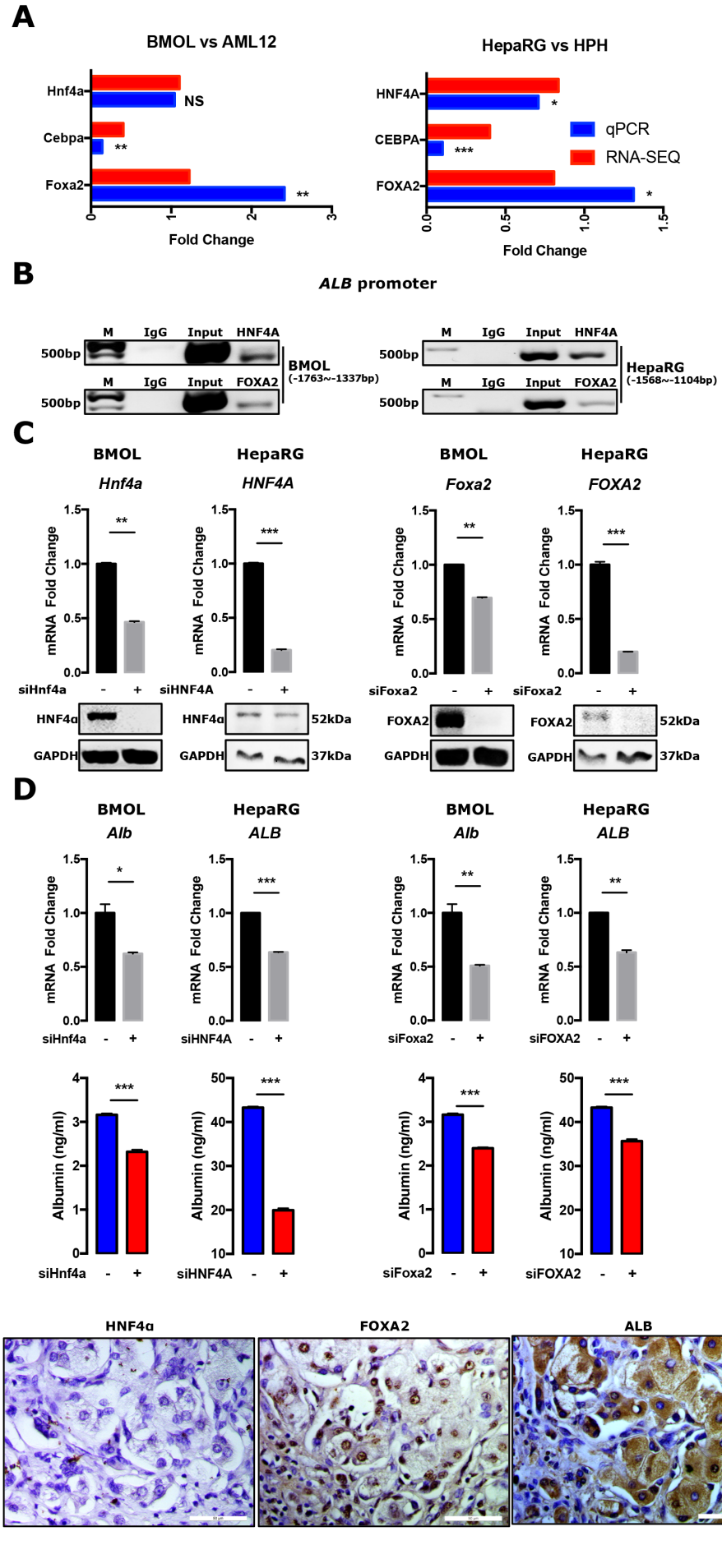
A
BMOL vs AML12
Hnf4a
NS
Cebpa
**
Foxa2
**
Fold Change
HepaRG vs HPH
HNF4A
*
CEBPA
***
FOXA2
*
qPCR
RNA-SEQ
Fold Change
B
ALB promoter
M IgG Input HNF4A
500bp
BMOL
(-1763~-1337bp)
M IgG Input FOXA2
500bp
M IgG Input HNF4A
500bp
HepaRG
(-1568~-1104bp)
M IgG Input FOXA2
500bp
C
BMOL
Hnf4a
HepaRG
HNF4A
BMOL
Foxa2
HepaRG
FOXA2
mRNA Fold Change
siHnf4a - +
siHNF4A - +
siFoxa2 - +
siFoxa2 - +
HNF4α
GAPDH
52kDa
37kDa
FOXA2
GAPDH
52kDa
37kDa
D
BMOL
Alb
HepaRG
ALB
BMOL
Alb
HepaRG
ALB
mRNA Fold Change
siHnf4a - +
siHNF4A - +
siFoxa2 - +
siFOXA2 - +
Albumin (ng/ml)
siHnf4a - +
siHNF4A - +
siFoxa2 - +
siFOXA2 - +
E
HNF4α
FOXA2
ALB

Figure 7. HNF4α and FOXA2 upregulate albumin transcription in liver progenitor cells in patients with massive hepatocyte loss.
A. Expression of HNF4A, CEBPA, and FOXA2 in liver progenitor cells and hepatocytes (BMOL vs. AML12, HepaRG vs. HPH) was analyzed by RNA sequencing and qPCR. The fold change from the qPCR was calculated using the 2-ΔΔCt method [77]. **B.** ChIP assays measured HNF4α and FOXA2 binding to the promoter of the *ALB* (-1568~-1104bp)/*Alb* (-1763~-1337bp) gene in HepaRG and BMOL cells. **C-D.** qPCR and western blotting (C) showed the knockdown efficiency of HNF4α and FOXA2 by RNAi in HepaRG and BMOL cells for 48 h. qPCR and ELISA (D) analyzed the effects on albumin expression in two cells, with or without HNF4α or FOXA2 siRNA treatment for 48 h. **E.** IHC staining shows HNF4α, FOXA2, and Albumin expression in liver progenitor cells of the representative patients with ALF using series sections. Original magnification: x40. Data information: *P*-values were calculated by unpaired Student's t-test (A, C, D). Bars represent the mean ± SD. *: *P*<0.05; **: *P*<0.01; ***: *P*<0.001; and NS, no significance. Except RNA sequencing, experiments were repeated for three times.

3.6 Hedgehog regulates FOXA2 expression in both hepatocytes and liver progenitor cells

To clarify the factors upregulating FOXA2 expression in hepatocytes losing HNF4α and C/EBPα expression, we scrutinized the transcriptome alteration in hepatocytes with HNF4α and C/EBPα knockdown by RNAi. RNA sequencing analysis showed that hepatocytes lacking both HNF4α and C/EBPα expression significantly increased hedgehog ligand biosynthesis (**Figure 8A**). Given that Gli2, a hedgehog canonical downstream transcription factor, possesses binding sites on the *Foxa2* promoter (**Figure 8B**), it reminds us that the hedgehog signaling might up-regulate FOXA2 expression in the hepatocytes losing HNF4α and C/EBPα expression. ChIP assay revealed that incubation of recombinant sonic hedgehog (SHH) protein for 24 hours induced GLI2 binding to the *Foxa2* promoter in hepatocytes (**Figure 8C**). qPCR analyses further showed that SHH or SAG treatment significantly increased Gli2 and Foxa2 mRNA expression in MPH and HepaRG (**Figure 8D**). Knockdown of Gli2 by RNAi inhibited FoxA2 mRNA expression in hepatocytes (**Figure 8E**). Subsequently, we examined GLI2 expression in 11 patients (6 decompensated cirrhosis and 5 ALF) expressing FOXA2 but lacking both HNF4α and C/EBPα. IHC based on series sections revealed that among 11 patients, 9 demonstrated robust GLI2 and FOXA2 expression in hepatocytes and LPC (**Table 13**, **Figure 8F**). Two patients with FOXA2 expression did not have detectable GLI2 expression (**Table 13**), indicating GLI2 is

not the only factor regulating FOXA2 transcription. These results suggest that hedgehog-GLI2 signaling contributes to the regulation of FOXA2 expression in hepatocytes and LPC lacking both HNF4α and C/EBPα.

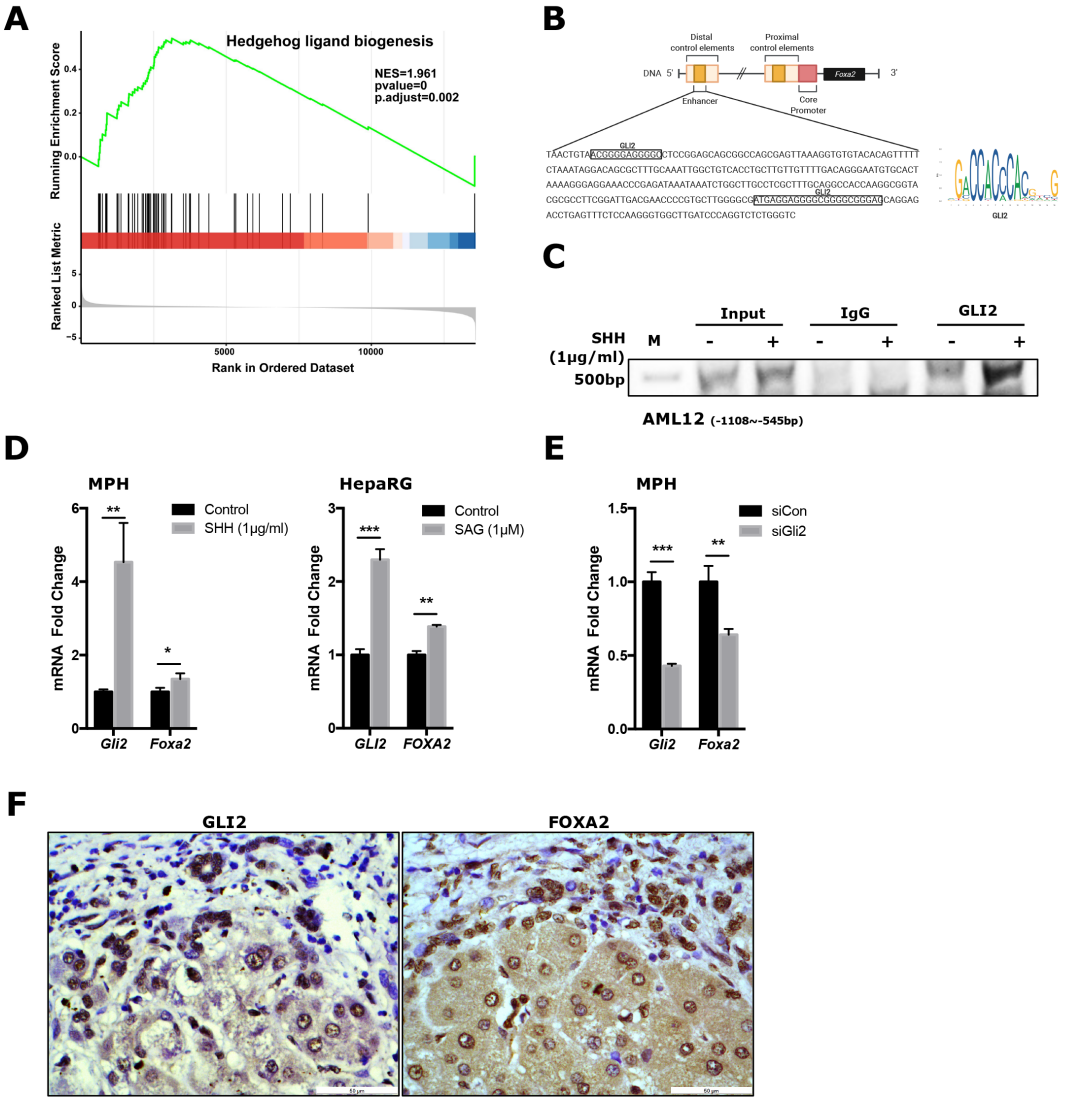

Figure 8. Hedgehog regulates FOXA2 expression in both hepatocytes and liver progenitor cells.

A. RNA sequencing was performed in mouse primary hepatocytes (MPH) with or without both Hnf4a and Cebpa siRNA treatment. GSEA reveals an upregulated gene set associated with hedgehog ligand biogenesis in MPH with both Hnf4a and Cebpa knockdown. **B.** In silico analysis shows the predictive binding sites of GLI2 on the *Foxa2* promoter [84]. **C.** ChIP assays were performed to examine the effect on GLI2 binding to the *Foxa2* promoter in AML12 cells with SHH (1 μg/mL) incubation for 24 h. **D.** qPCR analyzed the effects of SHH (1 μg/mL) or SAG (1 μM) on FOXA2 expression in MPH and HepaRG, respectively. Incubation time: 24 h. **E.** qPCR analyzed the effects of Gli2 on Foxa2 expression in MPH. The cells were transfected by Gli2 RNAi for 48 h. **F.** IHC staining shows GLI2 and FOXA2 expression in a representative patient with decompensated cirrhosis using series sections. Original

magnification: x40. Data information: *P*-values were calculated by unpaired Student's t-test (D, E). Bars represent the mean ± SD. *: *P*<0.05; **: *P*<0.01; ***: *P*<0.001. Except RNA sequencing, other experiments were repeated for three times.

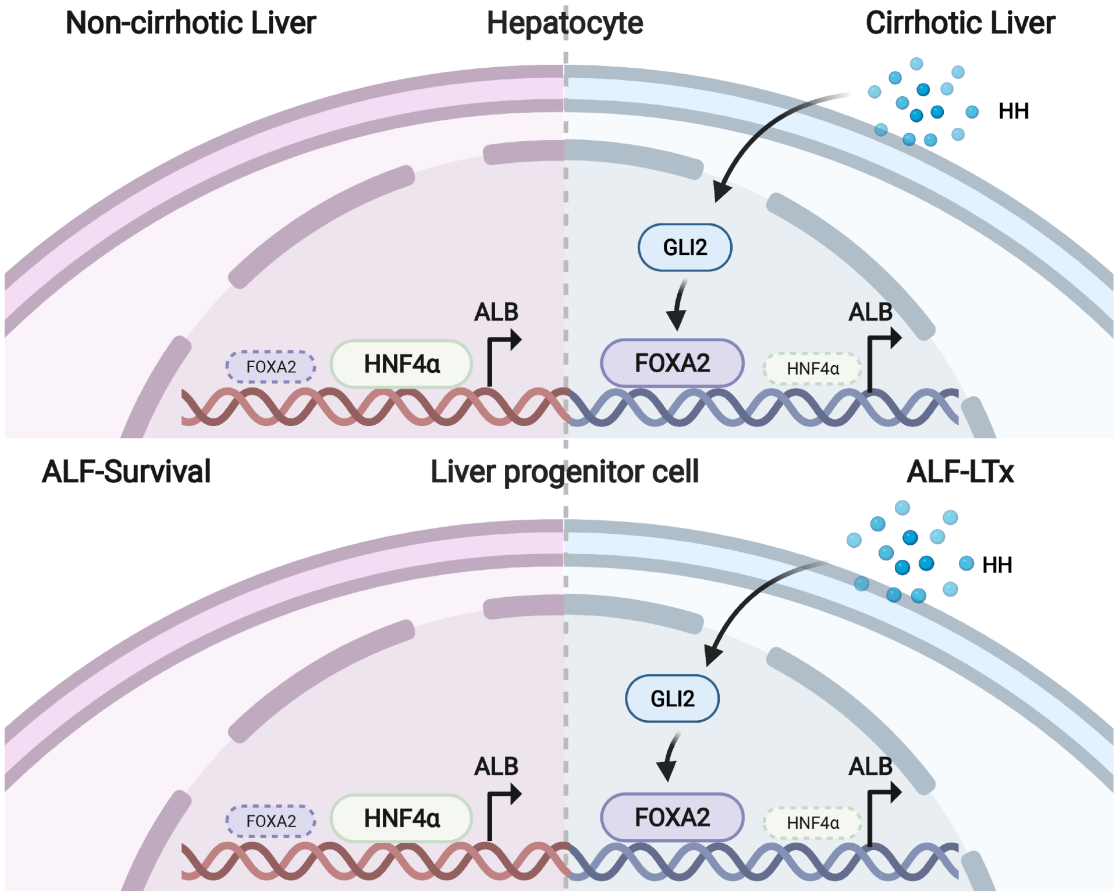

Figure 9. A scheme depicts the regulation of albumin expression in response to different pathophysiological challenges. Adapted from “Intracellular Comparison”, by BioRender.com (2020). Retrieved from https://app.biorender.com/biorender-templates.

Part II Insulin determines the impact of TGF-β on HNF4α transcription by maintaining C/EBPα expression

3.7 In normal hepatocytes, constitutive HNF4α expression requires TAF6/9 and H3K4me3

As a master lineage transcription factor, HNF4α is constitutively expressed in normal hepatocytes (**Figure 10A**). To clarify how hepatocytes constitutively express HNF4α, we first scrutinized the binding of RNA polymerase II (Pol II) to the core promoter of the *HNF4A* gene. In freshly isolated human primary hepatocytes (HPH) and mouse hepatocyte line AML12 cells, ChIP assays showed that the *HNF4A* core promoter was bound by Pol II with phosphorylation on serine 5 (S5) and serine 2 (S2) of the heptapeptide repeats in the C-terminal domain (CTD) of the Rbp1 subunit (**Figure 10B**), indicating transcription initiation and elongation of this gene. DNA sequence analysis revealed that the *HNF4A* core promoter does not possess a classical TATA box but has a downstream promoter element (DPE) (**Figure 10D**). ChIP assay shows that the *HNF4A* core promoter is bound by histone 3 (**Figure 10C**). Given that TFIID binding to the core promoter of genes without TATA box usually requires H3K4me3-marked nucleosomes[86], we examined H3K4me3 binding in the *HNF4A* core promoter. ChIP assay shows that the *HNF4A* core promoter did bind with H3K4me3-marked nucleosomes in HPH and AML12 cells (**Figure 10B**). Inhibition of H3K4me3 with the demethylase KDM5C significantly reduced mRNA expression of HNF4α in AML12 cells and mouse primary hepatocytes (MPH) (**Figure 10E-F**).

Given that the DPE motif is bound by TAF6 or TAF9 subunit of TFIID [87], we knocked down TAF6 and TAF9 by RNAi in AML12 cells and MPH (**Figure 10G** and **Figure 10H**). qPCR assay showed that mRNA expression of HNF4α was significantly reduced when TAF6 or TAF9 were knocked down (**Figure 10G** and **Figure 10H**). ChIP assays further revealed that knockdown of TAF6 or TAF9 decreased both S5-P and S2-P Pol II binding to the *HNF4A* core promoter (**Figure 10I** and **Figure 10J**), mediating the effect of TAF9 and TAF6 on *HNF4A* transcription.

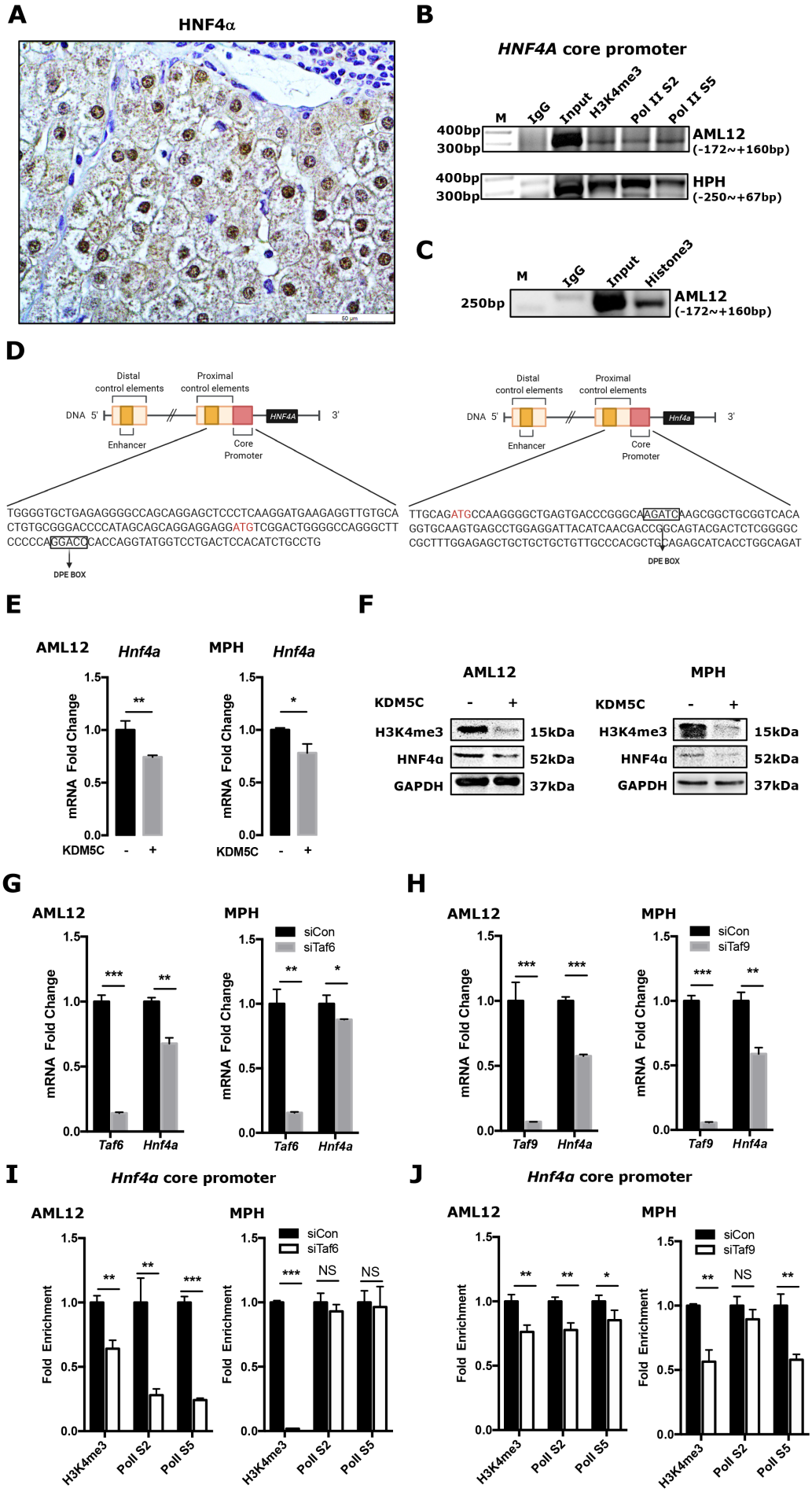
A
HNF4α
B
HNF4A core promoter
M
IgG
Input
H3K4me3
Pol II S2
Pol II S5
400bp
300bp
AML12
(-172~+160bp)
HPH
(-250~+67bp)
C
M
IgG
Input
Histone3
250bp
AML12
(-172~+160bp)
D
Distal control elements
Proximal control elements
DNA 5'
HNF4A
3'
Enhancer
Core Promoter
TGGGGTGCTGAGAGGGGCCAGCAGGAGCTCCCTCAAGGATGAAGAGGTTGTGCA
CTGTGCGGGACCCCATAGCAGCAGGAGGAGGATGTCGGACTGGGGCCAGGGCTT
CCCCCAGGACCCACCAGGTATGGTCCTGACTCCACATCTGCCTG
DPE BOX
Hnf4a
TTGCAGATGCCAAGGGGCTGAGTGACCCGGGCAAGATCAAGCGGCTGCGGTCACA
GGTGCAAGTGAGCCTGGAGGATTACATCAACGACCGGCAGTACGACTCTCGGGGC
CGCTTTGGAGAGCTGCTGCTGCTGTTGCCCACGCTGCAGAGCATCACCTGGCAGAT
DPE BOX
E
AML12
Hnf4a
MPH
Hnf4a
mRNA Fold Change
KDM5C
F
AML12
MPH
KDM5C
H3K4me3
HNF4α
GAPDH
15kDa
52kDa
37kDa
G
AML12
MPH
siCon
siTaf6
mRNA Fold Change
Taf6
Hnf4a
H
AML12
MPH
siCon
siTaf9
mRNA Fold Change
Taf9
Hnf4a
I
Hnf4α core promoter
AML12
MPH
siCon
siTaf6
Fold Enrichment
NS
H3K4me3
PolII S2
PolII S5
J
Hnf4α core promoter
AML12
MPH
siCon
siTaf9
Fold Enrichment
NS
H3K4me3
PolII S2
PolII S5

Figure 10. Constitutive HNF4α expression in hepatocytes requires TAF6, TAF9 and H3K4me3.

A. Immunohistochemical staining shows HNF4α expression in normal liver tissue. Original magnification: x40. **B.** ChIP assays were performed to examine H3K4me3, Pol II S2 and Pol II S5 binding to the core promoter of the *Hnf4a* (-172~+160bp) and the *HNF4A* (-250~+67bp) gene in AML12 cells and human HPH. **C.** ChIP assays measured Histone 3 binding to the core promoter of the *Hnf4a* (-172~+160bp) gene in AML12 cells. **D.** A scheme depicts the *HNF4A* core promoter sequence and DPE box in human and mouse species. **E-F.** Realtime qPCR (**E**) and Western blotting (**F**) were performed to analyze HNF4α expression in AML12 cells and MPH with or without KDM5C treatment for 24 hours. **G-H.** Realtime qPCR analyzed HNF4α mRNA expression in AML12 cells and MPH with or without Taf6 (**G**) or Taf9 (**H**) siRNA treatment for 24 h. **I-J.** ChIP-qPCR assays were performed to analyze H3K4me3, Pol II S2 and Pol II S5 binding to the core promoter of the *Hnf4a* (-172~+160bp) gene in AML12 cells and MPH with or without Taf6 (**I**) or Taf9 (**J**) siRNA treatment for 24 hours. Data information: *P*-values were calculated by unpaired Student's t-test (E, G, H, I, and J). Bars represent the mean ± SD, *, $P<0.05$; **, $P<0.01$; ***, $P<0.001$; and NS, No significance. Triple experiments were performed for A, B, C, and F and one representative result is shown.

3.8 Constitutive HNF4α transcription requires transcription factors SMADs and C/EBPα binding to the distal promoter

Core promoters only initiate low levels of transcription, while sufficient RNA transcription requires distal promoter activation by transcription activators [88]. To clarify the transcriptional activators that bind to the *Hnf4a* distal promoter, we analyzed the *Hnf4a* gene regulatory sequences. Transcription regulators SMADs and C/EBPα possess binding sites in the *Hnf4a* distal promoter (**Figure 11A**). ChIP assays confirmed that SMAD2, SMAD3 and C/EBPα bound to the *Hnf4a* distal promoter at 1172 – 1750 bp upstream from the transcription start site (TSS) in both AML12 cells and MPH (**Figure 11B**). Knockdown of SMAD2, SMAD3 and C/EBPα by RNAi not only reduced SMAD2, SMAD3 and C/EBPα binding to the *Hnf4a* distal promoter (**Figure 11C**), but also inhibited RNA polymerase II binding to the *Hnf4a* core promoter (**Figure 11D**) and mRNA and protein expression of HNF4α in hepatocytes (**Figure 11E-F**). Ectopic expression of C/EBPα robustly increased mRNA and protein expression of HNF4α in hepatocytes (**Figure 11E-F**).

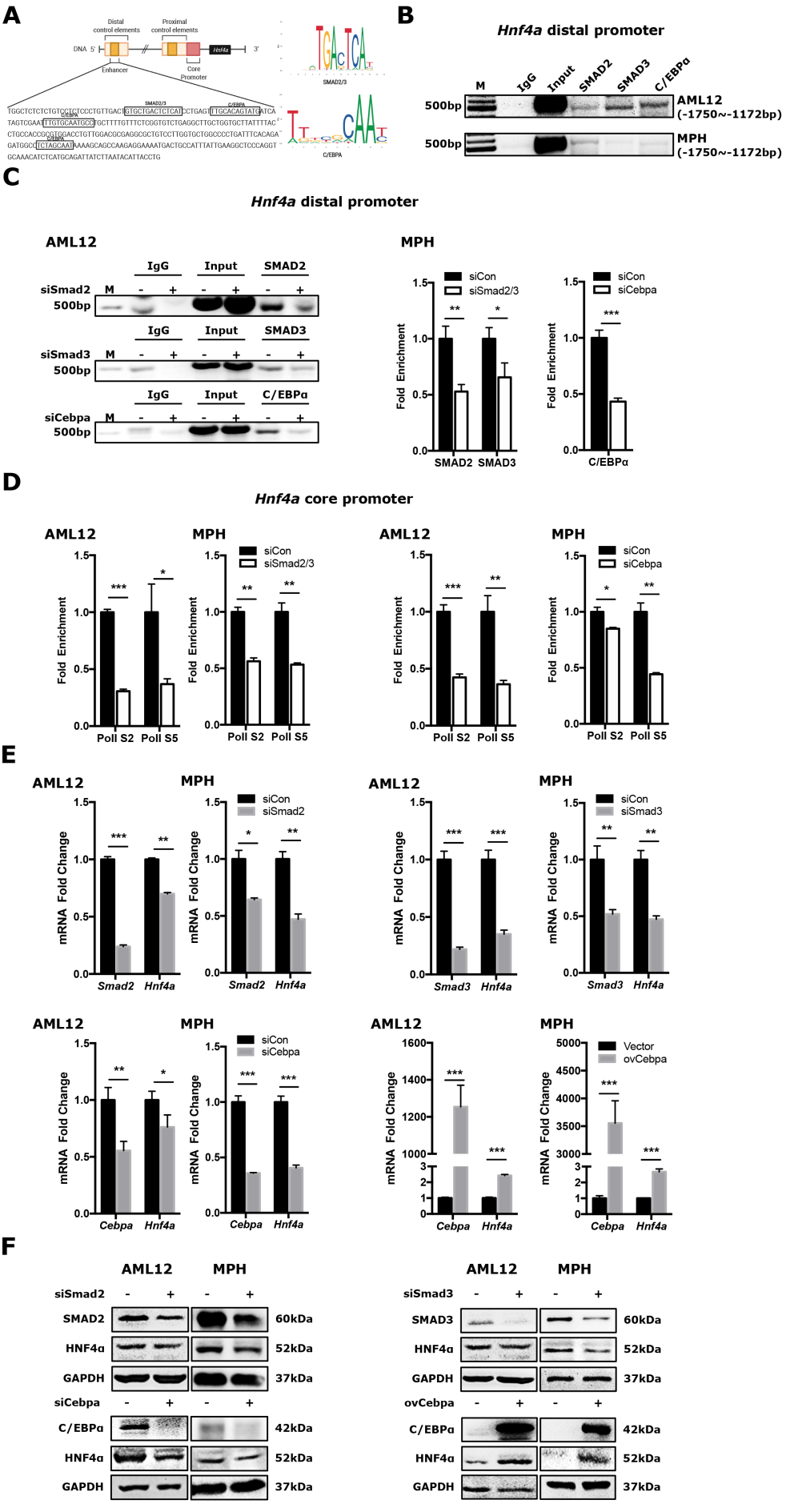
A
Distal control elements
Proximal control elements
DNA 5'
Hnf4a
3'
Enhancer
Core Promoter
SMAD2/3
C/EBPA
C/EBPA
B
Hnf4a distal promoter
M
IgG
Input
SMAD2
SMAD3
C/EBPα
500bp
AML12 (-1750~-1172bp)
MPH (-1750~-1172bp)
C
Hnf4a distal promoter
AML12
MPH
siSmad2
siSmad3
siCebpa
siCon
siSmad2/3
siCebpa
Fold Enrichment
SMAD2 SMAD3
C/EBPα
D
Hnf4a core promoter
PolI S2
PolI S5
E
mRNA Fold Change
Smad2
Smad3
Cebpa
Hnf4a
siSmad2
siSmad3
Vector
ovCebpa
F
siSmad2
siSmad3
siCebpa
ovCebpa
SMAD2
SMAD3
HNF4α
GAPDH
C/EBPα
60kDa
52kDa
37kDa
42kDa

Figure 11. Constitutive HNF4α transcription requires transcription factors SMADs and C/EBPα binding to the distal promoter.
A. The potential binding sites of SMAD2/3 and C/EBPα on the *Hnf4a* distal promoter (-1750~-1172bp) were predicted by Jaspar dataset [84]. **B.** ChIP assays were performed to examine SMAD2, SMAD3, and C/EBPα binding to the distal promoter of the *Hnf4a* (-1172~-1750bp) gene in AML12 cells and MPH. **C.** ChIP assays measured SMAD2, SMAD3, and C/EBPα binding to the distal promoter of the *Hnf4a* (-1172~-1750bp) in AML12 cells and MPH with or without Smad2/3 or Cebpa siRNA treatment for 24 hours. **D.** ChIP-qPCR analyzed Pol II S2 and Pol II S5 binding to the core promoter of the *Hnf4a* (-172~+160bp) in AML12 cells and MPH with or without Smad2/3 or Cebpa siRNA treatment for 24 hours. **E-F.** Realtime qPCR (**E**) and Western blotting (**F**) analyzed the effects of SMAD2/3 and C/EBPα on HNF4α expression in AML12 cells and MPH with or without Smad2/3 or Cebpa siRNA treatment for 24 hours, or Cebpa construct transfection for 48 hours. Data information: *P* values were calculated by unpaired Student's t-test (C, D, and E). Bars represent the mean ± SD, *, $P<0.05$; **, $P<0.01$, and ***, $P<0.001$. Triple experiments were performed for B, C, and F and one representative result is shown.

3.9 C/EBPα binding to the *HNF4A* distal promoter requires SMAD2/3, whereas SMAD2/3 binding to the *HNF4A* distal promoter is C/EBPα independent

Notably, knockdown of SMAD2/3 resulted in reduced binding of C/EBPα to the *Hnf4a* distal promoter in both AML12 cells and MPH (**Figure 12A**). On the other hand, SMAD2 and SMAD3 binding to the *Hnf4a* distal promoter was not altered when C/EBPα was knocked down (**Figure 12A**). qPCR and Western blotting analyses showed that forced overexpression of C/EBPα was not capable of restoring mRNA and protein expression of HNF4α when SMAD2/3 were reduced (**Figure 12B-C**). These results suggest that C/EBPα binding to the *HNF4A* distal promoter requires SMAD2/3, whereas SMAD2/3 binding to the *HNF4A* distal promoter is C/EBPα independent.

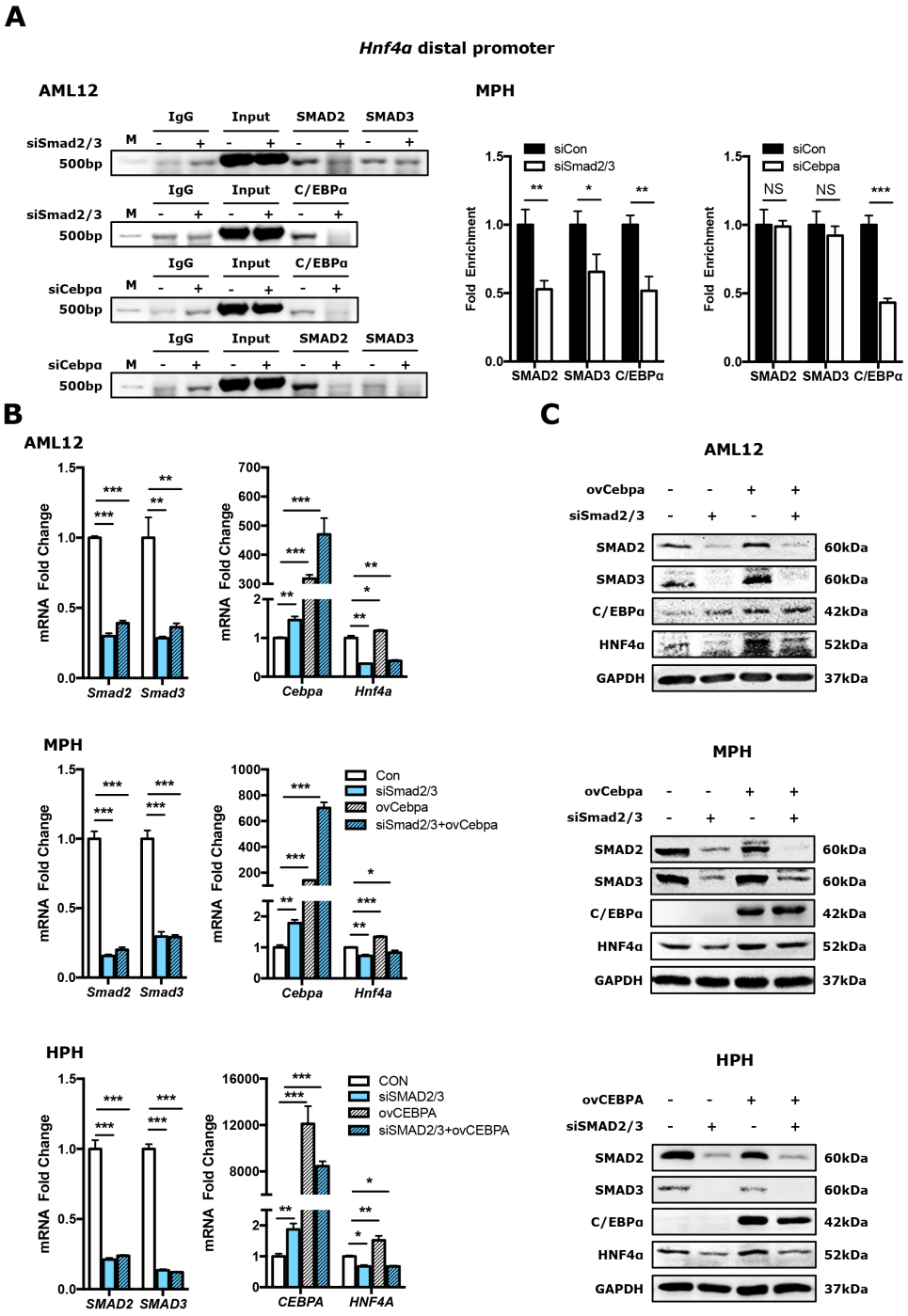

Figure 12. C/EBPα binding to the *HNF4A* distal promoter requires SMAD2/3, whereas SMAD2/3 binding to the *HNF4A* distal promoter is C/EBPα independent.

A. ChIP assays examined SMAD2, SMAD3, and C/EBPα binding to the *Hnf4a* distal promoter (-1750~-1172bp) in AML12 cells and MPH with or without Smad2/3 or Cebpa siRNA treatment for 24 hours. **B-C.** Realtime qPCR (**B**) and Western blotting (**C**) analyzed HNF4α expression in AML12, MPH and HPH with or without Smad2/3 siRNA treatment for 24 hours, followed by Cebpa construct transfection for 48 hours. Data information: *P*-values were calculated by unpaired Student's t-test (A-B). Bars represent the mean ± SD. *: *P*<0.05; **: *P*<0.01; ***: *P*<0.001; and NS, no significance. Triple experiments were performed for A and C and one representative result is shown.

3.10 Mediator complex is required for sufficient HNF4α transcription

To sufficiently initiate gene transcription, the Mediator protein complex linking transcriptional activator bound enhancer to general transcription factors is required for a large portion of genes [88]. We examined the effects of Mediator14 and CDK8, two components of the Mediator complex, on basal *HNF4A* transcription. In AML12 cells and MPH, knockdown of Mediator14 reduced mRNA and protein expression of HNF4α (**Figure 13A, C**), but did not alter the expression of C/EBPα (**Figure 13B**). Furthermore, knocking down Mediator14 reduced both S5-P Pol II and S2-P Pol II binding to the *Hnf4a* core promoter, as well as SMAD2/3 and C/EBPα binding to the *Hnf4a* distal promoter (**Figure 13D**). Like Mediator14, knocking down CDK8 by RNAi significantly reduced mRNA expression of HNF4α in AML12 cells and MPH (**Figure 13E**). CDK8 reduction did not alter C/EBPα mRNA expression in MPH but decreased C/EBPα mRNA expression in AML12 cells (**Figure 13F**). These results suggest that the Mediator complex is required for sufficient *HNF4A* transcription.

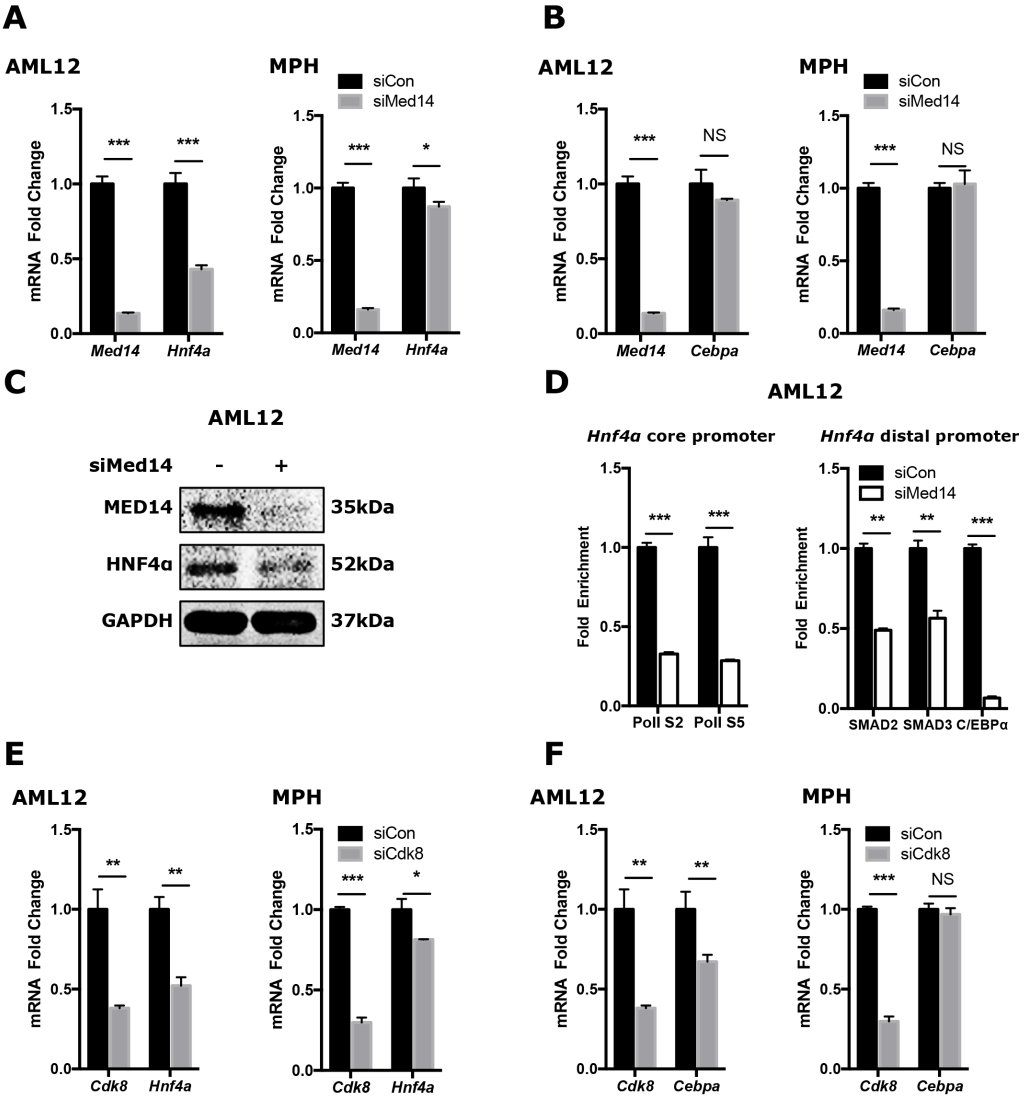

Figure 13. Mediator complex is required for sufficient *HNF4A* transcription.
A-B. Realtime qPCR analyzed the effect of Med14 on *Hnf4a* (**A**) and *Cebpa* (**B**) expression in AML12 cells and MPH. The cells were transfected by Med14 siRNA for 24 hours before measurement. **C.** Western blotting examined the effect of Med14 on *Hnf4a* expression in AML12 cells. The cells were transfected by Med14 siRNA for 48 hours before measurement. **D.** ChIP-qPCR assays examined Pol II S2 and Pol II S5 binding to the core promoter of the *Hnf4a* (-172~+160bp) gene, and SMAD2, SMAD3, and C/EBPα binding to the distal promoter of the *Hnf4a* (-1750~-1172bp) gene in AML12 cells with or without Med14 siRNA transfection for 24 hours. **E-F.** Realtime qPCR analyzed the effect Cdk8 on *Hnf4a* (**E**) and *Cebpa* (**F**) expression in AML12 cells and MPH transfected with Cdk8 or mock for 24 hours. Data information: *P*-values were calculated by unpaired Student's t-test (A, E, and F). Bars represent the mean ± SD. *: $P<0.05$; **: $P<0.01$; ***: $P<0.001$; and NS, no significance. Triple experiments were performed for C and one representative experiment is shown.

3.11 TGF-β reduces HNF4α transcription through inhibiting C/EBPα expression

SMAD proteins are canonical downstream transcription factors of TGF-β signaling [61]. The current finding that SMAD2/3 is required for HNF4α transcription seems to conflict with a commonly recognized notion, i.e., that TGF-β inhibits HNF4α expression in hepatocytes and thus drives epithelial-to-mesenchymal transition (EMT) [59]. To clarify the relationship between TGF-β, SMADs and HNF4α in hepatocytes, we initially performed qPCR to examine HNF4α mRNA expression in hepatocytes, which were treated with TGF-β for different times. Incubation with TGF-β for 2h and 6h significantly induced mRNA expression of HNF4α in MPH and AML12 cells (**Figure 14A**). However, TGF-β treatment for 24h inhibited HNF4α mRNA expression (**Figure 14A**). Western blotting showed that TGF-β-induced p-SMAD2 was expressed at high levels in all detected time points (**Figure 14B**). In AML12 cells and MPH, ChIP assays revealed that S5-P Pol II, S2-P Pol II and H3K4me3 binding to the *Hnf4a* core promoter were significantly increased after 2h TGF-β incubation but were remarkably reduced after 24h TGF-β administration (**Figure 14C**). Furthermore, TGF-β incubation for 2h increased SMAD2, SMAD3 and C/EBPα binding to the *Hnf4a* distal promoter, whereas TGF-β incubation for 24h remarkable inhibited C/EBPα binding to the *Hnf4a* distal promoter, although SMAD2 and SMAD3 binding to the distal promoter were significantly increased at this time point (**Figure 14D**). Impressively, ectopic C/EBPα expression restored TGF-β-inhibited *HNF4A* expression in MPH and

HPH (**Figure 14E-F**). These results strongly suggest that TGF-β might inhibit HNF4α transcription through influencing C/EBPα binding to the *HNF4A* distal promoter.

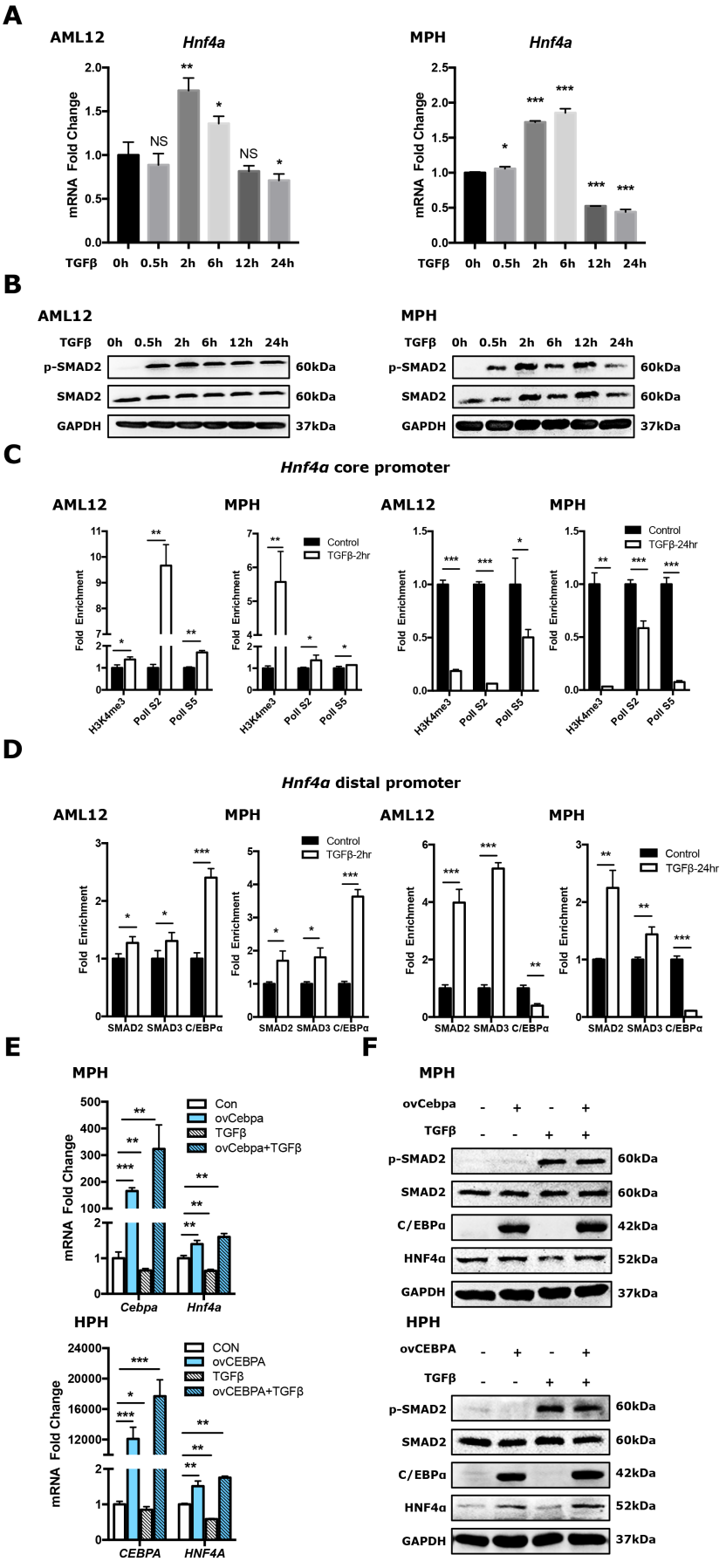

Figure 14. TGF-β reduces *HNF4A* transcription through inhibiting C/EBPα binding to the *HNF4A* distal promoter.

A. Realtime qPCR analyzed the effect of dynamic TGF-β (5 ng/mL) treatment on *Hnf4a* mRNA expression in AML12 cells and MPH. **B.** Western blotting examined p-SMAD2 expression in AML12 cells and MPH incubated with TGF-β (5 ng/ml) for different time as indicated. **C.** ChIP-qPCR assays were performed to examine H3K4me3, Pol II S2 and Pol II S5 binding to the core promoter of the *Hnf4a* (-172~+160bp) gene in AML12 cells and MPH. The cells were incubated with TGF-β (5 ng/mL) for 2 or 24 hours. **D.** ChIP-qPCR analyzed SMAD2, SMAD3, and C/EBPα binding to the *Hnf4a* distal promoter (-1750~-1172bp) in AML12 cells and MPH. The cells were incubated with TGF-β (5 ng/mL) for 2 or 24 hours. **E-F.** Realtime PCR (**E**) and Western blotting (**F**) analyzed the effect of TGF-β on *HNF4A* mRNA expression in MPH and HPH. The cells were transfected by CEBPA construct for 48 hours. Subsequently, incubate the cells with TGF-β (5 ng/ml) for 24 hours. Data information: *P*-values were calculated by unpaired Student's t-test (A, C, D, and E). Bars represent the mean ± SD, *, $P<0.05$; **, $P<0.01$, and ***, $P<0.001$. Triple experiments were performed for B and F and one representative result is shown.

3.12 TGF-β inhibits C/EBPα expression through SMAD binding to its distal promoter.

To clarify how TGF-β interferes with C/EBPα expression, we performed qPCR and Western blotting to examine the effects of TGF-β on C/EBPα expression in hepatocytes. Although C/EBPα mRNA expression was temporarily increased following administration of TGF-β, C/EBPα expression was subsequently inhibited following 6h of TGF-β treatment in MPH and AML12 cells (**Figure 15A-B**). DNA sequence analysis revealed that the *C/EBPA* distal promoter possesses SMAD2 and SMAD3 binding sites (**Figure 15C**), which were confirmed by ChIP assays in HPH and AML12 cells (**Figure 15D**). TGF-β treatment for 2h reduced SMAD binding but treatment for 24h further increased SMAD protein binding to the *C/EBPA* distal promoter in AML12 cells (**Figure 15E**). Knockdown of SMAD2 or SMAD3 increased mRNA and protein expression of C/EBPα in hepatocytes (**Figure 15F-G**). These results suggest that TGF-β inhibits C/EBPα transcription through driving SMAD2/3 binding to the *C/EBPA* distal promoter.

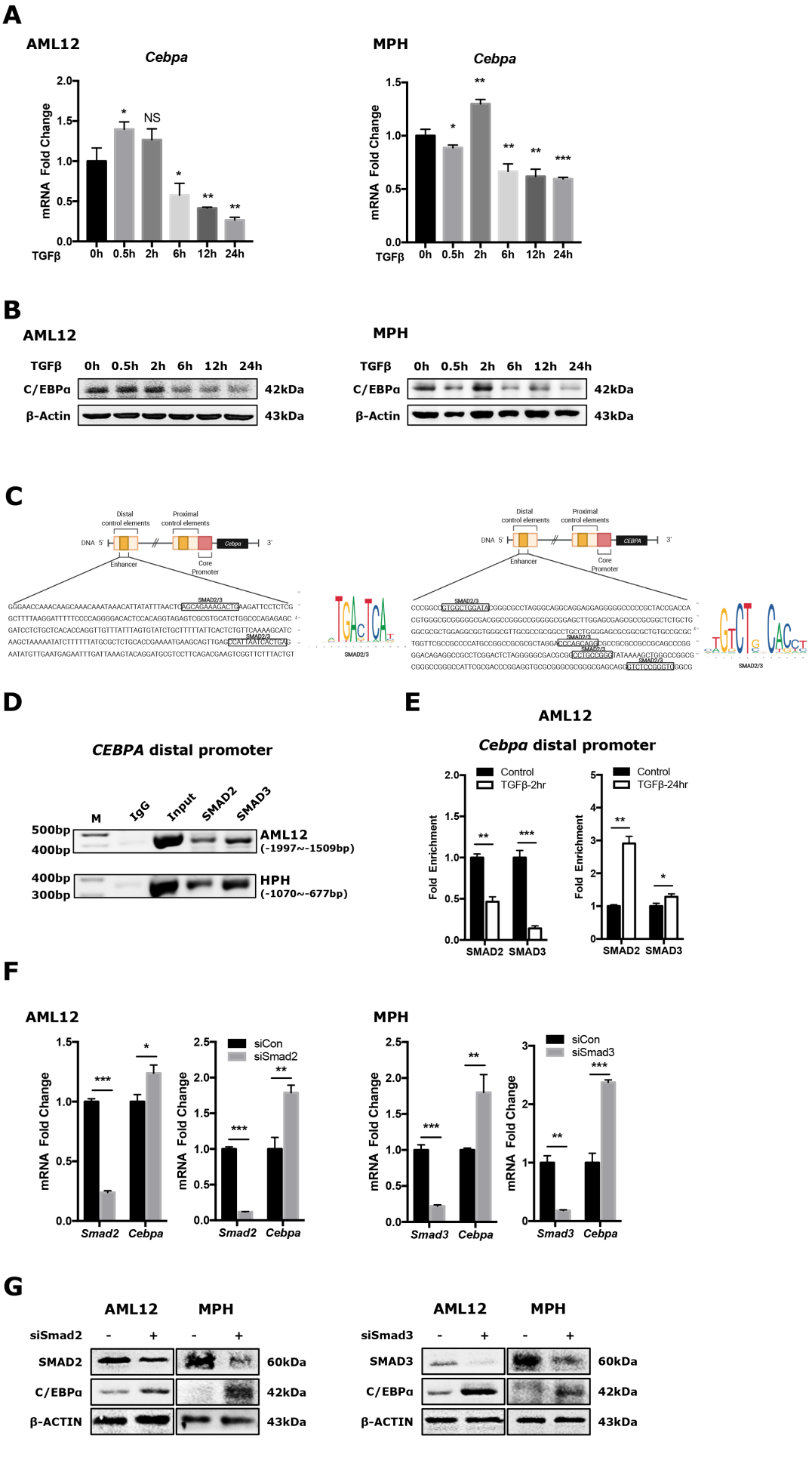
A
AML12
Cebpa
mRNA Fold Change
TGFβ 0h 0.5h 2h 6h 12h 24h
MPH
Cebpa
B
AML12
MPH
TGFβ 0h 0.5h 2h 6h 12h 24h
C/EBPα 42kDa
β-Actin 43kDa
C
Distal control elements
Proximal control elements
Enhancer
Core Promoter
Cebpa
CEBPA
SMAD2/3
D
CEBPA distal promoter
M IgG Input SMAD2 SMAD3
500bp 400bp AML12 (-1997~-1509bp)
400bp 300bp HPH (-1070~-677bp)
E
AML12
Cebpa distal promoter
Control TGFβ-2hr
Control TGFβ-24hr
Fold Enrichment
SMAD2 SMAD3
F
AML12
MPH
siCon siSmad2
siCon siSmad3
Smad2 Cebpa
Smad3 Cebpa
G
AML12 MPH
siSmad2 - + - +
SMAD2 60kDa
C/EBPα 42kDa
β-ACTIN 43kDa
siSmad3 - + - +
SMAD3 60kDa

Figure 15. TGF-β inhibits C/EBPα expression through SMAD2/3 binding to the *Cebpa* distal promoter.

A. Realtime qPCR analyzed the effect of TGF-β on *Cebpa* mRNA expression in AML12 cells and MPH. The cells were incubated with TGF-β (5 ng/ml) for different times. **B.** Western blotting measured C/EBPα expression in AML12 cells and MPH. The cells were incubated with TGF-β (5 ng/ml) for different times. **C.** DNA sequences of the mouse *Cebpa* (-1997~-1509bp) and human *CEBPA* (-1070~-677bp) distal promoter are shown. The binding sites of SMAD2/3 on the *Cebpa/CEBPA* distal promoter were predicted by Jaspar dataset [84]. **D.** ChIP assays examined SMAD2 and SMAD3 binding to the distal promoter of the *Cebpa/CEBPA* gene in AML12 (-1997~-1509bp) cells and HPH (-1070~-677bp). **E.** ChIP-qPCR analyzed SMAD2 and SMAD3 binding to the distal promoter of *Cebpa* (-1997~-1509bp) gene in AML12 cells. The cells were treated with TGF-β (5 ng/ml) for 2 or 24 hours. **F-G.** Realtime qPCR (**F**) and Western blotting (**G**) analyzed the effect of SMAD2 or SMAD3 on C/EBPα mRNA expression in AML12 cells and MPH with or without Smad2 or Smad3 siRNA treatment for 24 hours. Data information: *P*-values were calculated by unpaired Student's t-test (A, E, and F). Bars represent the mean ± SD. *: $P<0.05$; **: $P<0.01$; ***: $P<0.001$; and NS, no significance. Triple experiments were performed for B, D, and G and one representative experiment is shown.

3.13 Insulin is crucial for the maintenance of C/EBPα expression in hepatocytes

To further clarify the relationship between p-SMAD2, C/EBPα and HNF4α, we examined their expression levels by immunohistochemical staining (IHC) in liver tissues from 98 patients with chronic HBV infection, cirrhosis or acute decompensation (AD). Among these patients, hepatic p-SMAD2 levels in 86 patients had been examined previously [62]. In addition, we included an additional 12 cirrhotic patients with AD. IHC showed HNF4α immune positivity in hepatocytes of 74 patients (75.5%) (**Figure 16A**). Analyses based on serious sections further revealed that hepatocytes in 67 (68.4%) of patients simultaneously expressed robust p-SMAD2 and C/EBPα (**Figure 16A-B**). In 7 additional patients (7.1%) with HNF4α positive reaction, hepatocytes displayed positive p-SMAD2, but undetectable C/EBPα expression (**Figure 16A**). There were 24 (24.5%) patients who did not have detectable HNF4α levels in hepatocytes (**Figure 16A**). Among them, 5 (5.1%), 15 (15.3%) and 2 (2%) lacked both p-SMAD2 and C/EBPα, C/EBPα, and p-SMAD2 expression, respectively (**Figure 16A-B**). Impressively, all 6 cirrhotic patients with acute decompensation did not have detectable levels of the three transcription factors (see representative Pat.2 in **Figure 16B**). The remaining 2 patients (2%)

without hepatic HNF4α expression demonstrated both p-SMAD2 and C/EBPα immune reaction in hepatocytes (**Figure 16A**). Taken together, the expression of three transcription factors in most examined patients (90.9%) is consistent with the *in vitro* observation: HNF4α expression in hepatocytes requires both phosphorylated SMADs and C/EBPα.

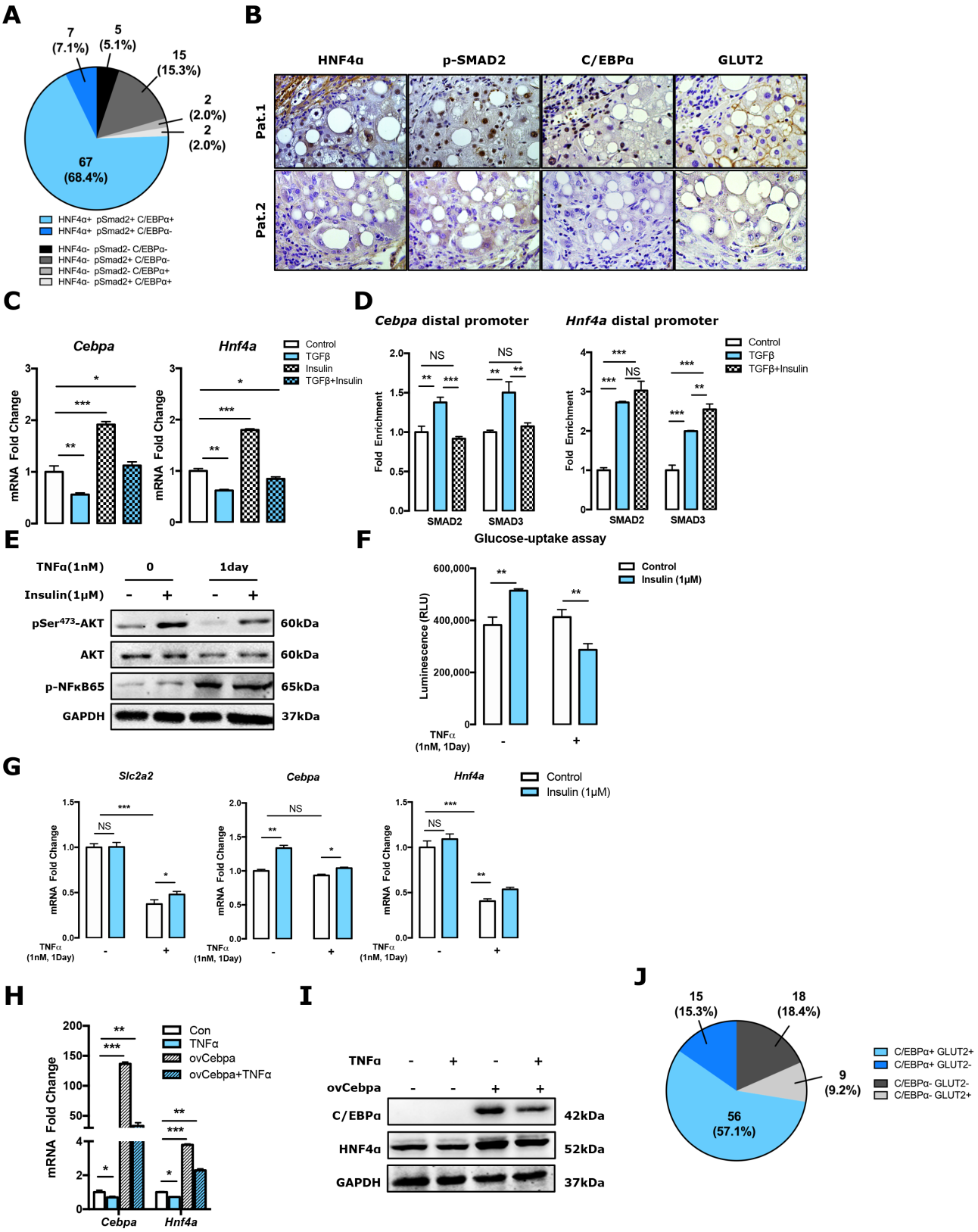

Figure 16. Insulin is crucial for the maintenance of C/EBPα expression in hepatocytes.

A. Quantification of HNF4α, p-SMAD2 and C/EBPα IHC staining in 98 patients described in Materials and Methods section. Values are presented as numbers and percentages. **B.** IHC staining for HNF4α, p-SMAD2, C/EBPα and GLUT2 in 2 representative cirrhotic patients (Pat.1 and Pat.2). Original magnification: x40. **C.** Realtime qPCR analyzed the effect of TGF-β and insulin on C/EBPα and HNF4α expression in AML12 cells. The cells were treated with TGF-β (5 ng/ml) and/or insulin (1 μM) for 24 hours. **D.** ChIP-qPCR assays examined SMAD2 and SMAD3 binding to the distal promoters of the *Cebpa* (-1997~-1509bp) and *Hnf4a* (-1750~-1172bp) gene in AML12 cells treated with TGF-β (5 ng/ml) and/or insulin (1 μM) for 24 hours. **E.** Western blotting analyzed $pSer^{473}$-AKT signaling in AML12 cells. The cells were incubated with TNFα (1 nM) for 1 day followed by insulin (1 μM) stimulation for 1 hour. **F.** Glucose uptake assay was performed in AML12 cells. The cells were incubated with TNFα (1 nM) for 1 day followed by insulin (1 μM) stimulation for 1 hour. **G.** Realtime qPCR analyzed the effect on *Slc2a2*, *Cebpa*, and *Hnf4a* expression in AML12 cells. The cells were incubated with TNFα (1 nM) for 1 day followed by insulin (1 μM) stimulation for 1 hour. **H-I.** Realtime qPCR (**H**) and Western blotting (**I**) analyzed the effect of TNFα on *Hnf4a* expression in MPH. The cells were transfected by Cebpa construct for 48 hours, followed by incubation with TNFα (1 nM) for 24 hours. **J.** Quantification of C/EBPα and GLUT2 IHC staining in 98 patients described in Materials and Methods section. Values are presented as number and percentage. Data information: *P*-values were calculated by unpaired Student's t-test (C, D, F, G and H). Bars represent the mean ± SD. *: $P<0.05$; **: $P<0.01$; ***: $P<0.001$; and NS, no significance. Triple experiments were performed for B, E, and I, and one representative experiment is shown.

The *in vitro* observation that TGF-β-induced SMAD activation contributes to HNF4α expression, but inhibits C/EBPα expression in hepatocytes raises an interesting question: why is hepatic C/EBPα expression only lost in patients with acute decompensation, a sepsis-like syndrome in cirrhotic patients, but not in patients with chronic HBV infection? We found that insulin prevented TGF-β from C/EBPα inhibition. Administration of 1 μM insulin for 24 hours induced mRNA expression of C/EBPα and HNF4α in AML12 cells (**Figure 16C**). Western blotting analyses showed that administration of insulin for 30 minutes was sufficient to upregulate protein expression of C/EBPα (**Figure 17A**). The upregulated C/EBPα levels were maintained for at least 24 hours (**Figure 17A**). Furthermore, TGF-β was not capable of inhibiting expression of C/EBPα and HNF4α when hepatocytes were treated with insulin (**Figure 16C**). ChIP assay shows that insulin inhibited TGF-β-dependent SMAD2 and SMAD3 binding to the *Cebpa* distal promoter (**Figure 16D**). However,

insulin promoted SMAD3 binding to the *Hnf4a* promoter (**Figure 16D**). Inhibition of phosphorylation of AKT by pan-AKT inhibitor MK2206 or knocking down AKT by RNAi blocked insulin-induced C/EBPα and HNF4α expression (**Figure 17B-D**). These results suggest a crucial role of insulin in the maintenance of C/EBPα and HNF4α. On the other hand, these data remind us that insulin resistance in acute decompensation might be a key event leading to C/EBPα and HNF4α suppression by TGF-β given that systemic inflammatory response results in insulin resistance in the liver [89].

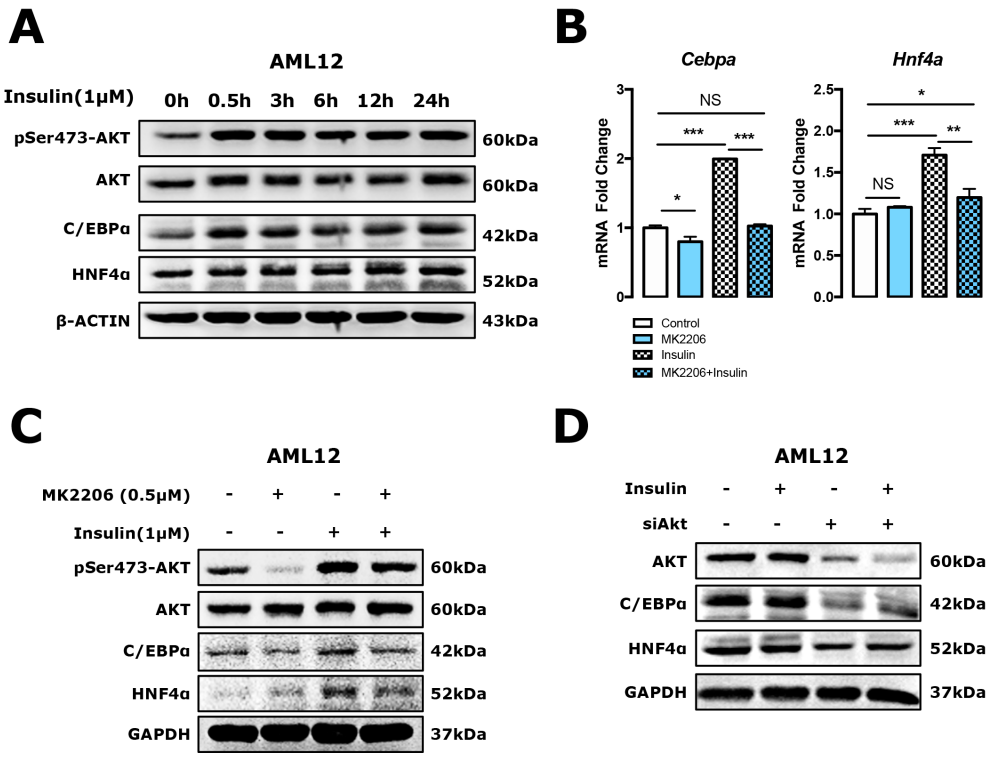

Figure 17. Insulin is crucial for the maintenance of C/EBPα expression in hepatocytes.

A. Wester blotting examined the expression of pSer^{473}-AKT, AKT, C/EBPα, and HNF4α in AML12 cells treated with insulin (1 μM) at different times. **B-C.** Realtime qPCR (**B**) and Western blotting (**C**) analyzed the effect of AKT inhibitor on *Cebpa* and *Hnf4a* expression in AML12 cells. The cells were treated with pan-AKT inhibitor MK2206 (0.5 μM) for 1 hour followed by insulin (1 μM) stimulation for 24 hours. **D.** Western blotting examined the expression of AKT, C/EBPα and HNF4α in AML-12 cells treated with AKT siRNA and/or insulin (1 μM) for 24 hours. Data information: *P*-values were calculated by unpaired Student's t-test (B). Bars represent the mean ± SD. *: $P<0.05$; **: $P<0.01$; ***: $P<0.001$; and NS, no significance. Triple experiments were performed for A, C, and D, and one representative experiment is shown.

Given the key role of TNF-α in the development of insulin resistance, we examined whether TNF-α-induced insulin resistance affected C/EBPα and HNF4α expression in hepatocytes. 1 nM TNF-α treatment for 24h inhibited p-AKT expression in hepatocytes (**Figure 16E**). Glucose uptake assay showed that TNF-α treatment for 2 days inhibited insulin-dependent glucose uptake in hepatocytes (**Figure 16F**). qPCR assays further revealed that TNF-α treatment significantly reduced mRNA expression of *Slc2a2*, *Cebpa* and *Hnf4a* in AML12 cells (**Figure 16G**), implying TNF-α-caused insulin resistance. When hepatocytes were transfected with C/EBPα construct, TNF-α-reduced HNF4α expression was partially restored (**Figure 16H-I**).

To confirm the impact of insulin signaling on C/EBPα expression, we performed IHC for the insulin-regulated glucose transporter GLUT2, the major transporter in charge of hepatocyte glucose uptake [90], in collected liver tissues. Among 71 patients with hepatic C/EBPα expression, 56 had robust GLUT2 expression in hepatocytes while 15 did not (**Figure 16A** and **16J**). In 27 patients without hepatic C/EBPα expression, 18 showed undetectable GLUT2, while 9 had GLUT2 expression in hepatocytes (**Figure 16A** and **16J**). In 6 patients with acute decompensation, none had detectable C/EBPα and GLUT2 immune reaction in hepatocytes. There were 75.5% of the patients showing positive nuclear C/EBPα and membrane GLUT2 expression in hepatocytes simultaneously.

These results strongly suggest a key role of insulin in the maintenance of C/EBPα and HNF4α expression under TGF-β challenge.

3.14 C/EBPα function in hepatocytes

To further clarify the role of C/EBPα in hepatocytes, we performed RNA sequencing in primary mouse hepatocytes with or without C/EBPα siRNA treatment (**Figure 18A**). A heat map shows the clustering situation of the examined samples (**Figure 18B**). Knockdown of C/EBPα significantly downregulated the transcription of 408 and upregulated 112 genes, respectively (**Figure 19A**). The most altered 50 significant genes are shown in **Figure 18C**. Downregulated genes were attributed to several functional categories, including essential hepatic transcription factors Hnf1b, Hnf4a, Hnf6a, Foxa1 and Foxa3, detoxification factors Cyp2c42, Cyp2d13, Cyp2d22, Cyp2d26, Cyp3a13, Cyp3a25, Cyp3a44, and Cyp21a1, membrane transporters

Abcc6, Atp7b, Slc10a1, Slc17a4, Slc27a2 and Slc27a5, coagulation factors F3, F5, F7, F9 and F11, and gluconeogenesis factors Fbp1, Fbp2, Gpt2, Serpina12, Erfe, Lepr, Foxk2 and Ppara (**Figure 19B**).

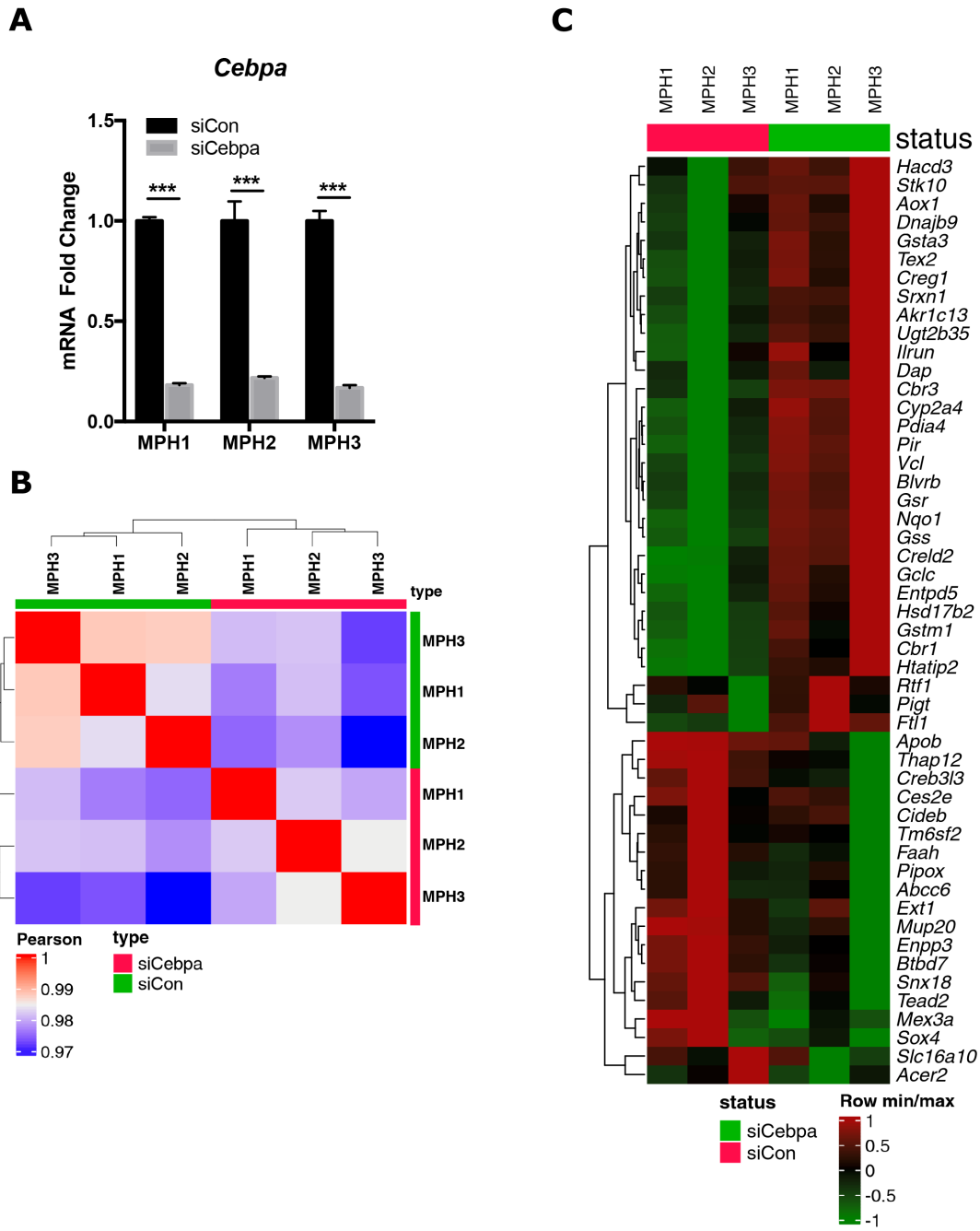

Figure 18. RNA-Sequencing in mouse primary hepatocytes with or without knock-down of Cebpa.

Primary hepatocytes were freshly isolated from three mice: Mouse1 (MPH1), Mouse2 (MPH2), Mouse3 (MPH3). MPH was transfected by Cebpa siRNA for 48 hours. The knockdown efficiency of siRNA is measured by qPCR (**A**). RNA extraction and sequencing were performed as described in Materials and Methods. The heatmap shows the clustering situation of the examined samples (**B**), and top altered 50 significant genes (**C**).

Subsequently, we performed qPCR assays to validate reduced transcription of the following hepatic gene in the C/EBPα knockdown hepatocytes: transcription factors Hnf4α and Foxa3, coagulation factors F5, F7, F9 and F11, detoxification factors Cyp2d26, Cyp3a25 and Cyp21a1, membrane transports Abcc6, Slc10a1, and Slc27a5, and gluconeogenesis factors Fbp2, Gpt2, and Ppara (**Figure 19C**). These results suggest that besides its contribution to HNF4α transcription, C/EBPα might play a crucial role in other essential hepatocyte functions, such as coagulation factor synthesis and bile transport.

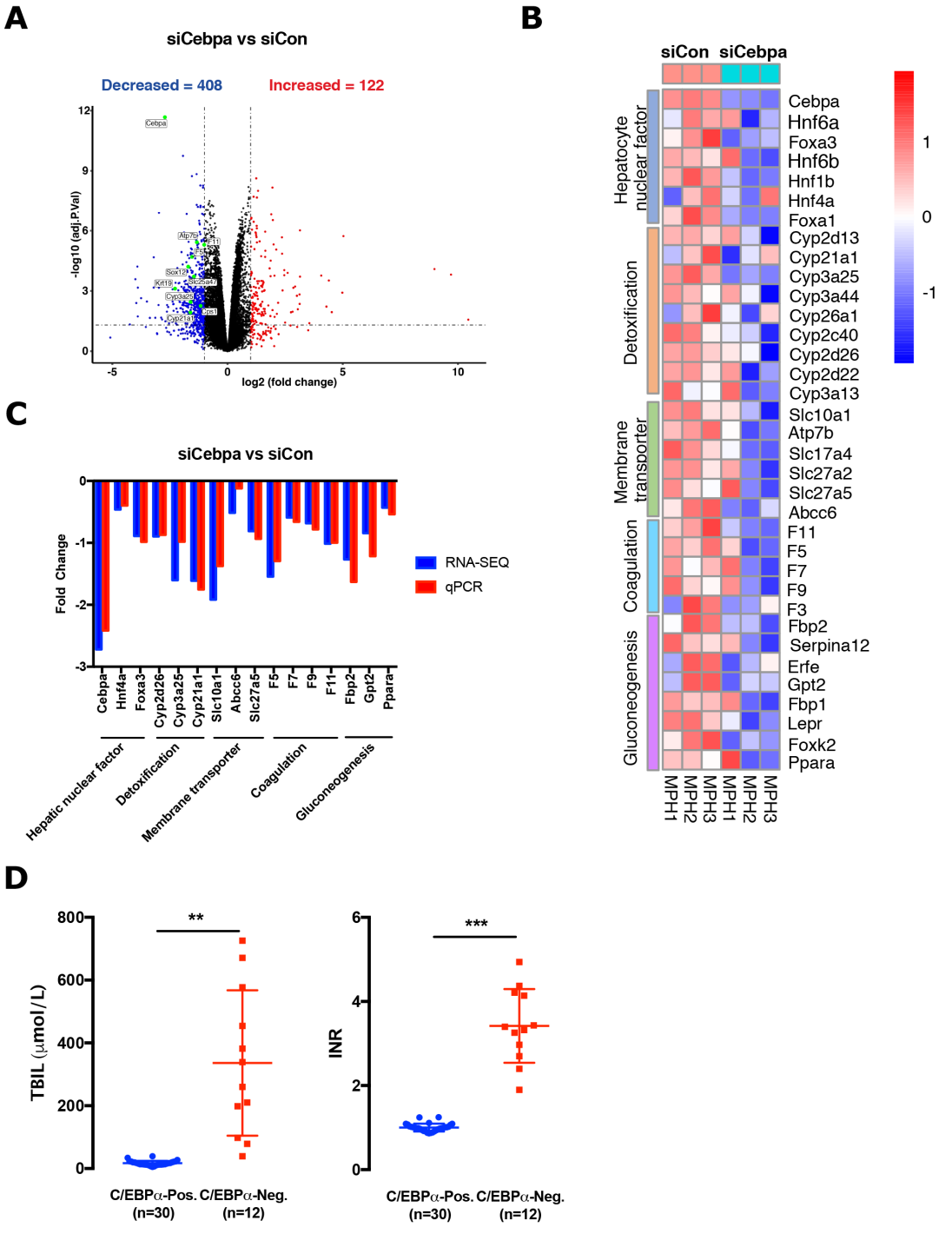

Figure 19. Lack of C/EBPα affects multiple key liver functions.
RNA sequencing was performed in mouse primary hepatocytes (MPH) with or without C/EBPα siRNA treatment for 48 hours (A-C). **A.** Volcano plot shows transcriptomic alteration in MPH treated with C/EBPα siRNA (Padj<0.05, |logFC|>1). **B.** A heat map depicts representative significantly reduced genes (Padj<0.05) related to five aspects of liver function in MPH treated with C/EBPα siRNA. **C.** Verification of selected genes by RT-PCR. **D.** Serum total bilirubin (TBIL) concentration and international normalized ratio (INR) were compared in 42 cirrhotic patients (30 compensated *versus* 12 acute decompensated).

Subsequently, we compared total serum bilirubin (TBIL) concentrations and international normalized ratio (INR) between 30 compensated liver cirrhosis and 12 cirrhotic patients with acute decompensation (AD). The two parameters in the compensated cirrhotic and AD patients were 16.94 ± 7.44 μmol/L versus 336.19 ± 231.56 μmol/L and 0.98 ± 0.10 versus 3.42 ±0.87, respectively (both $P<0.01$, **Figure 19D**). As shown in **Figure 16A**, the thirty compensated cirrhotic patients robustly expressed both C/EBPα and HNF4α, whereas the twelve AD patients had lost both transcription factors in hepatocytes. These results support essential roles of C/EBPα and HNF4α in the maintenance of key liver functions.

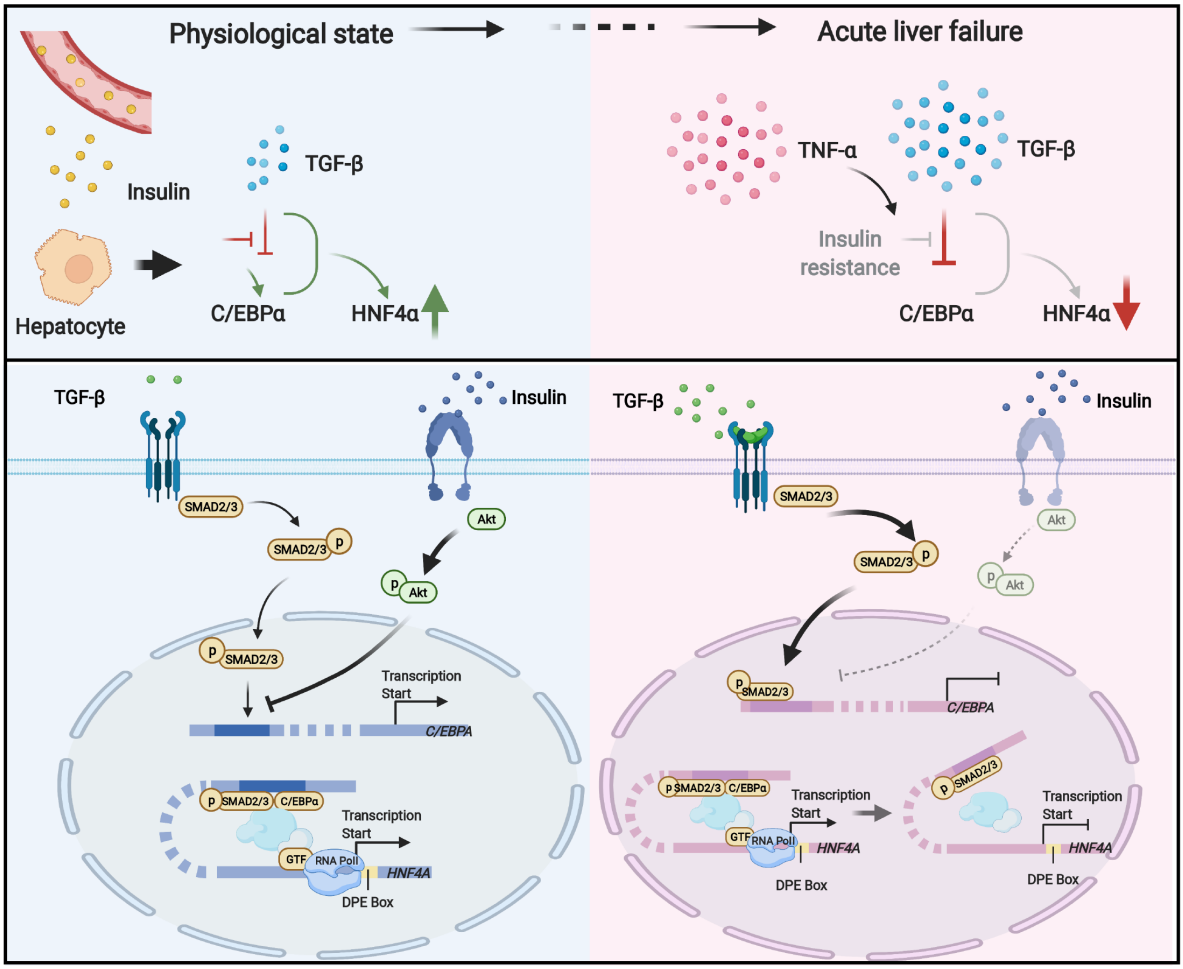

Figure 20. A scheme depicts how hepatocytes constitutively express HNF4α and why HNF4α is inhibited in severe liver disease: the key role of transcription factors SMAD2/3 and C/EBPα, and insulin signaling. Adapted from "Intracellular Comparison", by BioRender.com (2020).
Retrieved from https://app.biorender.com/biorender-templates

4 DISCUSSION

The current study found that there is a hierarchical regulatory network in the liver, which guarantees essential albumin synthesis under pathophysiological challenges. We realized that humans are capable of maintaining relatively normal serum albumin levels even in severe liver diseases such as decompensated cirrhosis and acute liver failure. We subsequently found that two types of liver cells, hepatocytes and liver progenitor cells, are in charge of producing albumin in different disease conditions. A hierarchical transcriptional network controls hepatocyte or LPC to maintain essential albumin expression in response to severe liver damage. The hierarchical regulatory mechanism comprises the following components: (1) In healthy subjects and patients with chronic liver disease, HNF4α and C/EBPα regulate albumin expression in hepatocytes; (2) In cirrhotic patients who lack hepatic HNF4α and C/EBPα expression, FOXA2 takes over the regulation of albumin transcription; (3) In patients suffering from massive hepatocyte necrosis, albumin is produced by LPC, where HNF4α and FOXA2 control albumin transcription. We summarize the hepatic hierarchical transcriptional network in Figure 9.

4.1 HNF4α and C/EBPα regulate albumin expression in normal hepatocytes

As a leading plasma volume expander, stable albumin levels are essential and indispensable for human homeostasis. Such a systemically physiological demand requires that hepatocytes constitutively maintain albumin transcription. We assume that at least two conditions are required for a constitutive gene transcription: (1) Chromatin structure of this gene is open; and (2) There are constitutive transcription factors initiating routine gene transcription. Consistent with previous studies [91,92,93], we found that the *ALB* core promoter possesses a TATA box. In addition, there is a nucleosome free area in the *ALB* core promoter. Such a DNA sequence element and chromatin structure facilitate binding of RNA polymerase II to the *ALB* core promoter in normal hepatocytes. To date, a plethora of transcription factors, including HNF4α, HNF1α, FOXAs, ubiquitous factor nuclear factor-Y, C/EBPα and C/EBPβ, are reported to contribute to albumin transcription in different settings [14,94–98]. Among these transcription factors, we firstly focused on two master hepatic transcription factors HNF4α and C/EBPα, given that they are constitutively expressed in normal

hepatocytes. Function loss experiments confirmed that both HNF4α and C/EBPα are required for albumin transcription in normal hepatocytes. These results provide an explanation of how normal hepatocytes constitutively express albumin.

4.2 FOXA2 takes over the regulation of albumin transcription in cirrhotic patients who lack hepatic HNF4α and C/EBPα expression

Expression of both HNF4α and C/EBPα in hepatocytes is inhibited in severely damaged livers, particularly in decompensated liver cirrhosis and acute liver failure. We examined serum albumin concentrations in 38 patients with decompensated cirrhosis. Interestingly, more than half of examined patients still maintain serum albumin concentration of more than 30 g/L. This raised an important question: which transcription factor controls albumin transcription in hepatocytes lacking HNF4α and C/EBPα? RNA sequencing analyses performed in hepatocytes with both HNF4α and C/EBPα knockdown provided a clue to this issue. In contrast to most hepatic enriched transcription factors, which were downregulated in hepatocytes with HNF4α and C/EBPα knockdown, FOXA2 transcription in hepatocytes was not affected. Like HNF4α and C/EBPα, FOXA2 possesses binding sites in the *ALB* promoter. A genetic analysis based on BXD mice shows that the hepatic expression of albumin is associated with genetic loci near HNF4α and FOXA2, indicating a sign of genetic regulation (http://www.genenetwork.org/show_trait?trait_id=ENSMUST00000031314 &dataset=UTHSC-BXD-Harv_Liv_TPM_log2_1019). Physiologically, FOXA2 expression and localization are regulated by insulin and glucagon: insulin inhibits, whereas glucagon promotes FOXA2 nuclear translocation [99]. FOXA2 is rarely localized in nuclei in normal hepatocytes (unpublished data). In cirrhotic patients suffering from acute liver failure, FOXA2 nuclear expression is robust. These patients underwent systemic inflammatory syndrome, which resulted in insulin resistance [89]. Considering the loss of insulin sensitivity in hepatocytes, it is not surprising that FOXA2 translocated into the nuclei of the cells.

4.3 FoxA2 is controlled by Hedgehog signaling.

Insulin resistance does not explain why high levels of FOXA2 are expressed in the hepatocytes of patients with decompensated cirrhosis and ALF. In normal hepatocytes, FOXA2 is undetectable by IHC, implying low basal levels of the transcription factor. Hepatic insulin resistance occurs in patients with non-alcoholic steatohepatitis (NASH). However, FOXA2 expression is not increased in NASH patients (unpublished data). Therefore, there must be additional signals that induce FOXA2 expression in diseases such as ALF. Based on RNA sequencing analyses, we found that hepatocytes with both HNF4α and C/EBPα knockdown had increased hedgehog ligand biosynthesis. In liver damage, inflammatory cytokines, e.g., TGF-β[66], platelet-derived growth factor (PDGF)[67], epidermal growth factor (EGF)[68], and insulin-like growth factor (IGF)[69], activate hedgehog. In addition, Gli2, a canonical hedgehog downstream transcription factor, possesses binding sites on the *Foxa2* promoter. In this study, GLI2 was robustly expressed in the nuclei of hepatocytes simultaneously with FOXA2 in 6 patients with ALF. *In vitro*, GLI2 binding to the *Foxa2* promoter was confirmed by ChIP. These results highlight a critical effect of hedgehog signaling in the regulation of FOXA2 expression in the patients lacking HNF4α and C/EBPα.

4.4 LPCs exploit HNF4α or FOXA2 to maintain albumin synthesis in patients with massive hepatic necrosis.

Patients with acute liver failure are at high risk of mortality, who suffer from massive hepatic necrosis. In such an urgent condition, most or all hepatocytes are destroyed [100]. Impressively, a large portion of ALF patients maintains relatively normal albumin levels. We found that LPC activation and albumin expression by LPC maintains albumin levels in these patients. Normal LPC are capable of expressing low levels of HNF4α and albumin. A previous study shows that LPC express remarkable HNF4α only in the areas lacking hepatocytes in the patients with massive hepatic necrosis (unpublished data). LPC lack C/EBPα. Therefore, HNF4α and FOXA2 might be the two transcription factors that regulate albumin transcription in LPC. However, we found that in the examined patients with ALF, HNF4α was undetectable. However, robust FOXA2 was expressed in the LPC of these patients. These results highlight the crucial role of FOXA2 in the regulation of albumin transcription in ALF patients.

Taken together, the maintenance of essential albumin synthesis in physiological and diseased conditions is dependent on hepatocytes and LPC. In these cells, HNF4α, C/EBPα and FOXA2 form a hierarchical regulatory network that controls constitutive albumin expression.

Given the key role of HNF4α in albumin transcription, the current study also focused on another key questions: why and how hepatocytes constitutively express HNF4α? We found that both SMAD2/3 and C/EBPα are required for constitutive HNF4α expression in hepatocytes. As a transcriptional regulator, TGF-β-activated SMAD2/3 complex is an activator of HNF4α transcription. On the other hand, the SMAD2/3 complex acts as a C/EBPα transcriptional repressor through binding to its promoter. However, TGF-β-induced SMAD2/3 binding to the *CEBPA* promoter is inhibited by insulin signaling. Therefore, TGF-β challenge usually does not lead to the loss of C/EBPα and HNF4α expression in the hepatocytes of healthy subjects and patients. In the condition of severe inflammation, however hepatocytes develop insulin resistance upon stimulation with pro-inflammatory factor TNF-α. In the absence of insulin signaling, C/EBPα and HNF4α are successively inhibited by TGF-β. We summarize these results in Figure 20.

4.5 Constitutive expression of HNF4α in hepatocyte

Although HNF4α is a recognized hepatocyte lineage transcription factor and is commonly used as a marker of hepatocytes [101], it is unclear to date how hepatocytes constitutively express HNF4α. The current study provides partial molecular details of this aspect. We confirmed that the *HNF4A* gene core promoter possesses a DPE, but not a TATA box, and it is occupied by nucleosomes. For a gene with a DPE box, H3K4me3 is required for providing a harbor for TAF6 and TAF9 to recruit RNA Pol II to initiate transcription [102]. In addition, sufficient HNF4α transcription requires that SMAD2/3 and C/EBPα simultaneously bind to its distal promoter. A Mediator complex links the active distal promoter to the RNA Pol II bound core promoter. Disruption of any component of this molecular machinery influences HNF4α expression in hepatocytes.

4.6 The central role of C/EBPα in maintaining HNF4α transcription under high levels of TGF-β

SMAD2/3 are canonical downstream transcription factors of TGF-β signaling[61]. Previous *in vitro* studies showed that TGF-β induces hepatocyte to undergo EMT through inhibiting HNF4α [59]. How to explain that HNF4α transcription requires TGF-β-activated SMAD2/3, whereas HNF4α expression is inhibited by TGF-β? We found that activated SMAD2/3 in hepatocyte nuclei are capable of binding to multiple target genes, including C/EBPα and HNF4α. Although the p-SMAD2/3 complex acts as an activator to promote transcription of the *HNF4A* gene, it equally acts as a transcription repressor of the *CEBPA* gene. Given that the half-life of C/EBPα is between 1-3 hours [103], C/EBPα protein is exhausted when hepatocytes are long-term stimulated with TGF-β (e.g., >12 hours). Therefore, dynamic *in vitro* observation showed that upon TGF-β incubation mRNA expression of HNF4α is rapidly increased until 6 hours. Later, HNF4α expression is inhibited following reduced C/EBPα protein expression. Ectopic C/EBPα expression prevents TGF-β-mediated HNF4α inhibition in hepatocytes. These results highlight a central role of C/EBPα in the initiation and maintenance of HNF4α transcription in hepatocytes exposed to high TGF-β concentrations.

4.7 Insulin is a key factor that prevents C/EBPα from TGF-β inhibition

TGF-β-activated p-SMAD2/3 complex inhibits C/EBPα transcription *in vitro*. However, we observed that a large portion of patients simultaneously express robust C/EBPα, HNF4α and p-SMAD2 in hepatocytes. This raises another interesting question: why does p-SMAD2 not inhibit C/EBPα expression in these patients? We found that insulin inhibits SMAD2/3 binding to the *CEBPA* promoter *in vitro* and thus maintains C/EBPα expression in cultured hepatocytes. However, insulin promotes SMAD2/3 binding to the *HNF4A* promoter. In the examined patients, 78.9% of the patients with C/EBPα expression show GLUT2 expression in the outer membranes of hepatocytes, indicating insulin sensitivity in these cells. In addition, among 27 patients lacking C/EBPα expression 66.7% of patients do not have GLUT2 expression in the hepatocyte membrane. These results suggest that insulin is a key factor that

prevents C/EBPα from TGF-β inhibition. How insulin signaling inhibits SMAD2/3 binding to the *CEBPA* promoter but promotes SMAD3 binding to the *HNF4A* promoter requires further investigation.

Insulin resistance in skeletal muscle, adipose tissue and hepatocytes is a critical reaction that re-allocates energy from peripheral to central processes in response to severe disease conditions such as sepsis [104]. TNF-α is the major inflammatory cytokine leading to insulin resistance [105]. In this study, we confirmed that TNF-α incubation leads to insulin resistance *in vitro*. Concomitant with insulin resistance, both C/EBPα and HNF4α expression was inhibited. Ectopic C/EBPα expression partially restored TNF-α-reduced HNF4α expression, indicating a protective effect of C/EBPα on HNF4α expression. Among 98 observed patients, 6 suffered from acute liver failure and sepsis. It denotes that these patients had already undergone or were undergoing a systemic inflammatory response. In hepatocytes of these patients, nuclei do not show C/EBPα and HNF4α while membranes do not express GLUT2, indicating the occurrence of insulin resistance in hepatocytes. These results strongly highlight a crucial impact of the systemic hormone insulin on hepatocyte function.

4.8 C/EBPα function in hepatocyte

Besides promoting HNF4α transcription, C/EBPα is a crucial hepatic transcriptional regulator. In embryonic liver development, C/EBPα inhibits SOX9 through repressing the onecut transcription factor HNF6 expression and thus promotes hepatoblast differentiation towards hepatocytes [106]. On the other hand, suppression of C/EBPα expression results in hepatoblast-to-cholangiocyte differentiation [35]. In adult hepatocytes, C/EBPα controls proteins relevant to the metabolism of glucose and lipids, e.g., C/EBPα is capable of binding to the promoter of leptin [107]. In a mouse sepsis model, the binding activity of C/EBPα to the liver-specific genes such as the gluconeogenic enzymes phosphoenolpyruvate carboxykinase (PEPCK), is decreased [108]. Our RNA sequencing and subsequent qPCR analyses show that knockdown of C/EBPα affects not only the metabolism of glucose, lipids and ABC transporter families, but also key hepatocyte functional genes, e.g., coagulation factor synthesis. We subsequently compared blood total bilirubin concentrations and

INR levels, the two key parameters comprising the MELD score, in cirrhotic patients possessing or losing C/EBPα in hepatocytes. The latter patients also lost HNF4α and displayed extremely high bilirubin and INR levels. All patients in this cohort received liver transplantation. In contrast to the cirrhotic patients lacking C/EBPα expression, patients with intact C/EBPα expression were at the stage of compensated cirrhosis. They received histological examination because of the occurrence of hepatocellular carcinoma. These patients showed relatively normal bilirubin and INR levels. These results highlight a close relationship between C/EBPα and key liver functions.

4.9 The potential explanation of TGF-β and EMT *in vivo*

In addition to further clarifying the relationship between TGF-β signaling, SMADs, C/EBPα and HNF4α, the current study might be useful to explain a long-term controversial issue: whether diseased patients and animals undergo hepatocyte EMT *in vivo*. Although *in vitro* studies undoubtedly confirmed EMT in cultured hepatocytes [59], animal studies based on lineage tracing strategy did not detect hepatocytes undergoing EMT in carbon tetrachloride (CCl_4) and bile duct ligation (BDL)-treated mice [109]. The current study provides a potential explanation for this conundrum, indicating that the animals did not undergo EMT, because the disease models used do not lead to hepatic insulin resistance. When we performed GLUT2 staining in CCl_4 or BDL-treated mice, hepatocytes showed intact GLUT2 expression (data not shown). However, a detailed analysis of this issue is beyond the scope of the current study and deserves further investigation.

The current study highlights a crucial role of SMAD proteins in determining the hepatocellular expression of HNF4α as well as C/EBPα. It also raises an unanswered question: why does the SMAD2/3 complex activate the HNF4α transcription, but repress the C/EBPα expression? As canonical downstream transcriptional regulators of TGF-β signaling, the affinity of SMAD proteins for the SMAD-binding element (SBE) is too low to support a SMAD complex binding to a single SBE [110]. High-affinity binding between SMAD complex and SBE requires a co-factor [111,112]. Whether SMAD2/3 combines with different co-factors to exert opposite effects on the transcription of *HNF4A* and *CEBPA* requires further investigation.

5 SUMMARY

The results of my investigations reveal a hierarchical transcriptional network that controls the maintenance of essential albumin levels by hepatocytes or LPCs in response to severe liver damage. The hierarchical regulatory mechanism comprises the following components: (1) In healthy subjects and patients with chronic liver disease, HNF4α and C/EBPα regulate albumin expression in hepatocytes; (2) In cirrhotic patients who lack HNF4α and C/EBPα expression in hepatocytes, FOXA2 takes over albumin transcription; (3) In patients suffering from massive hepatocyte necrosis, albumin is produced by LPC, where HNF4α and FOXA2 control albumin transcription. (4) Hedgehog-GLI2 signaling might play a crucial role in the regulation of FOXA2 expression in hepatocytes lacking both HNF4α and C/EBPα.

In addition, this study provides data showing how hepatocytes constitutively express HNF4α. I found that (1) HNF4α transcription in hepatocytes required binding of both SMAD2/3 and C/EBPα to its promoters; (2) As a transcriptional regulator, TGF-β-activated SMAD2/3 complex is an activator of HNF4α transcription. On the other hand, the SMAD2/3 complex acts as a C/EBPα transcriptional repressor through binding to its promoter; (3) TGF-β-induced SMAD2/3 binding to the *CEBPA* promoter is inhibited by insulin signaling. Therefore, TGF-β challenge usually does not lead to the loss of C/EBPα and HNF4α expression in the hepatocytes of healthy subjects and patients. (4) In the condition of severe inflammation, however hepatocytes develop insulin resistance upon stimulation with pro-inflammatory factor TNF-α; (5) In the absence of insulin signaling, C/EBPα and HNF4α are successively inhibited by TGF-β.

In conclusion, my work described in this thesis revealed that the liver possesses a hierarchical regulatory network to stably maintain essential albumin expression in physiological conditions and under various pathological challenges. Furthermore, data from my investigations help to explain the long-term controversial issue that TGF-β inhibits HNF4α and thus induces hepatocyte EMT *in vitro*, but not *in vivo*.

6 REFERENCES

1. Hall JE, Guyton AC. *Guyton and Hall Textbook of Medical Physiology*. 12th ed. Saunders/Elsevier; 2011.

2. Theise ND, Saxena R, Portmann BC, et al. The canals of Hering and hepatic stem cells in humans. *Hepatology*. 1999;30(6):1425-1433. doi:10.1002/hep.510300614

3. Peters T. *All about Albumin: Biochemistry, Genetics, and Medical Applications*. Academic Press; 1996.

4. Jalan R, Bernardi M. Effective albumin concentration and cirrhosis mortality: from concept to reality. *J Hepatol*. 2013;59(5):918-920. doi:10.1016/j.jhep.2013.08.001

5. Garcia-Martinez R, Caraceni P, Bernardi M, Gines P, Arroyo V, Jalan R. Albumin: Pathophysiologic basis of its role in the treatment of cirrhosis and its complications. *Hepatology*. 2013;58(5):1836-1846. doi:10.1002/hep.26338

6. Spinella R, Sawhney R, Jalan R. Albumin in chronic liver disease: structure, functions and therapeutic implications. *Hepatol Int*. 2016;10(1):124-132. doi:10.1007/s12072-015-9665-6

7. Levitt DG, Levitt MD. Human serum albumin homeostasis: a new look at the roles of synthesis, catabolism, renal and gastrointestinal excretion, and the clinical value of serum albumin measurements. *Int J Gen Med*. 2016;9:229-255. doi:10.2147/IJGM.S102819

8. Arroyo V, García-Martinez R, Salvatella X. Human serum albumin, systemic inflammation, and cirrhosis. *J Hepatol*. 2014;61(2):396-407. doi:10.1016/j.jhep.2014.04.012

9. Keaney JF, Simon DI, Stamler JS, et al. NO forms an adduct with serum albumin that has endothelium-derived relaxing factor-like properties. *J Clin Invest*. 1993;91(4):1582-1589. doi:10.1172/JCI116364

10. Fernández J, Clària J, Amorós A, et al. Effects of Albumin Treatment on Systemic and Portal Hemodynamics and Systemic Inflammation in Patients With Decompensated Cirrhosis. *Gastroenterology*. 2019;157(1):149-162. doi:10.1053/j.gastro.2019.03.021

11. Fernández J, Angeli P, Trebicka J, et al. Efficacy of Albumin Treatment for Patients with Cirrhosis and Infections Unrelated to Spontaneous Bacterial Peritonitis. *Clin Gastroenterol Hepatol*. 2020;18(4):963-973.e14. doi:10.1016/j.cgh.2019.07.055

12. China L, Freemantle N, Forrest E, et al. A Randomized Trial of Albumin Infusions in Hospitalized Patients with Cirrhosis. *N Engl J Med*. 2021;384(9):808-817. doi:10.1056/NEJMoa2022166

13. Cereghini S, Raymondjean M, Carranca AG, Herbomel P, Yaniv M. Factors involved in control of tissue-specific expression of albumin gene. *Cell*. 1987;50(4):627-638. doi:10.1016/0092-8674(87)90036-5

14. Lichtsteiner S, Wuarin J, Schibler U. The interplay of DNA-binding proteins on the promoter of the mouse albumin gene. *Cell*. 1987;51(6):963-973. doi:10.1016/0092-8674(87)90583-6

15. Costa RH, Grayson DR, Darnell JE. Multiple hepatocyte-enriched nuclear factors function in the regulation of transthyretin and alpha 1-antitrypsin genes. *Mol Cell Biol*. 1989;9(4):1415-1425. doi:10.1128/mcb.9.4.1415

16. Cereghini S. Liver-enriched transcription factors and hepatocyte differentiation. *FASEB J*. 1996;10(2):267-282.

17. Costa RH, Kalinichenko VV, Holterman A-XL, Wang X. Transcription factors in liver development, differentiation, and regeneration. *Hepatology*. 2003;38(6):1331-1347. doi:10.1016/j.hep.2003.09.034

18. Duncan SA, Navas MA, Dufort D, Rossant J, Stoffel M. Regulation of a transcription factor network required for differentiation and metabolism. *Science*. 1998;281(5377):692-695. doi:10.1126/science.281.5377.692

19. Zaret KS. Regulatory phases of early liver development: paradigms of organogenesis. *Nat Rev Genet*. 2002;3(7):499-512. doi:10.1038/nrg837

20. Lemaigre F, Zaret KS. Liver development update: new embryo models, cell lineage control, and morphogenesis. *Curr Opin Genet Dev*. 2004;14(5):582-590. doi:10.1016/j.gde.2004.08.004

21. Lee CS, Friedman JR, Fulmer JT, Kaestner KH. The initiation of liver development is dependent on Foxa transcription factors. *Nature*. 2005;435(7044):944-947. doi:10.1038/nature03649

22. Li J, Ning G, Duncan SA. Mammalian hepatocyte differentiation requires the transcription factor HNF-4alpha. *Genes Dev*. 2000;14(4):464-474.

23. Zhao R, Watt AJ, Li J, Luebke-Wheeler J, Morrisey EE, Duncan SA. GATA6 is essential for embryonic development of the liver but dispensable for early heart formation. *Mol Cell Biol*. 2005;25(7):2622-2631. doi:10.1128/MCB.25.7.2622-2631.2005

24. Tomizawa M, Garfield S, Factor V, Xanthopoulos KG. Hepatocytes deficient in CCAAT/enhancer binding protein alpha (C/EBP alpha) exhibit both hepatocyte and biliary epithelial cell character. *Biochem Biophys Res Commun*. 1998;249(1):1-5. doi:10.1006/bbrc.1998.8999

25. Clotman F, Lannoy VJ, Reber M, et al. The onecut transcription factor HNF6 is required for normal development of the biliary tract. *Development*. 2002;129(8):1819-1828.

26. Coffinier C, Gresh L, Fiette L, et al. Bile system morphogenesis defects and liver dysfunction upon targeted deletion of HNF1beta. *Development*. 2002;129(8):1829-1838.

27. Hayhurst GP, Lee YH, Lambert G, Ward JM, Gonzalez FJ. Hepatocyte nuclear factor 4alpha (nuclear receptor 2A1) is essential for maintenance of hepatic gene expression and lipid homeostasis. *Mol Cell Biol*. 2001;21(4):1393-1403. doi:10.1128/MCB.21.4.1393-1403.2001

28. Watt AJ, Garrison WD, Duncan SA. HNF4: a central regulator of hepatocyte differentiation and function. *Hepatology*. 2003;37(6):1249-1253. doi:10.1053/jhep.2003.50273

29. Odom DT, Zizlsperger N, Gordon DB, et al. Control of pancreas and liver gene expression by HNF transcription factors. *Science*. 2004;303(5662):1378-1381. doi:10.1126/science.1089769

30. Stoffel M, Duncan SA. The maturity-onset diabetes of the young (MODY1) transcription factor HNF4alpha regulates expression of genes required for glucose transport and metabolism. *Proc Natl Acad Sci USA*. 1997;94(24):13209-13214. doi:10.1073/pnas.94.24.13209

31. Limaye PB, Alarcón G, Walls AL, et al. Expression of specific hepatocyte and cholangiocyte transcription factors in human liver disease and embryonic development. *Lab Invest*. 2008;88(8):865-872. doi:10.1038/labinvest.2008.56

32. Nishikawa T, Bell A, Brooks JM, et al. Resetting the transcription factor network reverses terminal chronic hepatic failure. *J Clin Invest*. 2015;125(4):1533-1544. doi:10.1172/JCI73137

33. Miller M, Shuman JD, Sebastian T, Dauter Z, Johnson PF. Structural basis for DNA recognition by the basic region leucine zipper transcription factor CCAAT/enhancer-binding protein alpha. *J Biol Chem*. 2003;278(17):15178-15184. doi:10.1074/jbc.M300417200

34. Ramji DP, Foka P. CCAAT/enhancer-binding proteins: structure, function and regulation. *Biochem J*. 2002;365(Pt 3):561-575. doi:10.1042/BJ20020508

35. Yamasaki H, Sada A, Iwata T, et al. Suppression of C/EBPalpha expression in periportal hepatoblasts may stimulate biliary cell differentiation through increased Hnf6 and Hnf1b expression. *Development*. 2006;133(21):4233-4243. doi:10.1242/dev.02591

36. Qiao L, MacLean PS, You H, Schaack J, Shao J. knocking down liver ccaat/enhancer-binding protein alpha by adenovirus-transduced silent interfering ribonucleic acid improves hepatic gluconeogenesis and lipid homeostasis in db/db mice. *Endocrinology*. 2006;147(6):3060-3069. doi:10.1210/en.2005-1507

37. Tao L-L, Zhai Y-Z, Ding D, Yin W-H, Liu X-P, Yu G-Y. The role of C/EBP-α expression in human liver and liver fibrosis and its relationship with autophagy. *Int J Clin Exp Pathol*. 2015;8(10):13102-13107.

38. Costa RH, Grayson DR, Xanthopoulos KG, Darnell JE. A liver-specific DNA-binding protein recognizes multiple nucleotide sites in regulatory regions of transthyretin, alpha 1-antitrypsin, albumin, and simian virus 40 genes. *Proc Natl Acad Sci U S A*. 1988;85(11):3840-3844. doi:10.1073/pnas.85.11.3840

39. Herbst RS, Nielsch U, Sladek F, Lai E, Babiss LE, Darnell JE. Differential regulation of hepatocyte-enriched transcription factors explains changes in albumin and transthyretin gene expression among hepatoma cells. *New Biol*. 1991;3(3):289-296.

40. Monaghan AP, Kaestner KH, Grau E, Schütz G. Postimplantation expression patterns indicate a role for the mouse forkhead/HNF-3 alpha, beta and gamma genes in determination of the definitive endoderm, chordamesoderm and neuroectoderm. *Development*. 1993;119(3):567-578.

41. Lantz KA, Vatamaniuk MZ, Brestelli JE, Friedman JR, Matschinsky FM, Kaestner KH. Foxa2 regulates multiple pathways of insulin secretion. *J Clin Invest*. 2004;114(4):512-520. doi:10.1172/JCI21149

42. Zaret KS, Lerner J, Iwafuchi-Doi M. Chromatin Scanning by Dynamic Binding of Pioneer Factors. *Mol Cell*. 2016;62(5):665-667. doi:10.1016/j.molcel.2016.05.024

43. Iwafuchi-Doi M, Donahue G, Kakumanu A, et al. The Pioneer Transcription Factor FoxA Maintains an Accessible Nucleosome Configuration at Enhancers for Tissue-Specific Gene Activation. *Mol Cell*. 2016;62(1):79-91. doi:10.1016/j.molcel.2016.03.001

44. Wolfrum C, Besser D, Luca E, Stoffel M. Insulin regulates the activity of forkhead transcription factor Hnf-3 /Foxa-2 by Akt-mediated phosphorylation and nuclear/cytosolic localization. *Proceedings of the National Academy of Sciences*. 2003;100(20):11624-11629. doi:10.1073/pnas.1931483100

45. von Meyenn F, Porstmann T, Gasser E, et al. Glucagon-Induced Acetylation of Foxa2 Regulates Hepatic Lipid Metabolism. *Cell Metabolism*. 2013;17(3):436-447. doi:10.1016/j.cmet.2013.01.014

46. De Feo P, Gaisano MG, Haymond MW. Differential effects of insulin deficiency on albumin and fibrinogen synthesis in humans. *J Clin Invest*. 1991;88(3):833-840. doi:10.1172/JCI115384

47. Peavy DE, Taylor JM, Jefferson LS. Correlation of albumin production rates and albumin mRNA levels in livers of normal, diabetic, and insulin-treated diabetic rats. *Proc Natl Acad Sci U S A*. 1978;75(12):5879-5883. doi:10.1073/pnas.75.12.5879

48. Lloyd CE, Kalinyak JE, Hutson SM, Jefferson LS. Stimulation of albumin gene transcription by insulin in primary cultures of rat hepatocytes. *Am J Physiol*. 1987;252(2 Pt 1):C205-214. doi:10.1152/ajpcell.1987.252.2.C205

49. Stanchfield JE, Yager JD. Insulin effects on protein synthesis and secretion in primary cultures of amphibian hepatocytes. *J Cell Physiol*. 1979;100(2):279-290. doi:10.1002/jcp.1041000209

50. Leto D, Saltiel AR. Regulation of glucose transport by insulin: traffic control of GLUT4. *Nat Rev Mol Cell Biol*. 2012;13(6):383-396. doi:10.1038/nrm3351

51. Rommel C, Bodine SC, Clarke BA, et al. Mediation of IGF-1-induced skeletal myotube hypertrophy by PI(3)K/Akt/mTOR and PI(3)K/Akt/GSK3 pathways. *Nat Cell Biol*. 2001;3(11):1009-1013. doi:10.1038/ncb1101-1009

52. Burgering BM, Coffer PJ. Protein kinase B (c-Akt) in phosphatidylinositol-3-OH kinase signal transduction. *Nature*. 1995;376(6541):599-602. doi:10.1038/376599a0

53. Herzig S, Long F, Jhala US, et al. CREB regulates hepatic gluconeogenesis through the coactivator PGC-1. *Nature*. 2001;413(6852):179-183. doi:10.1038/35093131

54. Matsumoto M, Pocai A, Rossetti L, Depinho RA, Accili D. Impaired regulation of hepatic glucose production in mice lacking the forkhead transcription factor Foxo1 in liver. *Cell Metab*. 2007;6(3):208-216. doi:10.1016/j.cmet.2007.08.006

55. Wang ND, Finegold MJ, Bradley A, et al. Impaired energy homeostasis in C/EBP alpha knockout mice. *Science*. 1995;269(5227):1108-1112. doi:10.1126/science.7652557

56. Clowes GH, Martin H, Walji S, Hirsch E, Gazitua R, Goodfellow R. Blood insulin responses to blood glucose levels in high output sepsis and spetic shock. *Am J Surg*. 1978;135(4):577-583. doi:10.1016/0002-9610(78)90040-5

57. Bunout D, Muñoz C, López M, et al. Interleukin 1 and tumor necrosis factor in obese alcoholics compared with normal-weight patients. *Am J Clin Nutr*. 1996;63(3):373-376. doi:10.1093/ajcn/63.3.373

58. Reaven GM. Pathophysiology of insulin resistance in human disease. *Physiol Rev*. 1995;75(3):473-486. doi:10.1152/physrev.1995.75.3.473

59. Munker S, Wu Y-L, Ding H-G, Liebe R, Weng H-L. Can a fibrotic liver afford epithelial-mesenchymal transition? *World J Gastroenterol*. 2017;23(26):4661-4668. doi:10.3748/wjg.v23.i26.4661

60. Franco DL, Mainez J, Vega S, et al. Snail1 suppresses TGF-beta-induced apoptosis and is sufficient to trigger EMT in hepatocytes. *J Cell Sci*. 2010;123(Pt 20):3467-3477. doi:10.1242/jcs.068692

61. Shi Y, Massagué J. Mechanisms of TGF-beta signaling from cell membrane to the nucleus. *Cell*. 2003;113(6):685-700. doi:10.1016/s0092-8674(03)00432-x

62. Weng H-L, Liu Y, Chen J-L, et al. The etiology of liver damage imparts cytokines transforming growth factor beta1 or interleukin-13 as driving forces in fibrogenesis. *Hepatology*. 2009;50(1):230-243. doi:10.1002/hep.22934

63. Borst SE. The role of TNF-alpha in insulin resistance. *Endocrine*. 2004;23(2-3):177-182. doi:10.1385/ENDO:23:2-3:177

64. Alam T, An MR, Papaconstantinou J. Differential expression of three C/EBP isoforms in multiple tissues during the acute phase response. *J Biol Chem*. 1992;267(8):5021-5024.

65. Fleig SV, Choi SS, Yang L, et al. Hepatic accumulation of Hedgehog-reactive progenitors increases with severity of fatty liver damage in mice. *Lab Invest*. 2007;87(12):1227-1239. doi:10.1038/labinvest.3700689

66. Syn W-K, Jung Y, Omenetti A, et al. Hedgehog-mediated epithelial-to-mesenchymal transition and fibrogenic repair in nonalcoholic fatty liver disease. *Gastroenterology*. 2009;137(4):1478-1488.e8. doi:10.1053/j.gastro.2009.06.051

67. Omenetti A, Yang L, Li Y-X, et al. Hedgehog-mediated mesenchymal-epithelial interactions modulate hepatic response to bile duct ligation. *Lab Invest*. 2007;87(5):499-514. doi:10.1038/labinvest.3700537

68. Yang L, Wang Y, Mao H, et al. Sonic hedgehog is an autocrine viability factor for myofibroblastic hepatic stellate cells. *J Hepatol*. 2008;48(1):98-106. doi:10.1016/j.jhep.2007.07.032

69. Riobó NA, Lu K, Ai X, Haines GM, Emerson CP. Phosphoinositide 3-kinase and Akt are essential for Sonic Hedgehog signaling. *Proc Natl Acad Sci U S A*. 2006;103(12):4505-4510. doi:10.1073/pnas.0504337103

70. Hirose Y, Itoh T, Miyajima A. Hedgehog signal activation coordinates proliferation and differentiation of fetal liver progenitor cells. *Exp Cell Res*. 2009;315(15):2648-2657. doi:10.1016/j.yexcr.2009.06.018

71. Sasaki H, Hui C, Nakafuku M, Kondoh H. A binding site for Gli proteins is essential for HNF-3beta floor plate enhancer activity in transgenics and can respond to Shh in vitro. *Development*. 1997;124(7):1313-1322.

72. Moreau R, Jalan R, Gines P, et al. Acute-on-chronic liver failure is a distinct syndrome that develops in patients with acute decompensation of cirrhosis. *Gastroenterology*. 2013;144(7):1426-1437, 1437.e1-9. doi:10.1053/j.gastro.2013.02.042

73. Seglen PO. Preparation of isolated rat liver cells. *Methods Cell Biol*. 1976;13:29-83. doi:10.1016/s0091-679x(08)61797-5

74. Berry MN, Grivell AR, Grivell MB, Phillips JW. Isolated hepatocytes--past, present and future. *Cell Biol Toxicol*. 1997;13(4-5):223-233. doi:10.1023/a:1007402505482

75. Pear WS, Nolan GP, Scott ML, Baltimore D. Production of high-titer helper-free retroviruses by transient transfection. *Proc Natl Acad Sci U S A*. 1993;90(18):8392-8396. doi:10.1073/pnas.90.18.8392

76. Nelson JD, Denisenko O, Bomsztyk K. Protocol for the fast chromatin immunoprecipitation (ChIP) method. *Nat Protoc*. 2006;1(1):179-185. doi:10.1038/nprot.2006.27

77. Livak KJ, Schmittgen TD. Analysis of relative gene expression data using real-time quantitative PCR and the 2(-Delta Delta C(T)) Method. *Methods*. 2001;25(4):402-408. doi:10.1006/meth.2001.1262

78. H Backman TW, Girke T. systemPipeR: NGS workflow and report generation environment. *BMC Bioinformatics*. 2016;17:388. doi:10.1186/s12859-016-1241-0

79. Bray NL, Pimentel H, Melsted P, Pachter L. Near-optimal probabilistic RNA-seq quantification. *Nat Biotechnol*. 2016;34(5):525-527. doi:10.1038/nbt.3519

80. Ritchie ME, Phipson B, Wu D, et al. limma powers differential expression analyses for RNA-sequencing and microarray studies. *Nucleic Acids Res*. 2015;43(7):e47. doi:10.1093/nar/gkv007

81. Gu Z, Eils R, Schlesner M. Complex heatmaps reveal patterns and correlations in multidimensional genomic data. *Bioinformatics*. 2016;32(18):2847-2849. doi:10.1093/bioinformatics/btw313

82. Rach EA, Winter DR, Benjamin AM, et al. Transcription initiation patterns indicate divergent strategies for gene regulation at the chromatin level. *PLoS Genet*. 2011;7(1):e1001274. doi:10.1371/journal.pgen.1001274

83. Kadonaga JT. Perspectives on the RNA polymerase II core promoter. *Wiley Interdiscip Rev Dev Biol*. 2012;1(1):40-51. doi:10.1002/wdev.21

84. Fornes O, Castro-Mondragon JA, Khan A, et al. JASPAR 2020: update of the open-access database of transcription factor binding profiles. *Nucleic Acids Res*. 2020;48(D1):D87-D92. doi:10.1093/nar/gkz1001

85. Weng H-L, Cai X, Yuan X, et al. Two sides of one coin: massive hepatic necrosis and progenitor cell-mediated regeneration in acute liver failure. *Front Physiol*. 2015;6:178. doi:10.3389/fphys.2015.00178

86. Vermeulen M, Mulder KW, Denissov S, et al. Selective anchoring of TFIID to nucleosomes by trimethylation of histone H3 lysine 4. *Cell*. 2007;131(1):58-69. doi:10.1016/j.cell.2007.08.016

87. Burke TW, Kadonaga JT. The downstream core promoter element, DPE, is conserved from Drosophila to humans and is recognized by TAFII60 of Drosophila. *Genes Dev*. 1997;11(22):3020-3031. doi:10.1101/gad.11.22.3020

88. Bustin S. Molecular Biology of the Cell, Sixth Edition; ISBN: 9780815344643; and Molecular Biology of the Cell, Sixth Edition, The Problems Book; ISBN 9780815344537. *Int J Mol Sci*. 2015;16(12):28123-28125. doi:10.3390/ijms161226074

89. Van Wyngene L, Vandewalle J, Libert C. Reprogramming of basic metabolic pathways in microbial sepsis: therapeutic targets at last? *EMBO Mol Med*. 2018;10(8). doi:10.15252/emmm.201708712

90. Rui L. Energy metabolism in the liver. *Compr Physiol*. 2014;4(1):177-197. doi:10.1002/cphy.c130024

91. Nishio H, Dugaiczyk A. Complete structure of the human alpha-albumin gene, a new member of the serum albumin multigene family. *Proc Natl Acad Sci U S A*. 1996;93(15):7557-7561. doi:10.1073/pnas.93.15.7557

92. Tronche F, Rollier A, Herbomel P, et al. Anatomy of the rat albumin promoter. *Mol Biol Med*. 1990;7(2):173-185.

93. Schleef M, Zühlke C, Jockusch H, Schöffl F. The structure of the mouse parvalbumin gene. *Mamm Genome*. 1992;3(4):217-225. doi:10.1007/BF00355722

94. Wu KJ, Wilson DR, Shih C, Darlington GJ. The transcription factor HNF1 acts with C/EBP alpha to synergistically activate the human albumin promoter through a novel domain. *J Biol Chem*. 1994;269(2):1177-1182.

95. Milos PM, Zaret KS. A ubiquitous factor is required for C/EBP-related proteins to form stable transcription complexes on an albumin promoter segment in vitro. *Genes Dev*. 1992;6(6):991-1004. doi:10.1101/gad.6.6.991

96. Cereghini S, Blumenfeld M, Yaniv M. A liver-specific factor essential for albumin transcription differs between differentiated and dedifferentiated rat hepatoma cells. *Genes Dev*. 1988;2(8):957-974. doi:10.1101/gad.2.8.957

97. Maire P, Wuarin J, Schibler U. The role of cis-acting promoter elements in tissue-specific albumin gene expression. *Science*. 1989;244(4902):343-346. doi:10.1126/science.2711183

98. Frain M, Hardon E, Ciliberto G, Sala-Trepat JM. Binding of a liver-specific factor to the human albumin gene promoter and enhancer. *Mol Cell Biol*. 1990;10(3):991-999. doi:10.1128/mcb.10.3.991

99. Wolfrum C, Asilmaz E, Luca E, Friedman JM, Stoffel M. Foxa2 regulates lipid metabolism and ketogenesis in the liver during fasting and in diabetes. *Nature*. 2004;432(7020):1027-1032. doi:10.1038/nature03047

100. Lucké B, Mallory T. The Fulminant Form of Epidemic Hepatitis. *Am J Pathol*. 1946;22(5):867-945.

101. Kyrmizi I, Hatzis P, Katrakili N, Tronche F, Gonzalez FJ, Talianidis I. Plasticity and expanding complexity of the hepatic transcription factor network during liver development. *Genes Dev*. 2006;20(16):2293-2305. doi:10.1101/gad.390906

102. Haberle V, Stark A. Eukaryotic core promoters and the functional basis of transcription initiation. *Nat Rev Mol Cell Biol*. 2018;19(10):621-637. doi:10.1038/s41580-018-0028-8

103. Bahrami-Nejad Z, Zhao ML, Tholen S, et al. A Transcriptional Circuit Filters Oscillating Circadian Hormonal Inputs to Regulate Fat Cell Differentiation. *Cell Metab*. 2018;27(4):854-868.e8. doi:10.1016/j.cmet.2018.03.012

104. Wang A, Luan HH, Medzhitov R. An evolutionary perspective on immunometabolism. *Science*. 2019;363(6423). doi:10.1126/science.aar3932

105. de Alvaro C, Teruel T, Hernandez R, Lorenzo M. Tumor necrosis factor alpha produces insulin resistance in skeletal muscle by activation of inhibitor kappaB kinase in a p38 MAPK-dependent manner. *J Biol Chem*. 2004;279(17):17070-17078. doi:10.1074/jbc.M312021200

106. Clotman F, Lannoy VJ, Reber M, et al. The onecut transcription factor HNF6 is required for normal development of the biliary tract. *Development*. 2002;129(8):1819-1828.

107. Olofsson LE, Orho-Melander M, William-Olsson L, et al. CCAAT/enhancer binding protein alpha (C/EBPalpha) in adipose tissue regulates genes in lipid and glucose metabolism and a genetic variation in C/EBPalpha is associated with serum levels of triglycerides. *J Clin Endocrinol Metab*. 2008;93(12):4880-4886. doi:10.1210/jc.2008-0574

108. Haaxma CA, Kim PK, Andrejko KM, Raj NR, Deutschman CS. Transcription factors C/EBP-alpha and HNF-1alpha are associated with decreased expression of liver-specific genes in sepsis. *Shock*. 2003;19(1):45-49. doi:10.1097/00024382-200301000-00009

109. Taura K, Miura K, Iwaisako K, et al. Hepatocytes do not undergo epithelial-mesenchymal transition in liver fibrosis in mice. *Hepatology*. 2010;51(3):1027-1036. doi:10.1002/hep.23368

110. Shi Y, Wang YF, Jayaraman L, Yang H, Massagué J, Pavletich NP. Crystal structure of a Smad MH1 domain bound to DNA: insights on DNA binding in TGF-beta signaling. *Cell*. 1998;94(5):585-594. doi:10.1016/s0092-8674(00)81600-1

111. Massagué J, Seoane J, Wotton D. Smad transcription factors. *Genes Dev*. 2005;19(23):2783-2810. doi:10.1101/gad.1350705

112. Massagué J. TGFβ signalling in context. *Nat Rev Mol Cell Biol*. 2012;13(10):616-630. doi:10.1038/nrm3434

7 LISTS OF FIGURES AND TABLES

7.1 List of figures

7.2 List of tables

8 CURRICULUM VITAE

PERSONAL INFORMATION

Name:	Rilu Feng
Date of birth:	Jul. 3rd, 1991
Place of birth	Ningbo, Zhejiang Province, China
Marital status:	Married
Father:	Shanlun Feng
Mother:	Nengfei Zhou

EDUCATION

Oct.2017-Present	M.D. Student (Dr.med.) Department of Medicine II, University Medical Center Mannheim, Medical Faculty Mannheim, Heidelberg University, Mannheim, Germany Doctor Thesis: Hierarchical regulation of albumin expression under various pathophysiological challenges
Sept.2014-Jul.2017	Master's Degree of Medicine Department of Endocrinology and Metabolism, Renji Hospital, Shanghai Jiao Tong University School of Medicine, Shanghai, China Master Thesis: The regulation mechanism of gastrointestinal function on postprandial blood glucose in type 2 diabetes
Sept.2009-Jul.2014	Bachelor's Degree of Medicine Chongqing Medical University School of Medicine, Chongqing, China

SCHOLARSHIP

M.D. scholarship from China Scholarship Council (CSC)

PUBLICATIONS

First authorship

1. **Feng R**, Yuan X, Shao C, Ding H, Liebe R, Weng HL. Are we any closer to treating liver fibrosis (and if no, why not)? J Dig Dis. 2018, 19(3):118-126.
2. Zhang M[#], **Feng R[#]**, Yue J[#], Qian C, Yang M, Liu W, Rayner CK, Ma J. Effects of Metformin and Sitagliptin Monotherapy on Expression of Intestinal and Renal Sweet Taste Receptors and Glucose Transporters in a Rat Model of Type 2 Diabetes. Horm Metab Res. 2020 May;52(5):329-335.
3. Zhang M[#], **Feng R[#]**, Yang M, Qian C, Wang Z, Liu W, Ma J. Effects of metformin, acarbose, and sitagliptin monotherapy on gut microbiota in Zucker diabetic fatty rats. BMJ Open Diabetes Res Care. 2019 Sep 20;7(1): e000717.
4. **Rilu Feng[#]**, Cheng Qian[#], Lianyong Liu, Qianjing Liu, Yungqiu Jin, Shengxian Li, Wei Liu, Chris Rayner, Jing Ma. Secretion of Gut Hormones, and Expression of Sweet Taste Receptors and Glucose Transporters, in a Rat Model of Obesity. Obesity Facts. 2019 Mar 29; 12(2):190-198.
5. **Feng R[#]**, Qian C[#], Liu Q, Jin Y, Liu L, Li S, Liao Y, Zhou H, Liu W, Rayner CK, Ma J. Expression of sweet taste receptor and gut hormone secretion in modeled type 2 diabetes. Gen Comp Endocrinol. 2017, 252:142-149.

Co-authorship

1. Wang S, **Feng R**, Shi Y, Chen D, Weng H, Ding H, Zhang C. Intracellular alpha-fetoprotein interferes with all-trans retinoic acid induced ATG7 expression and autophagy in hepatocellular carcinoma cells. Sci Rep. 2021 Jan 25;11(1):2146.
2. Yang M, Shi FH, Liu W, Zhang MC, **Feng RL**, Qian C, Liu W, Ma J. Dapagliflozin Modulates the Fecal Microbiota in a Type 2 Diabetic Rat Model. Front Endocrinol (Lausanne). 2020 Nov 17;11:635.
3. Qian C, Qi Y, **Feng R**, Yang M, Zhang M, Liu W, Rayner CK, Ma J. Sucralose can improve glucose tolerance and upregulate expression of sweet taste receptors and glucose transporters in an obese rat model. Eur J Nutr. 2020 Aug 28.
4. Kim DK, Kim YH, Lee JH, Jung YS, Kim J, **Feng R**, Jeon TI, Lee IK, Cho SJ, Im SS, Dooley S, Osborne TF, Lee CH, Choi HS. Estrogen-related receptor γ controls sterol regulatory element-binding protein-1c expression and alcoholic fatty liver. Biochim Biophys Acta Mol Cell Biol Lipids. 2019 Dec;1864(12):158521.

5. Le Tao, Wenting Ma, Liu Wu, Mingyi Xu, Yanqin Yang, Wei Zhang, Wenjun Sha, Hongshan Li, Jianrong Xu, **Rilu Feng**, Dongying Xue, Jie Zhang, Steven Dooley, Ekihiro Seki, Ping Liu, Cheng Liu. Glial cell line-derived neurotrophic factor (GDNF) mediates hepatic stellate cell activation via ALK5/Smad signaling. Gut. 2019 Dec;68(12):2214-2227.
6. Ko S, Russell JO, Tian J, Gao C, Kobayashi M, **Feng R**, Yuan X, Shao C, Ding H, Poddar M, Singh S, Locker J, Weng HL, Monga SP, Shin D. Hdac1 Regulates Differentiation of Bipotent Liver Progenitor Cells During Regeneration via Sox9b and Cdk8. Gastroenterology. 2019 Jan; 156(1):187-202.
7. Lin TC, Li SX, Xu H, Zhou H, **Feng RL**, Liu W, Sun Y, Ma J. Gastrointestinal hormone secretion in women with polycystic ovary syndrome: an observational study. Human Reproduction, 2015, 30(11):2639–2644.

CONFERENCE PRESENTATIONS AND PUBLISHED ABSTRACTS

1. **Young Scholar Forum of "Asia Pacific Forum on Global Health - Through and Beyond the Pandemic" oral presentation-online** (May. 10. 2021, Hangzhou, China). " A hierarchical regulatory network guarantees Albumin synthesis in responding to severe infection".
2. **37th GASL Annual Meeting 2021 poster** (29.01-30.01.2021, Online) "HNF4α and FOXA2 form a hierarchical regulatory network to guarantee Albumin synthesis in response to pathophysiological challenge".
3. **Falk Foundation 2020 poster** (13.02-14.02.2020, Mainz) "Y-box binding protein-1 is critical in chemoresistance of intrahepatic cholangiocarcinoma".
4. **DGVS 2019 oral presentation** (03rd October, Wiesbaden). "Glial cell line-derived neurotrophic factor (GDNF) mediates hepatic stellate cell activation via ALK5/Smad signaling".

COURSES

EASL BASIC SCHOOL OF HEPATOLOGY:

Metabolism, immunity and liver disease

16-18 May, 2019

University Hospital Klinikum rechts der Isar, Technical University of Munich, Munich, Germany

EASL BASIC SCHOOL OF HEPATOLOGY:

Liver cell isolation and characterization

16-18 January, 2019

University Hospital Düsseldorf, Düsseldorf, Germany

9 ACKNOWLEDGEMENT

First of all, I sincerely thank my supervisor Professor Dr. Steven Dooley for providing me with the opportunity of my scientific research in liver disease. I am very thankful for all his valuable advice, suggestions as well as comments and moreover his constant support throughout the whole period of research and writing.

Secondly, the profound gratitude should go to my second supervisor Dr. Honglei Weng. He has given me valuable instructions and enough space throughout the process of my research work. His insight and accurateness about my project taught me a lot and trained my critical thinking. He provided me with beneficial help and offered me precious comments during the whole process of my writing, without which, the paper would not be what it is now.

Furthermore, I am very grateful for all the experiences I gained as a member of the AG-Dooley group. It was a pleasure to work with all the partners involved. I would like to take the opportunity to thank Kerry Gould, Sai Wang and Yujia Li for helping to isolate the mouse primary hepatocytes. I am very thankful to Stefan Munker for providing human primary hepatocytes. Besides, I would like to thank Dr. Carsten Sticht for helping me with the gene expression analysis, thanks Shanshan Wang for teaching me the experimental skills. A special thanks go to Dr. Roman Liebe for carefully reviewing and editing my thesis.

Particularly, China Scholarship Council (CSC) is gratefully acknowledged for financing all my study life in Germany.

Last but not least, I would like to express the deep gratitude to my family members. Thanks to my parents for their selfless support, concern and love. Thanks to my husband, who shared with me my worries, frustrations, and happiness and stood by me. They gave me the strength I often lacked.